

ANALYSIS OF PARTICULATE MATTER  
EMISSION IN DIESEL ENGINE OPERATED  
WITH WASTE COOKING OIL BIODIESEL



NUR FAUZIAH BINTI JAHARUDIN

MASTER OF ENGINEERING  
UNIVERSITI MALAYSIA PAHANG

# UNIVERSITI MALAYSIA PAHANG

## DECLARATION OF THESIS AND COPYRIGHT

Author's full name : NUR FAUZIAH BINTI JAHARUDIN  
Date of birth : 11<sup>th</sup> NOVEMBER 1988  
Title : Analysis of Particulate Matter Emission in Diesel Engine Operated with Waste Cooking Oil Biodiesel  
Academic Session : SEM I 2014/2015

I declare that this thesis is classified as:

- CONFIDENTIAL** (Contains confidential information under the Official Secret Act 1972)\*
- RESTRICTED** (Contains restricted information as specified by the Organization where research was done)\*
- OPEN ACCESS** I agree that my thesis to be published as online open access (Full text)

I acknowledge that Universiti Malaysia Pahang reserve the right as follows:

1. The Thesis is the Property of Universiti Malaysia Pahang
2. The Library of Universiti Malaysia Pahang has the right to make copies for the purpose of research only.
3. The Library has the right to make copies of the thesis for academic exchange.

Certified By:

(Student's Signature)

881111-08-6744

New IC / Passport Number

Date: SEPTEMBER 2015

(Supervisor's Signature)

Assoc. Prof. Dr. Abdul Adam Bin Abdullah

Name of Supervisor

Date: SEPTEMBER 2015

ANALYSIS OF PARTICULATE MATTER EMISSION IN DIESEL ENGINE  
OPERATED WITH WASTE COOKING OIL BIODIESEL

NUR FAUZIAH BINTI JAHARUDIN

Thesis submitted in fulfillment of the requirements  
for the award of the degree of  
Master of Engineering in Mechanical

Faculty of Mechanical Engineering  
UNIVERSITI MALAYSIA PAHANG

UMP

2015

## SUPERVISOR'S DECLARATION

We hereby declare that we have checked this thesis, and in my opinion, this thesis is adequate in terms of scope and quality for the award of the degree of Master of Engineering in Mechanical.

Signature

Name of Supervisor : ASSOC.PROF.DR. ABDUL ADAM BIN ABDULLAH

Position : SENIOR LECTURER

Date : SEPTEMBER 2015

Signature

Name of Co-supervisor : ASSOC. PROF. DR. RIZALMAN BIN MAMAT

Position : FACULTY DEAN OF MECHANICAL ENGINEERING

Date : SEPTEMBER 2015

The logo of Universiti Malaysia Perlis (UMP) is a large, downward-pointing triangle. The top part of the triangle is a light blue rectangle containing a yellow diamond with a purple and blue swirl around it. The bottom part of the triangle is split into two sections: a light blue section on the left and a light purple section on the right. The letters "UMP" are written in white, bold, sans-serif font across the bottom of the triangle.

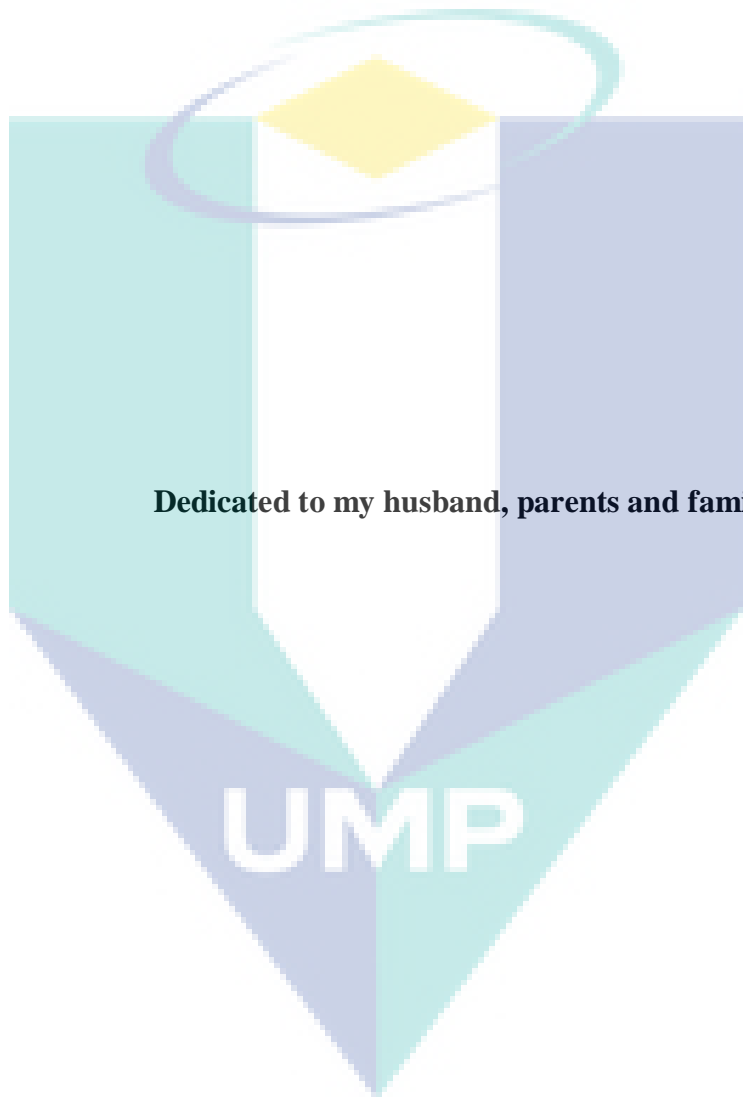
UMP

## STUDENT'S DECLARATION

I hereby declare that work in this thesis is my own except for quotations and summaries which have been duly acknowledged. The thesis has not been accepted for any degree and is not concurrently submitted for the award of the degree.

Signature :  
Name : NUR FAUZIAH BINTI JAHARUDIN  
Id Number : MMM 12002  
Date : SEPTEMBER 2015





**Dedicated to my husband, parents and family**

**UMP**

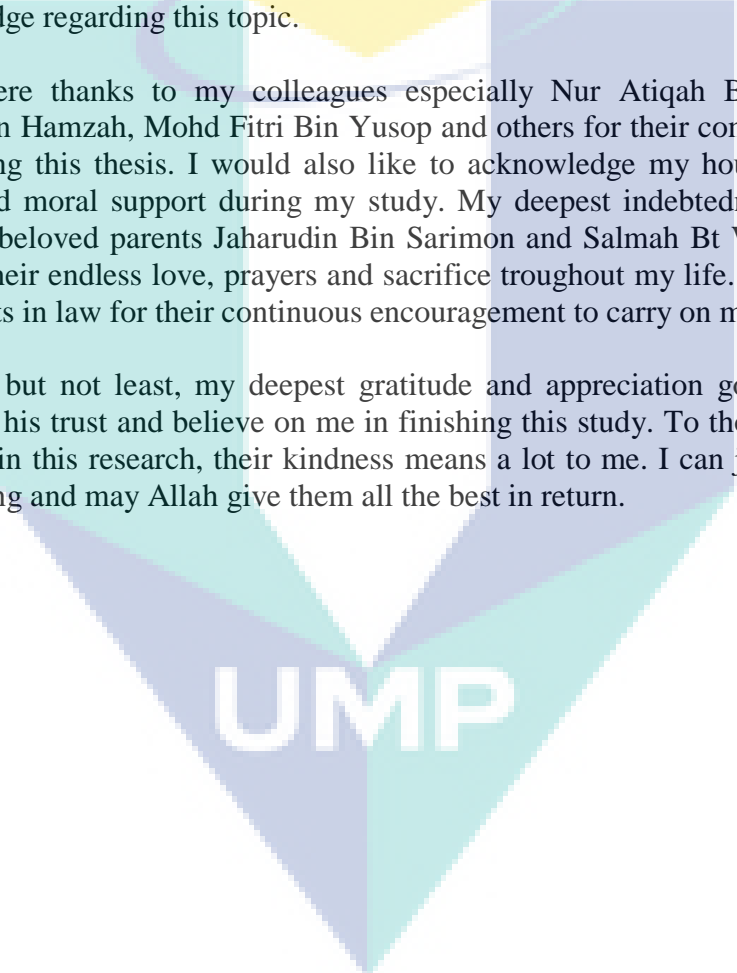
## ACKNOWLEDGEMENTS

*In the name of Allah, The most Beneficent, The Most Merciful*

Alhamdulillah, first and above all, I praise to Allah for the strengths and granting me the capability to proceed successfully. This thesis is completed due to assistance, guidance, support and contribution of several people throughout my study. I would like to express my sincerest gratitude to my supervisor Dr. Abdul Adam Bin Abdullah and my co-supervisor, Assoc. Prof Dr. Rizalman Bin Mamat for believing in my ability and providing invaluable guidance, advice and support. Not forgotten, my appreciation also goes to Assoc. Prof. Dr. Zafri Azran Bin Abdul Majid for his support and knowledge regarding this topic.

Sincere thanks to my colleagues especially Nur Atiqah Bt Ramlan, Mohd Herzwan Bin Hamzah, Mohd Fitri Bin Yusop and others for their contribution and help in completing this thesis. I would also like to acknowledge my housemates for their kindness and moral support during my study. My deepest indebtedness and gratitude goes to my beloved parents Jaharudin Bin Sarimon and Salmah Bt Wakhidon and my family for their endless love, prayers and sacrifice throughout my life. I am also grateful to my parents in law for their continuous encouragement to carry on my study.

Last but not least, my deepest gratitude and appreciation goes to my dearest husband for his trust and believe on me in finishing this study. To those who indirectly contributed in this research, their kindness means a lot to me. I can just say thank you for everything and may Allah give them all the best in return.

The logo of Universiti Malaysia Perlis (UMP) is a large, stylized letter 'V' shape. It is composed of several overlapping triangles in shades of teal, light blue, and yellow. The letters 'UMP' are printed in a bold, white, sans-serif font across the center of the 'V' shape.

UMP

## ABSTRACT

Diesel engines which is an attractive power unit used widely in many fields are among the main contributors to air pollutions for the large amount of emissions, especially particulate matter (PM) and nitrogen oxides (NO<sub>x</sub>). PM is one of the major pollutants emitted by diesel engine which have adverse effects on human health. Accordingly, many research have been done to find alternative fuels that are clean and efficient. In this study, waste cooking oil (WCO) biodiesel has been used as an alternative source for diesel engine which produces lower PM than diesel fuel. The emission of PM and gaseous emission (carbon monoxide (CO), carbon dioxide (CO<sub>2</sub>), nitric oxide (NO) and NO<sub>x</sub>) has been collected from single cylinder diesel engine fuelled with diesel and WCO biodiesel blends (B5, B10 B20 and B100) at five different engine speed (1200 rpm, 1500 rpm, 1800 rpm, 2100 rpm and 2400 rpm) with constant load of 20 Nm. The comparison between diesel and WCO biodiesel blends has been made in terms of PM characterization which is PM mass concentration, its component (soluble organic fraction (SOF) and soot) and its influence on PM formation, PM morphology and PM size distribution. In addition, combustion characteristic which is in-cylinder pressure of the engine as well as exhaust temperature also has been observed. The results show PM emission of B100 is lower than diesel fuel with variation of 5.56% to 21.82 % . This is due to oxygen content contained in B100. As for SOF concentration, blended fuels B10, B20, and B100 have higher SOF value (3.23 % to 82.36 % ) compared to diesel fuel at moderate and high engine speed. Meanwhile, soot concentration for blended fuels B10, B20 and B100 is lower (10 % to 62.50 % . ) compared to diesel fuel Observation on PM morphology shows that the images is chain-like agglomeration which is extremely small non uniform nanostructure. As for the PM size distribution, the trend were similar for diesel and WCO biodiesel blends. The size distribution of diesel fuel and WCO biodiesel blends were shifted to the larger size as the engine speed is increased. Simultaneously, the size distribution is shifted to the smaller PM diameter as blending ratio of WCO biodiesel in the fuel blend is increase. The observation of in-cylinder pressure shows uncertain trend with the WCO biodiesel ratio in the fuel blend while decreasing with the increasing engine speed due to the prolong ignition delay period. At the same time, WCO biodiesel blends gives higher value of exhaust temperature which is 1.49 % compared to diesel fuel and it increases as the engine speed increase. In terms of gaseous emission, increasing engine speed increased the CO, CO<sub>2</sub>, NO<sub>x</sub> and NO emission while decrease the O<sub>2</sub> emission. The effect of WCO biodiesel blends on the gaseous emission shows uncertain trend while PM-NO<sub>x</sub> trade off observation shows B100 simultaneously decrease both NO<sub>x</sub> and PM emission at the same time. This study shows that the PM and gaseous emission as well as combustion characteristic of the WCO biodiesel are comparable with diesel fuel thus WCO biodiesel has potential as an alternative fuel to be used in diesel in the future.

## ABSTRAK

Enjin diesel yang merupakan unit kuasa yang digunakan secara meluas dalam pelbagai bidang adalah penyumbang utama kepada pencemaran udara yang dikeluarkan oleh ekzos, terutamanya bahan zarah (PM) dan oksida nitrogen (NO<sub>x</sub>). PM merupakan bahan pencemar utama yang dihasilkan oleh enjin diesel yang boleh memberikan kesan buruk terhadap kesihatan manusia. Oleh itu, banyak kajian telah dilakukan untuk mencari bahan api yang bersih dan cekap. Kajian ini menggunakan sisa minyak masak (WCO) sebagai sumber alternatif untuk enjin diesel yang menghasilkan PM lebih rendah berbanding bahan api diesel. Pengeluaran PM dan pencemaran gas (karbon monoksida (CO), karbon dioksida (CO<sub>2</sub>), nitrik oksida (NO) and NO<sub>x</sub>) telah dikumpulkan dari enjin diesel yang menggunakan bahan api diesel dan adunan biodiesel WCO (B5, B10 B20 dan B100) pada lima kelajuan enjin berbeza (1200 rpm, 1500 rpm, 1800 rpm, 2100 rpm dan 2400 rpm) dengan beban enjin 20 Nm. Perbandingan antara diesel dan adunan biodiesel WCO telah dibuat dari segi pencirian PM antaranya kepekatan jisim PM, komponen yang terdapat dalam PM (SOF dan jelaga) dan pengaruhnya terhadap pembentukan PM, morfologi PM dan taburan saiz PM. Di samping itu, ciri-ciri pembakaran iaitu tekanan dalam silinder enjin serta suhu ekzos juga telah dikaji. Keputusan menunjukkan PM dari B100 lebih rendah berbanding bahan api diesel dengan variasi dari 5.56% to 21.82 % Ini adalah kerana kandungan oksigen yang terkandung dalam B100. Bagi kepekatan SOF, adunan bahan api B10, B20, dan B100 mempunyai nilai SOF yang lebih tinggi (3.23 % ke 82.36 % ) berbanding bahan api diesel pada kelajuan enjin sederhana dan tinggi. Sementara itu, kepekatan jelaga untuk bahan api B10, B20 dan B100 adalah lebih rendah (10 % ke 62.50 %). berbanding bahan api diesel. Pemerhatian ke atas morfologi PM menunjukkan imej yang terbentuk adalah seperti penggumpalan zarah bersambung yang amat kecil dan tidak seragam. Bagi taburan saiz PM, bahan api diesel dan adunan biodiesel WCO menunjukkan trend yang sama yang mana taburan saiz telah beranjak kepada saiz yang lebih besar apabila kelajuan enjin meningkat. Pada masa yang sama, taburan saiz beranjak kepada saiz yang lebih kecil apabila nisbah biodiesel WCO dalam adunan bahan api meningkat. Pemerhatian bagi tekanan dalam silinder menunjukkan trend yang tidak menentu dengan nisbah biodiesel WCO dalam adunan bahan api manakala ia menurun dengan kelajuan enjin yang semakin meningkat disebabkan oleh tempoh lengah pencucuhan yang semakin meningkat. Pada masa yang sama, adunan biodiesel WCO memberikan nilai yang lebih tinggi bagi suhu ekzos iaitu 1.49 % berbanding bahan api diesel dan ia meningkat dengan peningkatan kelajuan enjin. Dari segi pencemaran gas, peningkatan kelajuan enjin meningkatkan pengeluaran CO, CO<sub>2</sub>, NO<sub>x</sub> dan NO dan menurunkan pengeluaran O<sub>2</sub>. Walaubagaimanapun, kesan adunan biodiesel WCO pada pencemaran gas menunjukkan trend yang tidak menentu. Pemerhatian terhadap keseimbangan pengeluaran diantara PM-NO<sub>x</sub> menunjukkan B100 menurunkan jumlah pengeluaran NO<sub>x</sub> dan PM. Kajian ini menunjukkan bahawa PM dan pencemaran gas dan juga ciri-ciri pembakaran biodiesel WCO adalah setanding bahan api diesel. Oleh itu, biodiesel daripada WCO mempunyai potensi sebagai minyak alternatif yang boleh digunakan dalam enjin diesel pada masa akan datang.

## TABLE OF CONTENTS

	<b>Page</b>
<b>SUPERVISOR'S DECLARATION</b>	ii
<b>STUDENT'S DECLARATION</b>	iii
<b>ACKNOWLEDGEMENTS</b>	iv
<b>ABSTRACT</b>	v
<b>ABSTRAK</b>	vi
<b>TABLE OF CONTENTS</b>	vii
<b>LIST OF TABLES</b>	x
<b>LIST OF FIGURES</b>	xi
<b>LIST OF SYMBOLS</b>	xiv
<b>LIST OF ABBREVIATION</b>	xv
<b>CHAPTER 1 INTRODUCTION</b>	
1.1 Introduction	1
1.2 Problem Statement	5
1.3 Objectives of the Study	7
1.4 Scope of the Study	7
1.5 Overview of the Thesis	8
<b>CHAPTER 2 LITERATURE REVIEW</b>	
2.1 Introduction	9
2.2 Diesel Engine Combustion	9
2.3 Exhaust Emission From Diesel Engine	12
2.3.1 Carbon Monoxide (CO)	13
2.3.2 Carbon Dioxide (CO <sub>2</sub> )	14
2.3.3 Oxygen (O <sub>2</sub> )	15
2.3.4 Nitrogen Oxides (NO <sub>x</sub> )	15
2.3.5 Particulate Matter (PM)	17
2.4 Health Effect of Diesel Engine Emission	18
2.5 Worldwide Emission Regulation	20

2.6	Particulate Matter	22
2.6.1	Particulate Matter Composition and Structure	23
2.6.2	Mechanism of Particulate Matter Formation	26
2.6.3	Particulate Matter Measurement Methods	31
2.6.4	Overview on Particulate Matter study	33
2.7	Biodiesel as an Alternative Fuel	36
2.7.2	Production of Waste Cooking Oil as a Biodiesel	40
2.7.3	Waste Cooking Oil Biodiesel Properties	41
2.8	Summary	45

### **CHAPTER 3 RESEARCH METHODOLOGY**

3.1	Introduction	47
3.2	Engine and Instrumentation	48
3.2.1	Engine	50
3.2.2	Hydraulic Dynamometer	50
3.2.3	Data Acquisition System	52
3.2.4	Temperature and Speed Measurement	52
3.3	Exhaust Emission Measurement	53
3.3.1	Exhaust Gas Analyzer	54
3.3.2	Filter Holder	55
3.3.3	Filter Paper	56
3.3.4	Sampling Pump	58
3.3.5	Forced Convection Oven	59
3.3.6	High Precision Electric Balance	59
3.3.7	Dichloromethane	60
3.3.8	Field Element Scanning Electron Micrograph (FE-SEM)	61
3.4	Test Fuel	61
3.5	Test Operating Condition	62
3.6	Particulate Matter Analysis	63
3.6.1	Gravimetric Analysis	63
3.6.2	Image Analysis	64
3.7	Summary	69

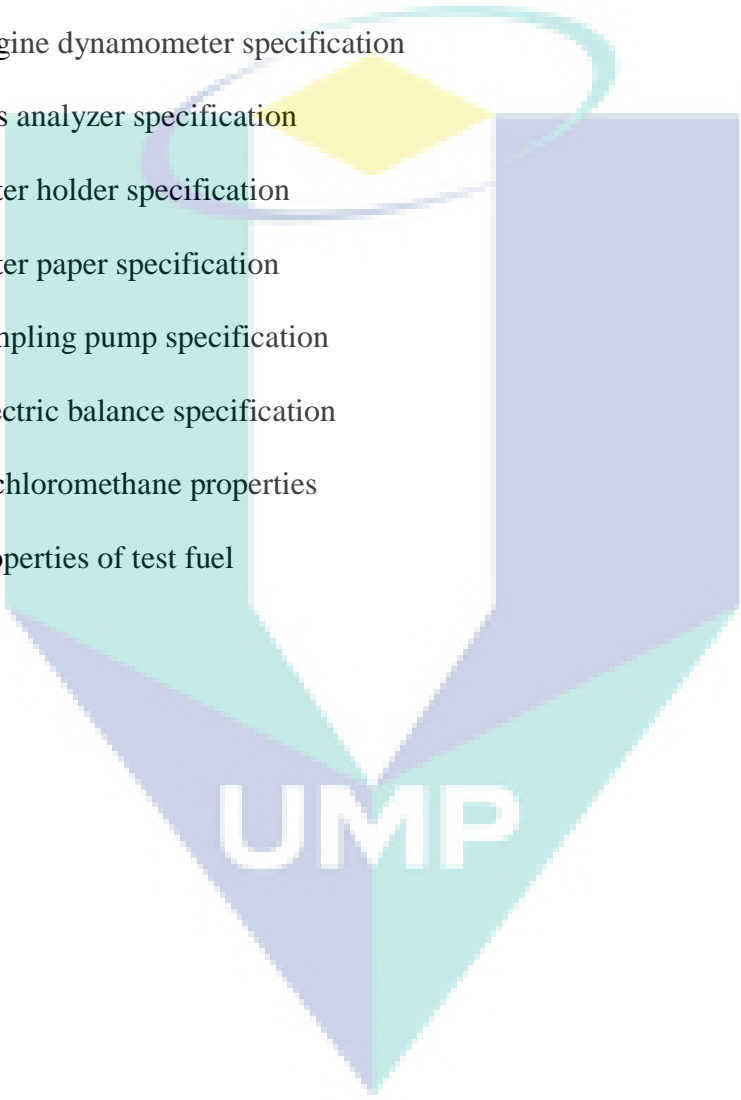
### **CHAPTER 4 RESULT AND DISCUSSIONS**

4.1	Introduction	70
-----	--------------	----

4.2	In-Cylinder Pressure	71
4.3	Exhaust Temperature	75
4.4	PM Mass Concentration	77
	4.4.1 SOF Component	79
	4.4.2 Soot Component	80
4.5	PM morphology	81
4.6	PM Size Distribution	85
	4.6.1 Effect of Engine Speed on PM Size Distribution	85
	4.6.2 Effect of WCO Biodiesel Blends on PM size Distribution	97
4.7	Gaseous Emission	99
	4.7.1 CO Emission	99
	4.7.2 O <sub>2</sub> Emisison	100
	4.7.3 CO <sub>2</sub> Emission	101
	4.7.4 NO <sub>x</sub> Emission	102
	4.7.5 NO Emission	103
4.8	PM - NO <sub>x</sub> Trade Off	104
4.9	Summary	106
<b>CHAPTER 5 CONCLUSION AND RECOMMENDATION</b>		
5.1	Conclusion	107
5.2	Summary of Findings	109
5.2	Recommendations	110
	5.2.1 TEM Employment to Obtain PM Image	110
	5.2.3 PM Chemical Composition Analysis	111
	5.2.4 Transient Mode Testing	111
	5.2.5 Specific Sources for WCO Biodiesel	111
<b>REFERENCES</b>		112
<b>APPENDIX</b>		126

**LIST OF TABLES**

<b>Table No.</b>	<b>Title</b>	<b>Page</b>
2.1	PM (TSP, PM <sub>10</sub> , PM <sub>2.5</sub> ) Standards in selected asian countries ( $\mu\text{g}/\text{m}^3$ )	22
3.1	Engine Specification	50
3.2	Engine dynamometer specification	51
3.3	Gas analyzer specification	55
3.4	Filter holder specification	56
3.5	Filter paper specification	57
3.6	sampling pump specification	58
3.7	Electric balance specification	60
3.8	Dichloromethane properties	60
3.9	Properties of test fuel	62

The logo is a large, downward-pointing arrow shape composed of four triangular segments in shades of teal and light blue. The letters 'UMP' are printed in white, bold, sans-serif font across the center of the arrow.

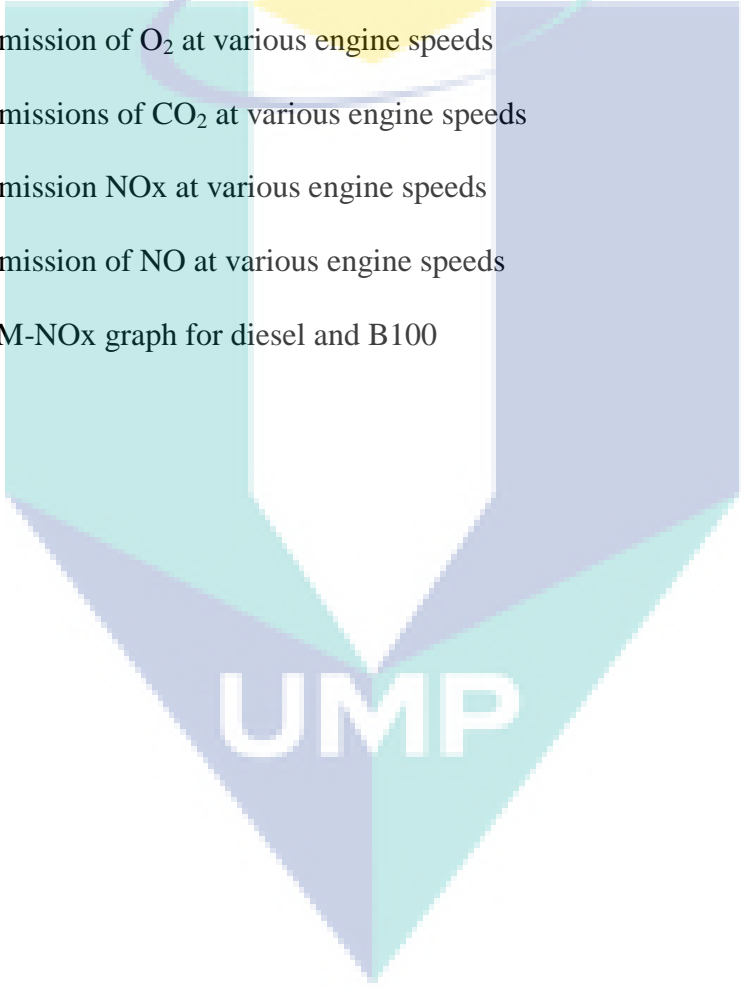
**UMP**

## LIST OF FIGURES

<b>Figure No.</b>	<b>Title</b>	<b>Page</b>
1.1	Final consumption for petroleum product	3
1.2	PM deposition in human respiratory tract	5
2.1	Four stroke cycle of diesel engine	10
2.2	Pressure-time diagram and rate of heat release of diesel combustion process.	11
2.3	Structure and composition of engines particulate matter	24
2.4	Typical particle size and distribution from diesel engines	25
2.5	Steps in PM formation	28
2.6	Quasi steady diesel combustion plume	30
2.7	Feedstock price in United States	39
3.1	Flow chart	48
3.2	Schematic diagram of the test rig	49
3.3	Test engine	49
3.4	Dynamometer system	51
3.5	Data acquisition system	52
3.6	Temperature and speed measurement instrument	53
3.7	Exhaust sampling equipment setup	54
3.8	Exhaust gas analyzer	54
3.9	Filter holder parts	55
3.10	Placement of filter paper in filter holder	56
3.11	PM sample trapped on filter paper	57
3.12	Sampling pump	58

3.13	High Precision Electric Balance	59
3.14	Sample in dichloromethane	60
3.15	FE-SEM	61
3.16	Image analysis process	65
3.17	Scale bar in FE-SEM image	65
3.18	Image prior to threshold	66
3.19	A) Threshold adjustment, B) Binary image	67
3.20	Final binary image	68
4.1	Variation of in-cylinder pressure of diesel fuel	71
4.2	Variation of in-cylinder pressure of B100	72
4.3	In-cylinder pressure of WCO biodiesel blends at 1800 rpm	74
4.4	Variation of exhaust temperature with different engine speed and fuel	76
4.5	PM concentration of WCO biodiesel blends and diesel fuel	78
4.6	Percentage of PM reduction of B100 compare to diesel fuel	78
4.7	SOF concentration of WCO biodiesel blends and diesel fuel	79
4.8	Soot concentration of WCO biodiesel blends and diesel fuel	81
4.9	FE-SEM images of B100 and diesel fuel	83
4.10	FE-SEM images of B5, B10 and B20	84
4.11	PM size distribution for diesel fuel	86
4.12	Average particle count of diesel fuel for each engine speed	87
4.13	PM size distribution for B5	88
4.14	Average particle count of B5 for each engine speed	89
4.15	PM size distribution for B10	90
4.16	Average particle count of B10 for each engine speed	91

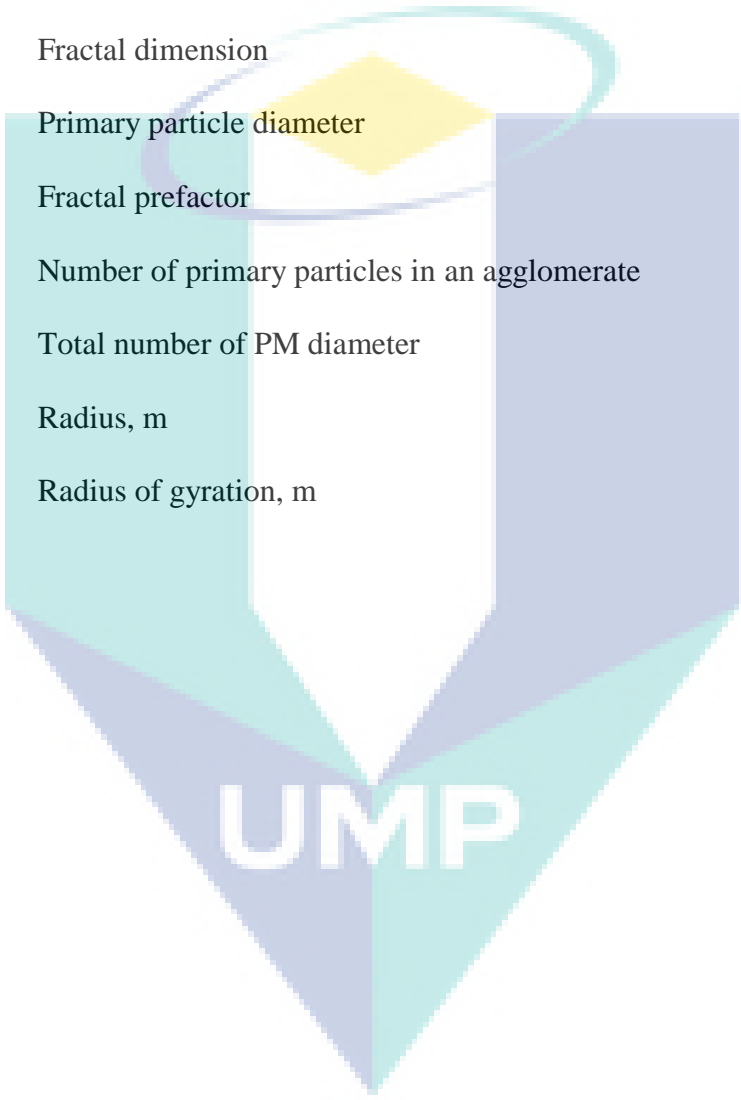
4.17	PM size distribution for B20	92
4.18	Average particle count of B20 for each engine speed	94
4.19	PM size distribution for B100	95
4.20	Average particle count for B100 for each engine speed	96
4.21	PM size distribution at engine speed 1800 rpm	98
4.22	Emission of CO at various engine speeds	99
4.23	Emission of O <sub>2</sub> at various engine speeds	101
4.24	Emissions of CO <sub>2</sub> at various engine speeds	102
4.25	Emission NO <sub>x</sub> at various engine speeds	103
4.26	Emission of NO at various engine speeds	104
4.27	PM-NO <sub>x</sub> graph for diesel and B100	105

The logo for UMP (Universiti Malaysia Perlis) is a large, downward-pointing arrow shape. It is composed of four triangular sections meeting at a central point. The top-left and bottom-right sections are light blue, the top-right and bottom-left sections are light purple, and the bottom-most section is light green. The letters 'UMP' are written in white, bold, sans-serif font across the center of the arrow.

UMP

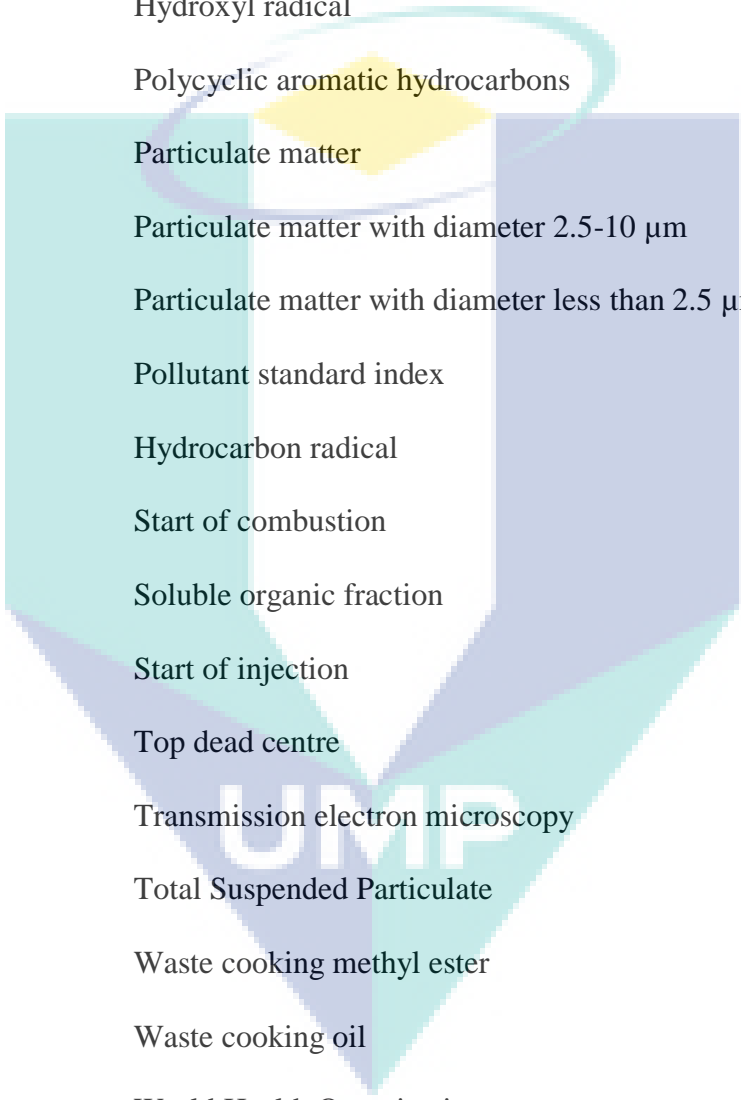
**LIST OF SYMBOLS**

$\bar{d}$	Mean diameter, m
A	Area, m <sup>2</sup>
D	Diameter, m
D <sub>f</sub>	Fractal dimension
d <sub>p</sub>	Primary particle diameter
K <sub>g</sub>	Fractal prefactor
N <sub>p</sub>	Number of primary particles in an agglomerate
n	Total number of PM diameter
r	Radius, m
R <sub>g</sub>	Radius of gyration, m



## LIST OF ABBREVIATION

ASTM	American Society for Testing and Materials
ATDC	After top dead centre
BDC	Bottom dead centre
BP	British Petroleum
BTDC	Before top dead centre
C	Carbon
CO	Carbon monoxide
CO <sub>2</sub>	Carbon dioxide
EGR	Exhaust gas recirculation
EIA	Energy Information Administration
EPA	Environment Protection Agency
EU	European Union
FE-SEM	Field emission scanning electron microscopy
H <sub>2</sub> O	Water
HAPs	Hazardous air pollutants
HC	Hydrocarbon
HCCI	Homogeneous compression charge ignition
HDDE	Heavy duty diesel engine
HO <sub>2</sub>	Hydroperoxil
IEA	International Energy Agency
N	Nitrogen
N <sub>2</sub>	Nitrogen gas
NO	Nitric acid



NO <sub>2</sub>	Nitrogen dioxide
NO <sub>x</sub>	Nitrogen oxides
O <sub>2</sub>	Oxygen
O <sub>3</sub>	Ozone
OH	Hydroxyl radical
PAHs	Polycyclic aromatic hydrocarbons
PM	Particulate matter
PM <sub>10</sub>	Particulate matter with diameter 2.5-10 μm
PM <sub>2.5</sub>	Particulate matter with diameter less than 2.5 μm
PSI	Pollutant standard index
RH	Hydrocarbon radical
SOC	Start of combustion
SOF	Soluble organic fraction
SOI	Start of injection
TDC	Top dead centre
TEM	Transmission electron microscopy
TSP	Total Suspended Particulate
WCME	Waste cooking methyl ester
WCO	Waste cooking oil
WHO	World Health Organization

## CHAPTER 1

### INTRODUCTION

#### 1.1 INTRODUCTION

Demand for fossil fuel is likely to keep increasing due to significant growth of population, transportation and the basic industry sectors (Asif and Munir, 2007). The trend can be seen growing since the industrial revolution took off in the 18<sup>th</sup> century in Europe where vast quantities of fossil fuel have since been used to power the economy. However, it is becoming global issue when reports say that world oil reserves are depleting while at the same time the prices keep increasing. On the other hand, the increasing consumption of fossil fuel also gives significant effect on environmental problems. Data from BP Statistical Review of world energy Jun 2014 stated that global primary energy consumption in 2013 accelerated about 2.3 % over 2012 despite stagnant global economic growth. Consumption and production for all fuels had increased, reaching record levels for every fuel type except nuclear power. For each of the fossil fuels, global consumption rose more rapidly than production. The data suggests that growth in global carbon dioxide (CO<sub>2</sub>) emissions from energy use also accelerated in 2013, although it remained below average (BP, 2014).

According to International Energy Agency (IEA) in its latest World Energy Outlook released on 12 November 2014, global energy consumption will rise by 37 % by 2040 while crude-oil consumption is expected to rise from the current 90 million barrels a day to 104 million barrels a day, but demand for oil will plateau by 2040. Besides that, the report also stated that the global supply of crude oil, other liquid

hydrocarbons and biofuels is expected to be sufficient to meet the world demand for liquid fuel for at least the next 25 years. However, there is substantial uncertainty about the levels of future liquid fuels supply and demand. After the oil crises of the 1970s and 1980s, much of the debate about world oil markets focused on the limitations of supply (IEA, 2014).

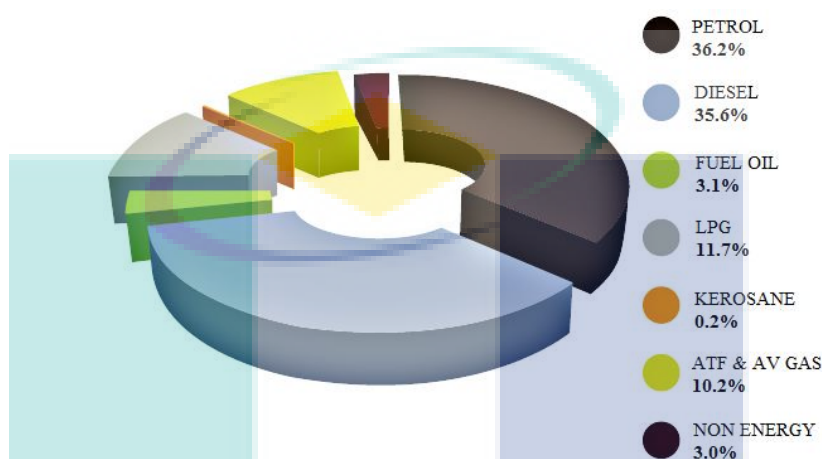


**Figure 1.1:** Final consumption for petroleum product

Source: Energy Commission (2014)

In Malaysia, the total primary energy supply increased by 5.9 % in 2012 compared to 3.2 % during 2011. The increase of 2.8 % was a result of increase production of crude oil from 28,325 kilo tonne of oil equivalent (ktoe) in 2011 to 29,115 ktoe in 2012. Accordingly, the final energy consumption in 2012 also increased at a higher pace of 7.5 % which reach 46,711 ktoe compared to 4.8 % in 2011. The highest energy demand was contributed by the transport sector which is 36.8 % followed by the industrial sector at 29.8 %, 16.0 % from the non-energy sector, the residential and commercial sectors at 15.1 % and 2.3 % from the agriculture sector. The total final energy consumption for petroleum products increased by 3.4 % in 2012 with the major increase coming from kerosene and fuel oil. The consumption of petroleum product is illustrated in Figure 1.1. Final consumption for kerosene increased by 100.1 % while final consumption for fuel oil increased by 85.5 %. Petrol and diesel continued to be the largest contributors to the total consumption for petroleum products with 36.2 % and 35.6 % respectively (Energy Commission, 2014).

Diesel engine which is one of the larger contributors to total consumption for petroleum has been used widely in many fields such as transportation, agriculture, marine, aircraft and industrial application. These facts make diesel engine the main contributor to total consumption for petroleum. It has several advantages compared to gasoline engines such as lower fuel consumption, lower carbon monoxide emissions (CO), better torque characteristics and higher reliability (Heywood, 1988). However, due to its lean-burning nature and high temperatures and pressures of the combustion process, diesel engine becomes main contributors to air pollutions as it produce large quantity of emissions, especially particulate matter (PM) and nitrogen oxides (NO<sub>x</sub>) (Heywood, 1988). Many research have been done to overcome this emission problem. For example, the research on fuel injection to influence the fuel sprays formation and improves fuel-air mixing in the combustion chamber (Agarwal et. al, 2015 and Herfatmanesh et. al, 2013). However, the trade-off trend between NO<sub>x</sub> and PM of diesel combustion is still not yet completely solved. One of the solutions focused by many researchers is by replacing diesel fuel with an alternative fuel. Many agree that this solution can solve the problem of diesel emission and also reduce the dependence on crude oil.

In this regard, biodiesel as an alternative fuels are becoming important increasingly due to environmental and energy concerns. The Ministry of Plantation Industries and Commodities of Malaysia (MPIC) has implemented B7 programme for the agriculture sector beginning November 2014. B7 involves the blending of 7 % of palm biodiesel with 93 % of petroleum diesel. The implementation of B7 program would consume 575,000 tonnes of biodiesel which contribute towards a savings of 667.6 million litres of diesel a year (MPIC, 2014). Biodiesel, which is considered to be a low-carbon clean fuel, can be blended with different proportions and directly used in diesel engine without modification. It has been found that engines fuelled with biodiesel run successfully for longer durations. The performance and emission characteristics are also quite comparable to that of petroleum based diesel fuel (Nantha Gopal et al., 2014).

Biodiesel is now mainly being produced primarily from food crops such as rapeseed, soy bean and palm oil. However, the use of edible oil to produce biodiesel in

many countries is not feasible in view of a big gap in the demand and supply of such oils for food consumption. In addition, use of edible and non-edible vegetable oil makes the process of production of biodiesel expensive. About 75-90 % of the total production cost for biodiesel comes from the cost of the feedstock (Talebian-Kiakalaieh et al., 2013). Therefore, inexpensive raw material is required to lower the cost of biodiesel. High potential of waste cooking oil (WCO) can be obtained all over the world. The production of large amount of WCO has increased due to the increasing food consumption. In addition, WCO also cause many disposal problems all around the world by polluting river water and choking of drainage. Thus, conversion of WCO into biodiesel may bring many benefits. The production of biodiesel from WCO is one of the better ways to utilize it efficiently and economically eliminating the disposal related problems (Nantha Gopal et al., 2014 and Can, 2014).

Research showed that diesel engine fuelled with WCO could decrease the emission produce in terms of smoke, particulate matter (PM), hydrocarbon, sulphur oxide and carbon monoxide (Lapuerta et al., 2008 and Lin et al., 2011). However, there are growing concerns in negative impact of PM emission from diesel engine on human health and the environment. Diesel vehicles contribute significantly to the particulate air pollution problem, especially in metropolitan areas of Asian developing countries (Jin et al., 2014). The size of the particle determines where it will deposit in the human respiratory tract when inhaled as shown in Figure 1.2. Report by Peng said that PM with size of 10 micrometre ( $PM_{10}$ ) can enter into the lungs causing health problems such as coughing, wheezing to asthma attacks and severe bronchitis to high blood pressure and heart attack. Similarly, smaller PM with size 2.5 micrometre and less ( $PM_{2.5}$ ) tends to penetrate deep into the lungs that will cause damage to the alveoli tissues which further results in cough and other severe respiratory problems for individuals with asthma or heart diseases. While extremely small particles with diameter less than 100 nm may pass through the lungs and affect other vital organs such as brain (Peng et al., 2008 and WHO, 2013).

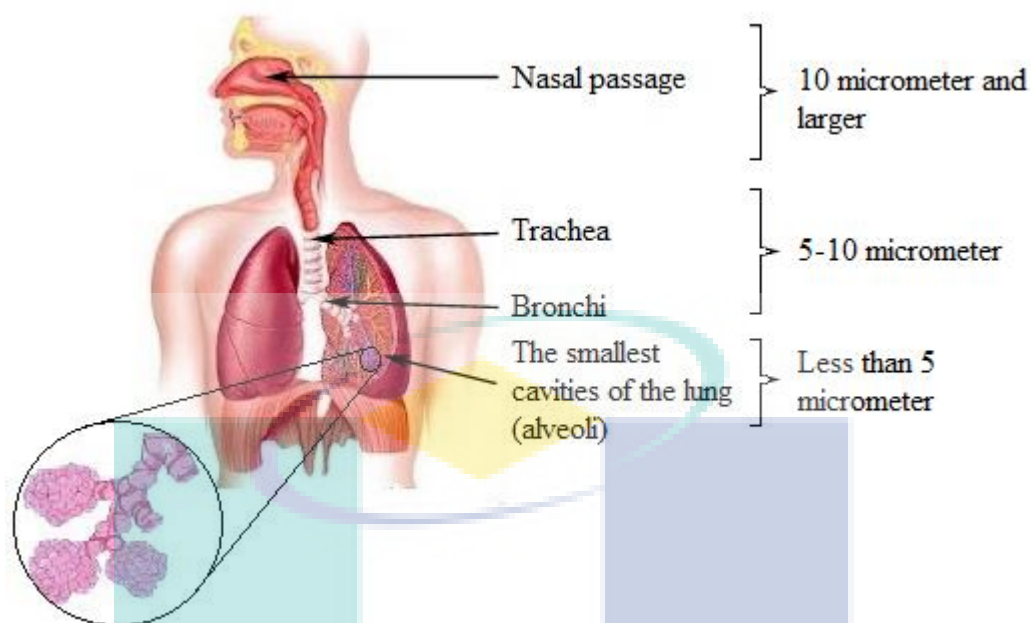


**Figure 1.2:** PM deposition in human respiratory tract

Source: Home Air Purifier Expert (2010)

## 1.2 PROBLEM STATEMENT

Global modernization from industrial era of the 18<sup>th</sup> century has caused global energy crisis. As the world population increased about 57% in the mid-17<sup>th</sup> century until now and expansion of industrial activities, the need for energy such as fossil fuel to accommodate demand is increasing rapidly. However, since fossil fuel is non-renewable energy, the decreasing of fossil fuel stock and increasing in price accelerate the urgency to find the fuel replacement. Since 2004, demand for diesel fuel has continued to rise, especially high demand from China, Europe and United States (EPA, 2012a). Another global concern arises together with the increasing demand of diesel fuel is the growing concern in diesel exhaust emission. The exhaust emission from diesel engine combustion such as CO, CO<sub>2</sub>, hydrocarbon (HC), NO<sub>x</sub> and PM are constituted substances that include in the list of hazardous air pollutants (HAPs) by the Environmental Protection Agency (EPA) (EPA, 2012b). In order to improve the air quality standards, regulations on emission from mobile source has become stringent

drastically in USA, Europe and Japan over the decade. The Kyoto Protocol, for example, has an emphasis on lowering the greenhouse gas emission especially CO<sub>2</sub> produced by burning fossil fuels. These stringent emissions standards have forced the automotive industries to improve the engine efficiency and reduce the amount of exhaust emission to fulfill the regulatory requirement.

To overcome this crucial problem researchers have developed biodiesel as an alternative or additives to standard diesel fuel that can be used in diesel engines with little or no modification needed. However, due to high production cost of biodiesel and issues of crop production for food supply, use of biodiesel has become an obstacle in evolving this alternative fuel. Therefore, WCO is one of the promising feedstock that can be converted to biodiesel with lower production cost at the same time providing a solution to its disposal problem. The study on biodiesel performance and exhaust emission has become a major focus among researchers over the world (Kumar et al., 2013; Chauhan et al., 2013; Can, 2014 and Öztürk, 2015). Yet, there is serious concern about the negative impact of exhaust emission from diesel engine especially PM emission on human health and the environment. Controlling the PM emission requires the development of more efficient diesel engine and improvement of the fuel. To achieve this, better understanding of chemical and physical of the diesel combustion process is needed. Therefore, in order to improve emission control and engine performance, it is necessary to understand the structure and the formation mechanism of PM. Understanding the component and size of PM are also important to estimate the effect of PM on human health and the environment.

This thesis has been motivated by interest in diesel aerosols from diesel engines combustions which are becoming one of the biggest contributors to overall PM emissions, and yet not well investigated. The study mainly focuses on characterization of PM component, number size distributions, morphology and overall mass concentrations of particulates emitted by diesel engines operated on the typical diesel engine as well as on potential WCO biodiesel. Other than that, gaseous emissions from the engine exhaust also have been discussed in this thesis. Although recent (2007-2015) on-road diesel engine implement some form of after-treatment system in the exhaust

and thus change the emission quality that comes out of the exhaust, this study will only focus on emission without after-treatment.

### **1.3 OBJECTIVES OF THE STUDY**

The overall objectives of this study is to understand the formation of the PM emission from diesel engine as it will be useful in order to meet more stringent emission regulation imposed by many nations currently and in the future. The specified objective of this study are:

- (i) To compare the engine exhaust PM emission of WCO biodiesel and diesel fuelled engine
- (ii) To analyze the influence of soluble organic fraction (SOF) and soot in particulate matter (PM) formation using various waste cooking (WCO) biodiesel blends.
- (iii) To study the PM characteristics and gaseous emissions from WCO biodiesel blends.

### **1.4 SCOPE OF THE STUDY**

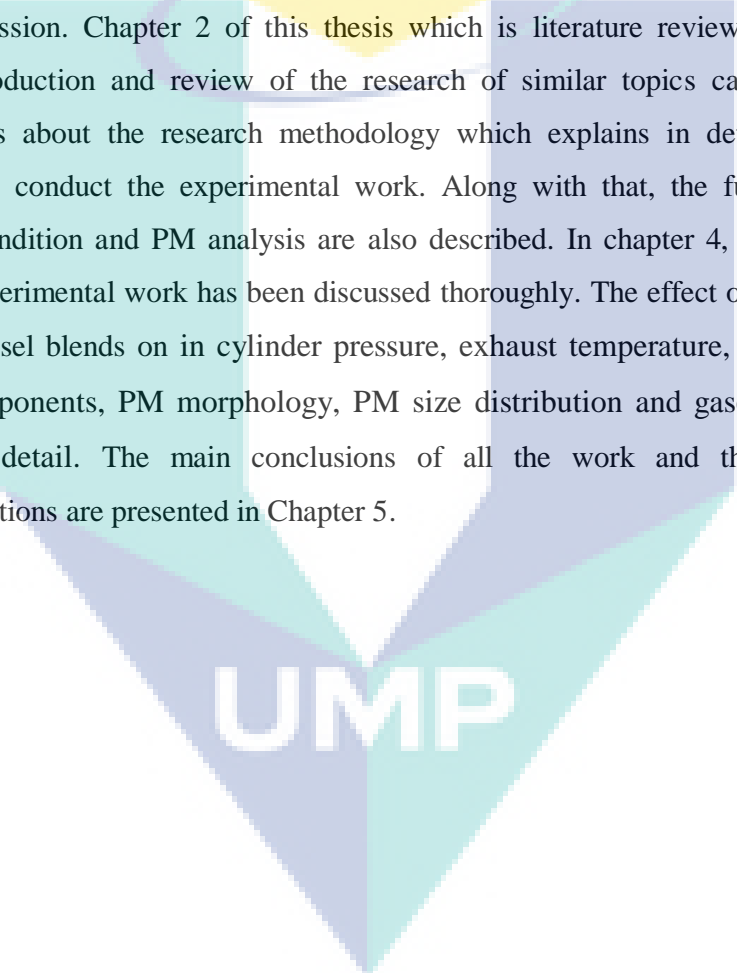
In order to achieve the objectives of this study, the research was carried out within the following scope:

- (i) An emission measuring equipment setup which includes gas analyzer for measure gaseous emission and PM sampling equipment.
- (ii) Data collection at engine speeds 1200 rpm, 1500 rpm, 1800 rpm, 2100 rpm and 2400 rpm with engine constant load of 20 Nm using five fuels, which is diesel fuel, WCO B5, WCO B10, WCO B20 and WCO B100.
- (iii) Determine in-cylinder pressure and peak pressure from the result obtain.
- (iv) Gravimetric analysis of PM to obtain mass concentration of PM and its component which is SOF and soot.
- (v) PM sample preparation for FE-SEM observation.

- (vi) PM image analysis to obtain PM diameter for characterization of PM with different fuels at different engine speeds.

## 1.5 OVERVIEW OF THE THESIS

This chapter has explained deliberately on the background research, problem statement, objectives and the scope of the study. The main focus is on the most critical problem caused by diesel engine which is related to exhaust emission such as PM as well as gaseous emission. Chapter 2 of this thesis which is literature review, intend to give a general introduction and review of the research of similar topics carried out globally. Chapter 3 is about the research methodology which explains in detail the equipment employed to conduct the experimental work. Along with that, the fuel properties, test operating condition and PM analysis are also described. In chapter 4, the result obtained from the experimental work has been discussed thoroughly. The effect of engine speed and WCO biodiesel blends on in cylinder pressure, exhaust temperature, PM concentration and its components, PM morphology, PM size distribution and gaseous emission are explain in detail. The main conclusions of all the work and the future research recommendations are presented in Chapter 5.

The logo of UMP (Universiti Malaysia Perlis) is a large, stylized letter 'V' shape. The left side of the 'V' is light blue, the right side is light green, and the bottom point is a darker blue. The letters 'UMP' are written in white, bold, sans-serif font across the center of the 'V'.

## CHAPTER 2

### LITERATURE REVIEW

#### 2.1 INTRODUCTION

This chapter covers some basic knowledge on the diesel engine and crucial issue on diesel engine exhaust emission which includes CO, CO<sub>2</sub>, NO<sub>x</sub>, nitric acid (NO) and PM. The exhaust emission of the diesel engine will be discussed in term of the formation, the effect on human health and comparison between diesel and biodiesel fuel. In detail, explanation on the formation mechanism of PM, their composition and structure, and current emission regulation over the world is also included in this chapter. Moreover, this chapter also discusses on the potential of WCO biodiesel that has the possibility to replace diesel fuel in order to improve the efficiency and reduce the emission of diesel engines.

#### 2.2 DIESEL ENGINE COMBUSTION

Diesel engine operates according to the principle of internal combustion engine and can be operated as a four-stroke cycle engine. A cylinder needs two revolutions of the crankshaft to complete a working cycle in this principle. One complete working cycle consists of the intake stroke, compression stroke, power or working stroke and exhaust stroke. The movement of the piston from the point of the topmost displacement or top dead center (TDC) to the point of the lowest displacement or bottom dead center (BDC) and backward is denoted as one complete cycle. Figure 2.1 shows four stroke cycle diesel engines. At the intake stroke, the valve opens and air is sucked into the cylinder as the piston is moving downward. Then, the piston moves back up as the

valves are closed compressing the air in the cylinder. The temperature of the compressed air reaches about  $700 - 800^{\circ}\text{C}$  (Heywood, 1988). As the piston reaches the top, fuel is injected into the cylinder. The injected fuel drops mix with air, evaporate and ignite by high temperature. The piston moves back downwards in the power stroke due to increase of pressure caused by the combustion and performs mechanical work which is transferred to the crankshaft. The piston moves back to the top at exhaust stroke due to excess pressure as a consequence of opening the outlet valve and pushing the exhaust out of the cylinder. Each stroke in the cycle completes at TDC or BDC.

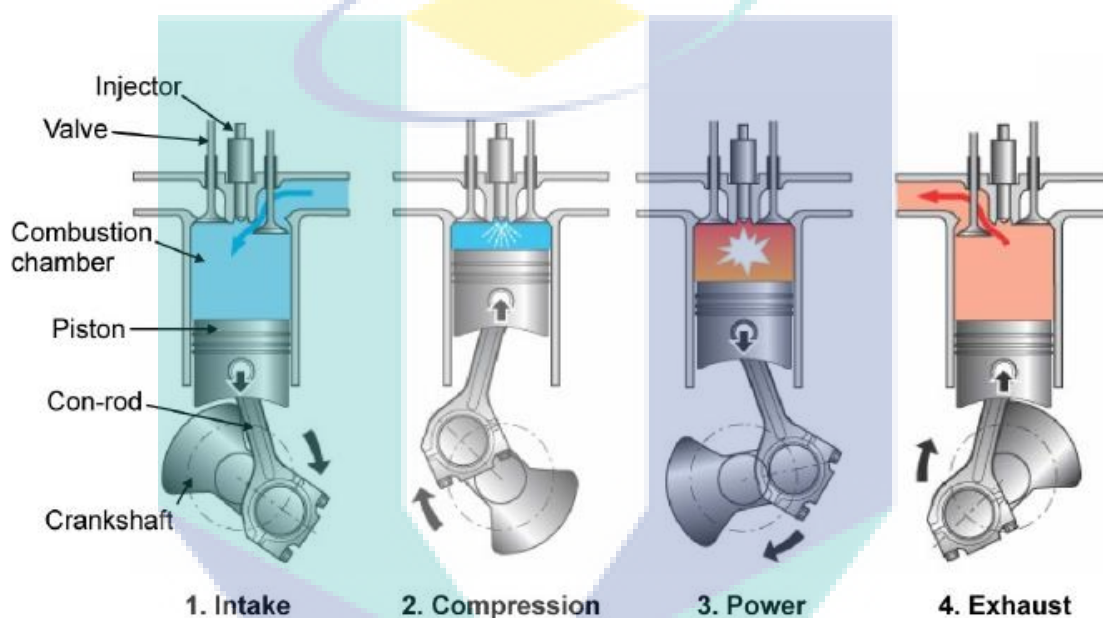


**Figure 2.1:** Four stroke cycle of diesel engine

Source: Mačković (2012)

Both physical and chemical processes are involved in the various phases of diesel operating cycle. Figure 2.2 shows the typical diesel combustion phases of a four-stroke cycle of diesel engines. The events during diesel combustion period can be categorized into four distinct phases as shown in Figure 2.2 (Heywood, 1988):

- 1: Ignition delay period.
- 2: Combustion phase I- premixed combustion phase.
- 3: Combustion phase II-mixing controlled phase.

## 4: Combustion phase III-late combustion.

The combustion process starts with the compression of air. Fuel injection occurs at the start of injection (SOI), as the fuel enters the engine cylinder it firstly evaporates and then mixes with the combustion air. The mixture is compressed and its pressure and temperature increase until the fuel's ignition point is reached and ignition occurs at the start of combustion (SOC). The period from SOI and SOC is known as the ignition delay period. During this period some particular processes occurs which is atomization, vaporization and mixture formation (Heywood, 1988).

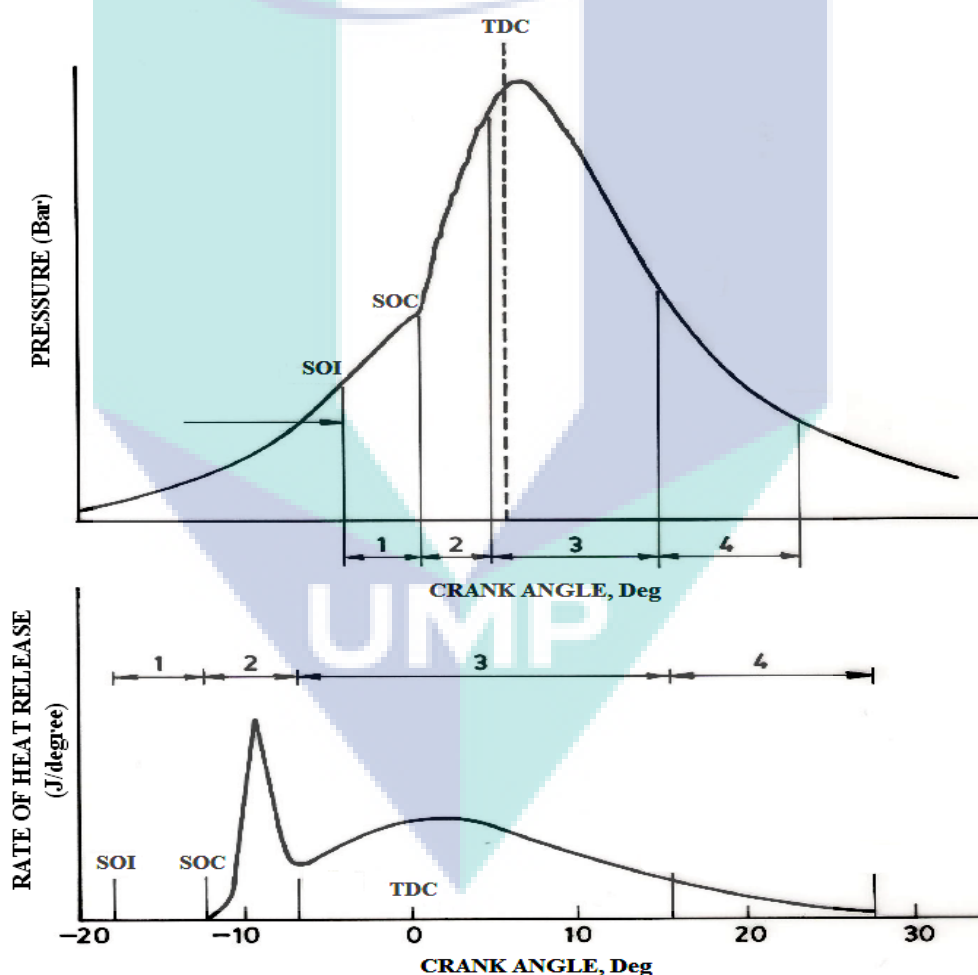


**Figure 2.2:** Pressure-time diagram and rate of heat release of diesel combustion process.

Source: Heywood (1988)

The first phase of combustion is the period of premixed combustion in which the rate of pressure rise increases continuously and rapidly before TDC to acquire its peak value. In this phase, the fuel accumulated during the ignition delay period forms a combustible mixture and is continuously burnt. This is also called the period of rapid combustion. Once the combustible mixture formed out of the fuel accumulated during the ignition delay period and that received during the first combustion phase is exhausted, the second phase of combustion begins which lasts a little longer. During the second phase, further burning of fuel is controlled by the rate at which combustible mixture becomes available. The rate of burning now depends upon the rate of fuel injection during this phase and the rate of formation of the combustible mixture and therefore, is called mixing controlled combustion. With the combustion process happening, it extends into the expansion stroke (late combustion phase). The burned products along with those unburned are then discharged into the after-treatment system, before being emitted to the atmosphere (Heywood, 1988).

### **2.3 EXHAUST EMISSION FROM DIESEL ENGINE**

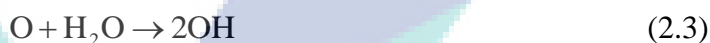
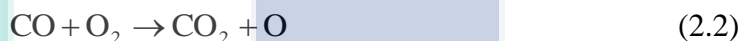
Although diesel engine provides better fuel efficiency than gasoline engine, diesel engine has a higher exhaust emission which has damaging effects upon the environment and human beings. Emissions from diesel engine are formed as a result of burning the heterogenous air/fuel mixture. Diesel engine emissions are composed of gaseous pollutants and particulate matter (PM). The emissions produce depend on the prevailing conditions not only during combustion, but also during the expansion and especially prior to the exhaust valve opening. Mixture preparation during the ignition delay, fuel ignition quality, residence time at different combustion temperatures, expansion duration, and general engine design features play a very important role in emission formation. In essence, the concentration of the different emission species in the exhaust is the result of their formation, and their reduction in the exhaust system. Incomplete combustion products formed in the early stages of combustion may be oxidized later during the expansion stroke. The exhaust emission components from diesel engine that discussed here are CO, NO<sub>x</sub>, O<sub>2</sub>, CO<sub>2</sub> and PM. In addition, the emission of diesel engine fuelled with biodiesel was compared with the conventional diesel fuel (Heywood, 1988).

### 2.3.1 Carbon Monoxide (CO)

CO is a colorless, odorless, poisonous, tasteless and non-irritant gas that is slightly less dense than air and is sparingly soluble in water. CO is one of the intermediate compounds formed by incomplete combustion of the fuel in an engine due to local areas with insufficient air supply. The formation of CO depends on the air fuel equivalence ratio, fuel type, combustion chamber design, starting of injection timing, injection pressure and speed. Oxidation reactions of hydrocarbon molecules lead to the formation of CO as shown below (Bowman, 1975):



RH represents a hydrocarbon with R as the hydrocarbon radical. Once the CO is formed, it's oxidized to CO<sub>2</sub> through the following steps:



As reaction 2.2 is slow, the primary oxidation of CO occurs through reaction 2.4. This reaction occurs when sufficient oxygen is available. On the other hand, reaction 2.5 is continuously produced hydroxyl radicals (OH) which is one of the principal oxidizing species and converts CO to CO<sub>2</sub>.

Even though CO emissions from compression ignition engines are normally low, they can be significantly higher at low loads or when idling. On this condition, the fuel air mixture is often over rich and the temperature is relatively low which results in incomplete combustion. In the upper atmosphere, CO reacts with ozone O<sub>3</sub> producing

CO<sub>2</sub>. This reaction contributed to the ozone layer depletion of the upper atmosphere. The ozone layer screens harmful sun rays from reaching the Earth's surface. Emission of CO can be lowered by using biodiesel in diesel engine (EPA, 2002a). According to most literature, it is a common trend that CO emission was reduced in diesel engine fuelled with biodiesel. Research done by Ozsezen et al. (2009) stated that CO emission was decreased by 9.52 % with use of the waste palm oil methyl ester and decreased by 67.65 % with the use of the canola oil methyl ester compared to diesel fuel. Recent study by Nantha et al. (2014) also showed the emission of CO from waste cooking methyl ester (WCME) blends are lower than diesel fuel. The reduction of CO emission of WCME20, WCME40, WCME80, and WCME100 are 59 %, 38 %, 35 %, and 31 % respectively, lesser than diesel fuel. This is due to the oxygen content in biodiesel, which allows more carbon molecules to oxidize when compared with diesel fuel.

However, some author has reported the significant increase in CO emissions by pure biodiesel. Lujan et al. (2009) has conducted the research on emission of diesel engine fuelled with biodiesel blends during the European MVEG-A cycle. CO emissions are reduced with the addition of moderate amounts of biodiesel on the fuel blend. However, important increases in biodiesel content invert the trend increasing these emissions where B50 and B100 showed an increment with 5.2 % and 9 % respectively. The reason for the increment of CO emission is that an increase in the lower heating power of biodiesel would improve CO and HC emission results.

### **2.3.2 Carbon Dioxide (CO<sub>2</sub>)**

One of the major greenhouse gases and normal product of combustion is CO<sub>2</sub>. Ideally, combustion of hydrocarbon fuel should produce only CO<sub>2</sub> and water (H<sub>2</sub>O). The relative proportion of these two depends on the carbon-to-hydrogen ratio of the fuel, about 1:1.75 for ordinary diesel fuel. Thus, CO<sub>2</sub> emission can be reduced by reducing the fuel's carbon content per unit energy, or by improving the fuel efficiency of the engine. The concentrations of global atmospheric CO<sub>2</sub> has been increased approximately 40 % since the Industrial Revolution. The combustion of fossil fuels is the largest source of CO<sub>2</sub> emissions, accounting for about 94.2 % of total U.S. CO<sub>2</sub> emissions and 82.5 % of total U.S. greenhouse gas emissions in 2012 (EPA, 2014).

Greenhouse gases absorb energy, slowing or preventing the loss of heat to space, hence, increasing the global temperature. Increasing global temperature may cause sea levels to rise, worsen the intensity of extreme weather events. The most effective way to reduce CO<sub>2</sub> emissions is to reduce diesel fuel consumption by blending or replace it with biodiesel.

Research by Gomez et al. (2000) showed that CO<sub>2</sub> was reduced approximately 7.5 % by waste cooking oil methyl ester compared to diesel fuel. In addition, Dorado et al. (2003) investigated the exhaust emission of diesel engine fuelled with waste olive oil methyl ester and found a significant reduction in CO<sub>2</sub> up to 8.6 % by olive oil methyl ester compared to diesel fuel. However, a study by Ulusoy and Tekin (2004) showed that the CO<sub>2</sub> emission of biodiesel from used frying oil was 5.03 % higher than diesel fuel. Similar results were shown by Usta et al. (2005) where the emission of CO<sub>2</sub> is increased by using biodiesel produce from hazelnut soapstock and waste sunflower oil mixture compared with diesel fuel.

### **2.3.3 Oxygen (O<sub>2</sub>)**

Emission of O<sub>2</sub> from diesel engine is not enacted in legislation. However, it is useful to be able to measure its concentration in the raw exhaust from diesel engine since it provides a review on other engine parameters. O<sub>2</sub> emissions are oxygen particles released into an exhaust system. O<sub>2</sub> release is required for an engine to work properly, as it supports the combustion process that makes an engine run. If the amount of O<sub>2</sub> is too much, it shows there is not enough fuel and will cause stress on the engine, which will result in damage to the engine. However, too little amount of O<sub>2</sub> means there is too much fuel saturating the engine's cylinders, which will result in bad fuel efficiency and possible loss of horsepower (Puhan et al., 2013).

### **2.3.4 Nitrogen oxides (NO<sub>x</sub>)**

The emission of NO<sub>x</sub> from diesel engines is a collection of nitric oxide (NO) and nitrogen dioxide (NO<sub>2</sub>). NO generally is the major component which contributes to 90 % of NO<sub>x</sub> (Benajes et al., 2014). The formation of NO can take place during both

the premixed and diffusion phases. The major part of NO from the diesel combustion is formed by the oxidation of atmospheric nitrogen ( $N_2$ ) via the extended Zeldovich mechanism (or thermal NO) (Heywood, 1988) that can be explained as follows:



This formation of NO is highly dependent on temperature reached during combustion due to large activation energies for the forward reaction 2.6 and the reverse reactions in 2.7 and 2.8. It is initiated at temperatures greater than 1900 K and the NO stays around during cooling since the reaction 2.7 and 2.8 is very slow. Therefore, high temperature and high oxygen concentrations result in high NO formation. Thermal NO formation is attributed to reaction 2.6 through reaction 2.8 is considered to be formed in the post combustion exhaust gas. The conversion of NO to  $NO_2$  in the flame zone considered as the final reaction mechanism of NOx formation and can be shown as follows:



Through the reaction 2.9, the hydroperoxyl ( $HO_2$ ) radicals form in the low temperature regions leading to  $NO_2$  formation. However,  $NO_2$  destruction can proceed via the reaction 2.10 and reaction 2.11 with active H and O radicals at high temperatures. Thus, during high temperatures, the majority of the NOx emitted from internal combustion engines is in the form of NO. According Flynn et al. (1999), two-thirds of the total NOx emissions are formed in the diffusion flame while one-third is

formed in the hot post-combustion gas regions. Chemical equilibrium considerations indicate that at typical flame temperatures, the  $\text{NO}_2/\text{NO}$  ratio should be negligibly small which is true for spark ignition (SI) engines. However, in compression ignition (CI) engines,  $\text{NO}_2$  can contribute 10 to 30 % of the total  $\text{NO}_x$  emissions because the back reaction from  $\text{NO}_2$  formed in the flame to  $\text{NO}$  (2.11) is quenched by mixing with cooler regions especially at light load (Heywood, 1988).

$\text{NO}_x$  leads to acid rain and contribute to unhealthy ground-level ozone and smog, often leading to severe respiratory problems among affected communities. Diesel engines produce unacceptably high levels of  $\text{NO}_x$  at high loads, and  $\text{NO}_x$  from non-road diesel engines represents an increasing percentage of the environmental pollution. The real challenge in designing modern diesel engines involves a trade-off between  $\text{NO}_x$  and PM emissions. Most engine modifications that decrease  $\text{NO}_x$  have a tendency to increase PM. Conversely, techniques to reduce PM tend to increase the production of  $\text{NO}_x$ . Both PM and  $\text{NO}_x$  are linked by combustion temperatures. With the increment of temperatures PM will decrease, but  $\text{NO}_x$  will increase and vice versa. Therefore, control strategies are primarily concerned with optimizing the control of these two constituents, either during combustion or after (Chryssakis et al., 2006).

### 2.3.5 Particulate Matter (PM)

PM consists of primary particles, whose diameters are between 20-50 nm and their sizes depend on the numbers of these spherules, which may vary from several to several thousands. Diesel particulates are mainly composed of three components which are soot, soluble organic fraction (SOF) and inorganic fraction. Soot originates from the carbon in the diesel fuels and generates in the combustion environment where the temperature and pressure can reach up to 2800 K and 100 Bar. Through the soot's surface growth, agglomeration as well as oxidation at the same time, the particulates form eventually after a final adsorption and condensation of hydrocarbons (Kittelson, 1998). The formation of PM, its composition and structure will be discussed in detail in section 2.5.

## 2.4 HEALTH EFFECT OF DIESEL ENGINE EMISSION

Diesel exhaust emission in term of gaseous and PM contains toxic air contaminants that can affect human health and the environment. NO<sub>x</sub> emissions from diesel engine are responsible for a large amount of environmental and health hazard. It becomes considerable problems in most major cities worldwide where NO<sub>x</sub> emission contributes acidification, the formation of ozone, nutrient enrichment, and smog formation (Grewe et al., 2012). NO and NO<sub>2</sub> are considered as toxic, however, NO<sub>2</sub> levels of toxicity are five times greater than that of NO. NO<sub>2</sub> can irritate the lungs and produce pulmonary edema and fatality if inhaled at high concentrations. Cough, hemoptysis, dyspnea, and chest pain can also be caused even when exposed to moderate levels of 50 ppm. NO<sub>2</sub> and airborne nitrate also contribute to pollutant haze, which impairs visibility (Hoeft et al., 2012)

Besides NO<sub>x</sub> emission, the acute toxicity of CO also has long been recognized and is well documented. Inhaled CO into the human body can block the delivery of oxygen and cause cellular hypoxia. CO is absorbed via the lungs into the bloodstream, where it replaces oxygen by attached chemically to hemoglobin forming carboxyhemoglobin. This reduces the oxygen carrying capacity of the blood. In addition the dissociation of oxyhemoglobin is also affected so that the supply of oxygen to tissues is further reduced. Thus, the human organs with the highest oxygen requirement such as the brain and heart can be affected more significantly, resulting in impaired of judgement, headaches, dizziness and confusion The cardiovascular and nervous systems can also be affected by long term exposure to low levels of CO (Kampa and Castanas, 2008)

On the other hand, emission of PM can cause a wide range of damage to surfaces and materials. If the particle is corrosive or has other pollutants, for example, sulphur dioxide attached to it, then it may also react with or corrode the surface or material. Health effects of PM under normal conditions of human respiratory which is in good health is able to deal with inhaled particles without undue stress or long-term effects. In sensitive individuals, or when high levels of particles are present, the PM may contribute to increased rates of respiratory illnesses and symptoms. Studies

indicate that such adverse effects are dependent on a number of factors, including: particle size, the intensity of the exposure, the chemical nature of the particles and their interaction with human tissue, the presence or absence of pre-existing conditions and meteorological factors such as winds, humidity, a temperature inversion, rain or thunderstorms. Environmental Protection Agency (EPA) is concerned about particles that are 10 micrometers in diameter or smaller because those are the particles that generally pass through the throat and nose and enter the lungs. There have been extensive studies into the health effects of different levels of particles and pollution mixes (Baccarelli et al., 2008).

PM<sub>10</sub> and PM<sub>2.5</sub> include inhalable particles that are small enough to penetrate the thoracic region of the respiratory system. The health effects of inhalable PM are well documented. They are due to exposure over both the short term (hours, days) and long term (months, years) and include respiratory and cardiovascular morbidity, such as aggravation of asthma, respiratory symptoms and an increase in hospital admissions also mortality from cardiovascular and respiratory diseases and from lung cancer. There is good evidence of the effects of short-term exposure to PM<sub>10</sub> on respiratory health, but for mortality, and especially as a consequence of long-term exposure, PM<sub>2.5</sub> is a stronger risk factor than the coarse part of PM<sub>10</sub>. All-cause daily mortality is estimated to increase by 0.2–0.6 % per 10 µg/m<sup>3</sup> of PM<sub>10</sub> (WHO, 2006 and Samoli E et al., 2008). Long-term exposure to PM<sub>2.5</sub> is associated with an increase in the long-term risk of cardiopulmonary mortality by 6–13% per 10 µg/m<sup>3</sup> of PM<sub>2.5</sub> (Beelen et al., 2008 and Pope III et al., 2002). Susceptible groups with pre-existing lung or heart disease, as well as elderly people and children, are particularly vulnerable. For example, exposure to PM affects lung development in children, including reversible deficits in lung function as well as chronically reduced lung growth rate and a deficit in long-term lung function (WHO, 2010). There is no evidence of a safe level of exposure or a threshold below which no adverse health effects occur. The exposure is universal and involuntary, increasing the significance of this determinant of health.

At present, there is not enough evidence to identify differences in the effects of particles with different chemical compositions or emanating from various sources (Stanek et al., 2011). It should be noted, however, that the evidence for the hazardous

nature of combustion-related PM (from both mobile and stationary sources) is more consistent than that for PM from other sources (WHO, 2007). The black carbon part of PM<sub>2.5</sub>, which results from incomplete combustion, has attracted the attention of the air quality community owing to the evidence for its contribution to harmful effects on health as well as on climate. Many components of PM attached to black carbon are currently seen as responsible for health effects, for instance organics such as Polycyclic aromatic hydrocarbons (PAHs) that are known carcinogens and directly toxic to the cells. Recently, the exhaust from diesel engines (consisting mostly of particles) was classified by the International Agency for Research on Cancer as carcinogenic to humans (IARC, 2012).

The component of PM which is SOF also brings harmful effect which it contains most of the PAHs and Nitro-PAHs emitted with diesel exhaust emissions. PAHs are carcinogens that are linked to heart diseases and respiratory disease. PAHs are made up of one to seven fused aromatic rings joined in various cluster forms. PAHs are under close observation by the EPA. They classify PAHs as an air toxin or polycyclic organic matter (POM). This is a class that is defined by having one or more benzene rings and a boiling point of 100°C and higher. Seven major POMs are classified as a major human carcinogen and include benz(a)anthracene, benzo(b)fluoranthene, benzo(k)fluoranthene, benzo(a)pyrene, chrysene, 7,12-dimethylbenz(a)anthracene, and indeno(1,2,3-cd)pyrene which all are found in SOF (Lee and Vu, 2010).

## **2.5 WORLDWIDE EMISSION REGULATION**

The diesel engine emission has been extensively discussed over the world. Concerning the diesel tailpipe emission regulations, they are categorized into three applications: light duty, on-road heavy duty and non-road heavy duty (Johnson, 2006). The first emission legislation was established in California in 1959 and followed by the first federal standard in 1966. Japan enacted similar regulation in 1996 while Europe in 1970 (Eastwood, 2008). U.S EPA has set diesel engine emission regulation for over forty years. This regulation governed primarily on highway engines in trucks and buses.

In 1971, EPA established the first PM National Ambient Air Quality Standard (NAAQS). The original PM standard was total suspended particulate (TSP). This standard was replaced in 1987 with PM less than 10  $\mu\text{m}$  in aerodynamic diameter ( $\text{PM}_{10}$ ) and specified an annual average concentration of  $50 \text{ mg/m}^3$  and a 24-h maximum of  $150 \text{ mg/m}^3$ , based on the highest value over 3-year period. In 1997, after reviewing scientific studies, the EPA concluded that particles with aerodynamic diameter less than  $2.5 \mu\text{m}$  ( $\text{PM}_{2.5}$ ) had a greater association with mortality and morbidity rates than  $\text{PM}_{10}$ . On this basis, the EPA established an annual  $\text{PM}_{2.5}$  standard level of  $15 \text{ mg/m}^3$ , and a 24-h  $\text{PM}_{2.5}$  standard level of  $35 \text{ mg/m}^3$ . Also, the EPA established the pollutant standard index (PSI) as an air pollution alert system to communicate to the general public information about the health risks of PM and other pollutants.

In 1998 EPA had brought non-road engines under the scope of regulation (EPA, 1988). The emission regulation for the off-highway scope includes farm and construction equipment, other mobile power sources like boats and locomotives, as well as stationary power sources. In July 2009, the European Union (EU) published its final Euro VI regulation for on-road heavy duty vehicles and set the limits to  $400 \text{ mg/kW-hr}$  for  $\text{NO}_x$  and  $10 \text{ mg/kW-hr}$  for PM on the European Transient and European Steady State Cycles (Johnson 2010). For light duty passenger cars and commercial vehicles, the limit for PM was set to  $5 \text{ mg/km}$ , both in Euro V and Euro VI. Currently, EPA is making revision on new PM pollution rules that will reportedly lower the exposure standard for  $\text{PM}_{2.5}$  and the final rule is effective on March 18, 2013. With regard to primary (health-based) standards for fine particles the EPA is revising the annual  $\text{PM}_{2.5}$  standard by lowering the level to  $12.0 \text{ mg/m}^3$  to provide increased protection against health effects associated with long and short-term exposures and to retain the 24-hour  $\text{PM}_{2.5}$  standard at a level of  $35 \text{ mg/m}^3$ .

Most of Asian countries also have adopted the  $\text{PM}_{10}$  standard in differing degree while more is needed in the development of a  $\text{PM}_{2.5}$  standard. Several Asian countries' have more lenient  $\text{PM}_{10}$  and  $\text{PM}_{2.5}$  standards when compared with EU air quality standards (EU AQS), World Health Organization (WHO), Air Quality Guidelines, EPA and NAAQS. Table 1 shows the summary of the PM standards in some Asian countries compared with EPA, EU NAAQS and WHO. China: Grade I is applies to specially

protected areas, such as natural conservation areas, scenic spots, and historical sites while China: Grade II applied to residential areas, mixed commercial/residential areas, cultural, industrial, and rural areas and China: Grade III applied to special industrial areas.

**Table 2.1:** PM (TSP, PM<sub>10</sub>, PM<sub>2.5</sub>) Standards in selected Asian countries ( $\mu\text{g}/\text{m}^3$ )

<b>Countries/ Organization standards</b>	<b>TSP 24-h</b>	<b>TSP annual</b>	<b>PM<sub>10</sub> 24-h</b>	<b>PM<sub>10</sub> annual</b>	<b>PM<sub>2.5</sub> 24-h</b>	<b>PM<sub>2.5</sub> annual</b>
EPA			150	50	35	12
EU			50	40	-	25
WHO			50	20	25	10
China: Grade I	120	80	50	40	-	-
China: Grade II	300	200	150	100	-	-
China: Grade III	500	300	250	150	-	-
Indonesia	230	90	150	-	-	-
Singapore	-	-	100	50	-	-
Republic of Korea	-	-	100	50	-	-
Malaysia	260	90	150	50	-	-

Source: CAI-Asia (2010)

The regulations, mostly in the form of statutory limits, have been tightened in a progressive way and that compels industry to develop its emission control technology accordingly. The manufacturers must have approval on their vehicles for this emissions compliance, when the vehicles are run on dynamometers over different standardized drive cycles based on their type and the emissions measured.

## 2.6 PARTICULATE MATTER

By definition, PM is a complex mixture of extremely small solids and liquid droplets found in the air. It is made up of a number of components, including acids (such as nitrates and sulfates), organic chemicals, metals, and soil or dust particles. Diesel particulates are sometimes referred to as fine particles (Heywood, 1988). Their sizes vary from several nanometers to several hundred microns (EPA, 2008). EPA

defines the particulate matter as any substance other than water that is collected by filtration of the diluted exhaust gases at or below 325 K (EPA, 2008).

### 2.6.1 Particulate Matter Composition and Structure

Diesel PM has two main components which are soot or solid carbon material and volatile or soluble organic compound commonly described as a soluble organic fraction (SOF). According to the conceptual model by Peter (Eastwood, 2008) PM can be divided into non-volatile/non-soluble, which are mainly generated in the engine, and volatile/soluble which form later in the exhaust. Figure 2.3 showed the schematic structure of PM for engines. Generally, soot is high agglomerated solid carbonaceous material and ash. Its typical chemical formulae are  $C_8H$ ,  $C_9H$  and  $C_{10}H$ . About 5 to 10 % by mass oxygen and 0.5 % nitrogen are also present. Typical empirical formula of soot is  $CH_{0.11}O_{0.065}N_{0.005}$ . When examined under electron microscope, soot appears as necklace-like agglomerates composed of a selection of small, basic particles with nearly spherical structure. Individual diesel soot particulates vary in shape from clusters of spherules to chains of spherules, where a soot cluster may contain as many as 4000 spherules. The size of spherules varies in diameter from 10 to 80 nm, but mostly lies between 15 and 30 nm. The spherules are called primary soot particles and the cluster or chain-like soot aggregates are defined as secondary particles, composed of tens to hundreds of primary spherical particles (Naydenova, 2007).

On the other hand, SOF which can be extracted by solvent like dichloromethane originates from the fuel and oil hydrocarbons. It comes from a tiny fraction of the fuel, which atomized and evaporated lube oil that escape oxidation and appear in the exhaust. Diesel lube contains hydrocarbons that range from  $C_{18}$  to  $C_{36}$  whereas diesel fuel contains hydrocarbons from  $C_{12}$  to  $C_{20}$ . The SOF contains polycyclic aromatic compounds containing oxygen, nitrogen and sulphur (Farrar-Khan et al., 1992). Most of the sulphur in the fuel is oxidized to sulphur dioxide ( $SO_2$ ), but a small fraction is oxidized to sulphur trioxide ( $SO_3$ ) that leads to sulphuric acid ( $H_2SO_4$ ) and sulfates ( $SO_4^{2-}$ ) in the exhaust particles. In addition to SOF, sulfates originating from fuel sulphur, nitrogen dioxide and water are also absorbed in the particle core formed by soot. Typically, SOF has an empirical formula  $CH_{1.65}O_{0.1}N_{0.007}$ . The mass content of

SOF varies significantly depending upon engine design and operating conditions, but mostly it is in the range from 20 % to 45 %. SOF values are highest at light engine loads when the exhaust temperature is low.

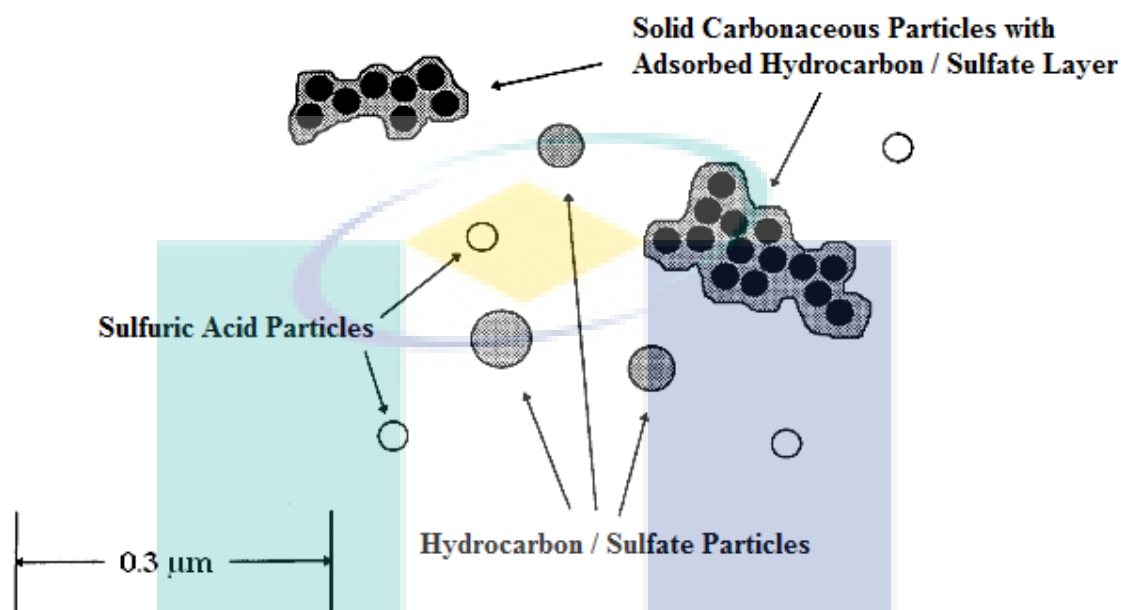


**Figure 2.3:** Structure and composition of engines particulate matter

Source: Kittelson (1998)

PM is divided by most authors into three distinct types which are nucleation mode (3-30 nm), accumulation mode (20-500 nm), and coarse mode (>500 nm). A typical size distribution of diesel exhaust PM is shown in Figure 2.4. The distribution shows in the figure are trimodal, lognormal in form. It's usually presented using either particle mass or particle number distribution. In mass distributions, the majority of the particulate mass is found in the accumulation mode. In number distributions, on the other hand, most particles are found in the nuclei mode. In other words, diesel particulate matter is composed of numerous small particles holding very little mass, mixed with relatively few larger particles which contain most of the total mass.

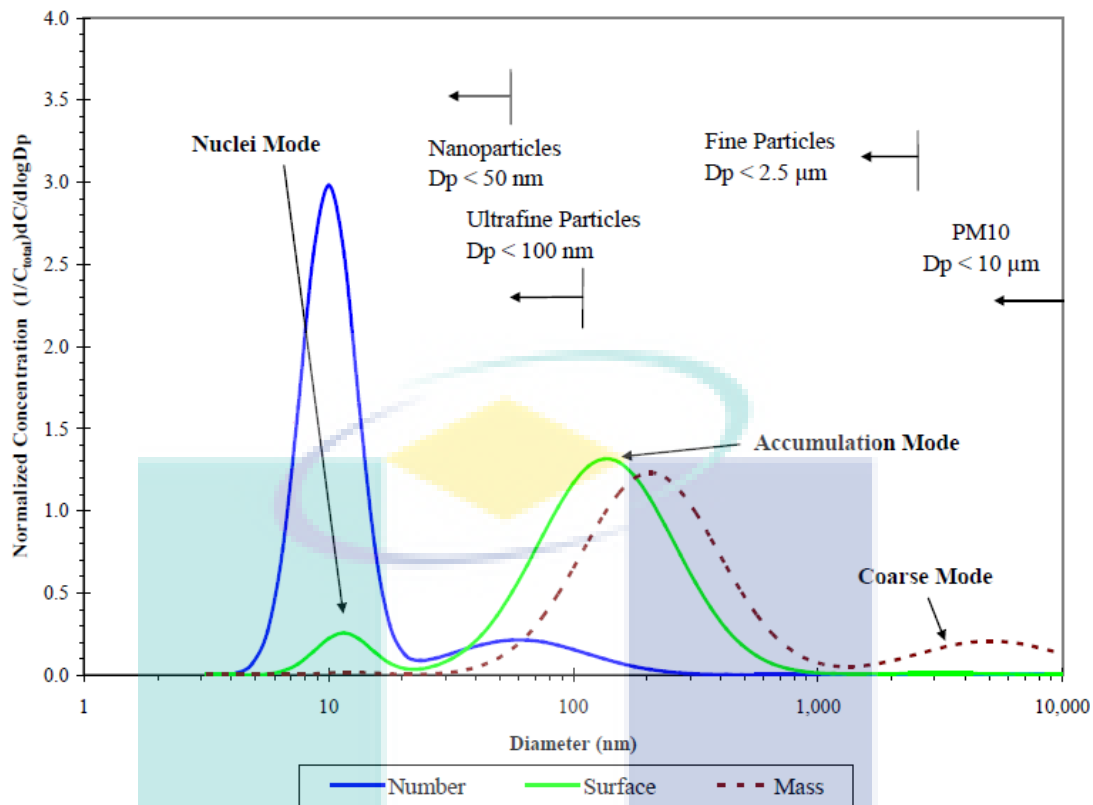


**Figure 2.4:** Typical particle size and distribution from diesel engines

Source: Kittelson and Kraft (2014)

According to various definitions, the diameters of nuclei mode particles are generally less than 40-50 nm. Based on particle size research in the 1990's technology heavy-duty diesel engines, it has been postulated that the nuclei mode extends through sizes from 3 to 30 nm (Kittelson et al., 2002). The size ranges place nuclei mode particles entirely within the nano size particle range. The maximum concentration of nuclei mode particles occurs at 10-20 nm. The nuclei mode, depending on the engine technology and particle sampling technique, typically contains only 1-20 % of the total PM mass, and more than 90 % of the total particle number (Kittelson, 1998). Sometimes the nuclei mode particles present as much as 99 % of the total PM number. Nuclei mode particles are composed mostly of volatile organic and sulphur compound that form during exhaust dilution cooling. Nuclei mode also contains solid carbon and metal compounds. This mode is relatively less studied because of their obscure and irreproducible nature.

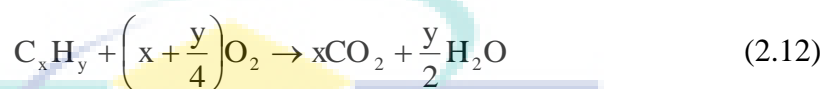
The accumulation mode where most of the particle mass exists is made of sub-micron particles of diameter ranging from 30 nm to 50 nm (Kittelson et al., 2002). As shown in Figure 2.4, accumulation mode extends through the fine, ultrafine, and the upper end of the nano size particles range. Accumulation mode particles are made of solids (carbon, metallic ash) intermixed with condensates and adsorbed material (heavy hydrocarbons, sulphur species). This is where the carbonaceous agglomerates and associated adsorbed materials reside. For the past few years, attention has been mainly drawn on the accumulation mode particles where it consists of primary particles or spherules (Heywood, 1988). The spherules diameter is around 20-50 nm and the size of the particles are determined by their numbers. The coarse mode is particles with aerodynamic diameter above 1000 nm contain 5-20 % of the particle mass. Practically this mode has no contribution to particle number (Kittelson et al., 2002). The coarse particles are not generated in the diesel combustion process. The particle mainly composed of accumulation and nuclei mode that have been deposited on cylinder and exhaust system surfaces and later re entrained. These coarse particles can easily be stored and released in the exhaust system. This inconsistencies behavior makes the coarse particles unpredictable and thus less studied (Eastwood, 2008).

Figure 2.4 shows the atmospheric PM. Many authors categorized the particles into four categories which were  $PM_{10}$  with diameter smaller than 10  $\mu\text{m}$ , fine particles which also known as  $PM_{2.5}$  with the diameter of smaller than 2.5  $\mu\text{m}$ , ultrafine particles with diameter smaller than 100 nm and nano particles which has a diameter smaller than 50 nm. The allocation is according to the aerodynamic diameter, which defined as the diameter of a 1  $\text{g}/\text{cm}^3$  density sphere of the same settling velocity in air as the measured particle.  $PM_{10}$  and  $PM_{2.5}$  are actually defined by standard sampling systems in which the sampling probability falls to 50 % of the designated aerodynamic diameter. An exact definition of ultrafine and nano particles have not been agreed upon. Nearly, all of the particles emitted by a diesel engine are nano particles (Kittelson et al., 2002).

## 2.6.2 Mechanism of Particulate Matter Formation

Soot formation is a complex process, which involves many chemical and physical phases. A detailed kinetic model of soot formation usually comprises of two

general parts which are gas-phase chemistry, initiating the soot precursors, and particulate-phase model which is the least explored area in soot formation theory. In a diesel engine, soot can be produced as a result of the pyrolysis of liquid fuel and by accumulation of oxygen depleted fuel vapor. Generally, the soot is formed in the fuel-rich region where the lack of oxygen prevents complete combustion of fuel. For a stoichiometric composition, the combustion reaction is (Frenklach, 2002):



Under these ideal combustion conditions, hydrocarbons combine with oxygen molecules to produce CO<sub>2</sub> and water. Although the total oxygen content within the combustion chamber of a diesel engine may be sufficient to produce a stoichiometric composition, localized oxygen depleted regions exist. These regions are usually caused by insufficient mixing and cause soot to be formed along with products such as hydrocarbons, carbon monoxide and hydrogen.

In general, the soot formation in diesel combustion involved four major processes: soot particle inception and nucleation, particle coagulation, particle surface reaction (growth and oxidation) and particle agglomeration. Figure 2.5 shows the steps involved in formation of PM. There have been several principal proposals made regarding the general nature of soot particle inception. Among these are polyacetylenes or polyynes, ionic species and polycyclic aromatic hydrocarbons (PAH) (Frenklach, 2002). Following the PAH hypothesis, a mechanism of soot formation should consist of several stages. The first stage occurs by pyrolysis or oxidation reactions where the fuel molecules are broken down into smaller hydrocarbon molecules and free radicals. Most of the energy release in these early reactions arises from the formation of water. The temperatures reached as a result of these reactions are of the order of 1600-1700 K. Then the key step occurs, the *first aromatic ring* in the system from small aliphatics, usually benzene or phenyl is formed. This first ring appears as the nucleus for the formation and growth of PAH, following different mechanisms.

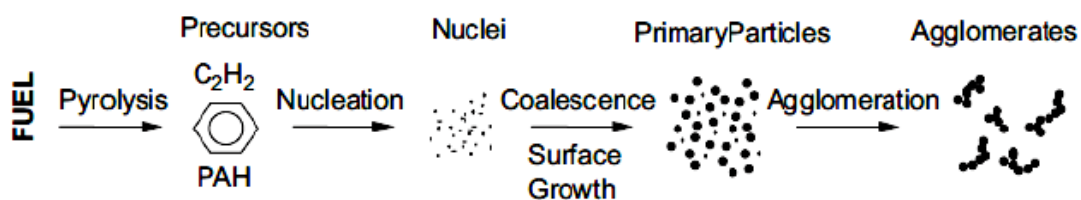


Figure 2.5: Steps in PM formation

Source: Banús et al., (2013)

The soot nucleation process is basically a continuous PAH growth and coagulation process that produce nuclei in the form of large condensed PAH particles (Richter and Howard, 2000). PAH species begin to stick to each other at some size during collision, thus forming PAH dimers. PAH dimers collide with PAH molecules forming PAH trimmers or with other dimers forming PAH tetramers, and so on. On the other hand, individual PAH species keep increasing in size via molecular chemical growth reactions. In this manner, the PAH clusters evolve into solid particles which formed the smallest identifiable soot particles with diameters of the order of 1 nm. These small soot particles then grow by particle growth. Almost 90 % of the total soot mass is produced as the result of particle growth. The particle growth usually involves two main processes which were the coalescence of soot nuclei into larger particles and the surface growth. On the other hand, during this growth process, the deposition of organic materials on the surface of primary particles due to absorption and condensation of the organic fractions can also be observed. Whereas, collision between larger particles starts to occur as the particles keep growing. As the result, the product of collisions between large particles often loses its spherical shape. This explains why the individual primary particles in the exhaust still maintain the overall spherical geometry while the soot agglomerate usually exhibit chain-like structure.

As the primary particles grow to a certain size, the agglomeration process occurs and form chains several hundred nanometers long, with primary diameters between 30 and 50 nm. The resulting soot particles are believed to contain between  $10^3$  and  $10^5$  carbon atoms on average. During this process, the primary particles agglomerate into

clusters that have chain-like structure. The surface growth process still continues to merge the primary particles on the aggregate during the agglomeration stage, which causes the demolition process to occur. The demolition process is responsible for increasing the diameter of the primary particles, reducing the number of primary particles within the aggregate, as well as partly restoring the spherical geometry of the primary particles. During and immediately after its formation and growth, oxidation of soot particles may occur which often results in a decrease of the soot concentration. Soot oxidation is classified as a heterogeneous (gas-solid) reaction, and generally occurs when the soot particles diffuse to lean parts of the flame where the temperature and oxygen concentration are high. The soot particles are usually oxidized when they are burned in the presence of oxidant species such as molecular and atomic  $O_2$  or the OH radical. During the oxidation process, the soot particles will react with the oxidants to produce gaseous products such as CO and  $CO_2$ . Almost 90 % of the soot formed will be completely burnt during the oxidation process, and only the remaining portion of soot particles that survive the oxidation at the end of the combustion will be emitted into the exhaust (Heywood, 1988).

Dec (1997) has presented the conceptual models of soot formation in spray combustion based on laser imaging studies in a supercharged engine at Sandia Laboratories. The formation and features of a quasi-steady diesel fuel jet was shown schematically in Figure 2.5. It is seen in these studies that the liquid jet is relatively short and the fuel ahead of liquid jet is in vapor phase. The soot appeared for the first time just downstream of a liquid jet in the rich premixed combustion region. The concentration of soot increases and particle size grows as soot flows downstream towards the spray boundary. The highest soot concentration and largest particle size are in the region, forming head or leading edge of the jet. The model suggests that the formation of soot precursors and consequent generation of soot particles takes place in the rich premixed flame where the fuel-air equivalence ratio is in the range, 2 to 4. The soot particles grow in size as they pass through the spray towards the spray leading edge. The soot finally gets oxidized in the diffusion flame at the spray boundaries by the OH radical rather than the molecular oxygen,  $O_2$ . While  $NO_x$  is produced on the outside of the diffusion flame, where temperatures are high and oxygen and nitrogen are abundant.

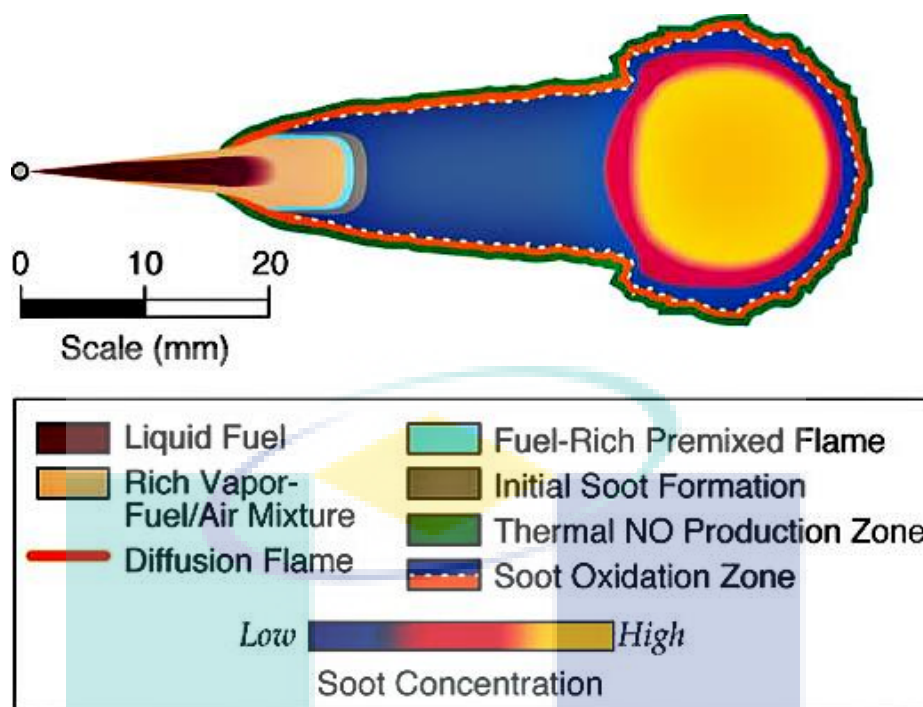


**Figure 2.6:** Quasi steady diesel combustion plume

Source: Dec (1997)

Initial pyrolysis of fuel usually identifies a very rich combustion region. The products of this initial pyrolysis have abundant amounts of soot precursors, like  $C_2H_2$ ,  $C_2H_4$ , and the radical  $C_3H_3$ , for seed particles, as well as unburned hydrocarbons, for growth species. Initial soot particles form and grow in size through agglomeration, direct deposit, and surface growth. The soot particles, soot precursors and growth species, are all oxidized as they mix with the surrounding air at high temperatures. Furthermore, just downstream of this reaction, observations from Dec have shown the existence of a zone where small soot particles begin to form. The particles take root and grow as they move down the turbulent fuel jet toward the head vortex. Oxidation of the soot particles occurs when they pass close to, or through the diffusion flame formed around the periphery of the spray plume, where the particles are exposed to  $O_2$ . A vast majority of the soot particles formed during the diesel combustion is oxidized before the combustion event is quenched (Heywood, 1988). In the final stage of the combustion event a “race” occurs between the dropping temperature due the expansion cooling and the rate of the soot oxidation. The PM left when the final stage of combustion is

quenched, becomes the soot expunged from the cylinder and into the exhaust of the engine.

### 2.6.3 Particulate Matter Measurement Methods

A comprehensive knowledge of PM size, morphology, and composition is needed to characterize them sufficiently since diesel PM are geometrically complex and consist of multi component mixtures including semi volatile compounds. These compounds may be in the gas phase or condensed on particles depending on the temperature. PM properties depend on the fuel, engine technology, operating conditions, and exhaust after treatment. The properties also change with time, as the particulates undergo transformation once released into the atmosphere or while in the sampling train or in the measurement apparatus. Measurement and sampling of diesel PM presents a challenge due to its complex nature. There are a number of methods for PM measurements and each method is dependent upon the information required.

For instance, the EPA defines PM produced by diesel fuel combustion as the mass of material collected on a filter at a temperature of 52°C or less after dilution of exhaust with air (EPA, 2002b). While Mine Safety and Health Administration (MSHA) regulate the exposure of underground metal/non-metal miners to diesel PM based on the mass concentration of elemental carbon (EC). Since diesel engines are the only source of submicron EC particles in this occupational environment, EC was found to be a suitable substitute for diesel PM in underground metal/non-metal mines (MSHA, 2005). Other measurement methods for diesel PM in occupational environments also include respirable particulates ( $<3.5\mu\text{m}$ ), smoking corrected respirable particulates and combustible respirable particulates among other methods (EPA, 2008). The mass measurement methods discussed above all are known as gravimetric approach where sample PM are collected on a filter, then sent to a laboratory for mass determination.

Recently, Concerns have been raised on which aspect of particles should be emphasized when it comes to health issues either a mass or number of particles. Historically, the emissions standards followed by researchers are based on the studies of particle mass concentration, from  $\text{PM}_{10}$  to  $\text{PM}_{2.5}$ . However, even  $\text{PM}_{2.5}$  is still very large compared to vehicle particulates (Eastwood, 2008). Consequently, it is becoming

increasingly clear that regulations on emitted particulate mass from diesel engines are not a proper measure for the health hazard as a particle of 10  $\mu\text{m}$  and 1 million particles of 100 nm diameter have similar weight, but the latter is much more dangerous to human health. For this reason, the researches on PM push forward the transition of the PM measurement from its mass to number and size distribution.

Currently, most particle-sizing devices observe the diameter of a particle in the measurement and this term is commonly used to present size in aerosol science. The diameter measured presents an equivalent diameter of a spherical particle, which has the same response to certain forces. These concepts include the Stoke diameter, aerodynamic diameter and electrical mobility diameter (Eastwood, 2008). One of the most popular equipment to measure the PM size and distribution, and the electrical mobility diameter is the scanning mobility particle sizer (SMPS). On the other hand, an electrical low pressure impactor (ELPI) is used for the aerodynamic diameter. Both of these equipments are suitable for steady state engine tests, but SMPS is more relevant to the smaller particles, and the ELPI to the larger particles (Eastwood, 2008). Other equipment includes a differential mobility spectrometer (DMS) and an engine exhaust particle sizer (EEPS), which also measure the electrical mobility diameter, just as the SMPS. They have a lower detection limit in particle size and a much quicker response than ELPI, thus are more widely used for transient engine tests (Johnson et al., 2013).

On the other hand, interest has increased in studies the aerosol morphological characteristics, which may lead to a better qualitative description of the PM. Scanning electron microscopy (SEM) is popular equipment in the identification of physical characterization of PM. The use of SEM has improved the understanding of the properties and source of PM in addition provides detailed information on particle morphology. This technique also allows the determination of PM size, mass, and chemical composition. It uses electrons to provide magnified images, better feature resolution, wider range of magnification, and a greater depth-of-field in comparison to the conventional light microscope (Shandilya et al., 2002). SEM, in association with an energy-dispersive X-ray (EDS) system, can identify chemical characterization of particles (Ferreira et al., 2013). The latest technology for identifying and analyzing PM with this technique is a computer vision based image processing methods. The imaging

method integrated with SEM is a highly efficient and automatic technique for PM characterization (Nazar et al., 1996). This method consists of two main steps; image acquisition and image analysis.

Image acquisition is the process of creating formatted numerical value from the micrograph of interest to be processed by computer. On the other hand, image analysis is the process of extracting meaningful information from images. Image analyzing software/techniques is used to analyze the particle images obtained from SEM to find sizes, shape and area of individual particle present in filter images. Generally five steps are involved in analyzing each image which is image reading, preprocessing, segmentation, feature extraction and representation. Field emission scanning electron microscopy (FE-SEM) is an alternate method for conventional SEM. FE-SEM produces clearer, less electrostatically distorted images with spatial resolution down to  $1 \frac{1}{2}$  nm. It is 3 to 6 times better than SEM. Many researchers used FE-SEM techniques for various researches on PM. Recently the most common method to characterize the structure of PM is transmission electron microscopy (TEM). This technique provides projected two-dimensional properties of PM agglomerates which give higher resolution compared to SEM and FE-SEM. Similar with SEM and FE-SEM, TEM also governed by computer based image processing in order to analyze PM characteristics.

#### **2.6.4 Overview on Particulate Matter study**

Study of PM from European light duty (LD) vehicle was carried out as early as in 1998 by a group of oil companies such as BP oil, Esso and Shell. The study was carried out by four diesel and three gasoline vehicles which were tested using limited fuel matrix and varied driving conditions. The result was analyzed in terms of PM size, number and mass distribution (Hall et al., 1998). The PM from LD diesel vehicles were much higher than from LD gasoline vehicles. The PM size distribution and chemical composition of diesel PM can vary greatly depending on the engine type, engine speed and load, composition of fuel and lubricating oil and emission control technology. In practice, vehicles operate at varying loads and at times the engine remains idle for long durations due to unorganized traffic and congestion.

Therefore, there is a need to characterize diesel PM with varying engine operating conditions and quality of fuel (Sharma et al., 2005). Tanaka et al. (2002) was studied on the PM composition under different engine operating conditions. By lowering the engine torque, the result showed that the small aerodynamic diameter particles were decreased when the ratio of the soluble organic fraction (SOF) was increased. In addition, the SOF ratio in the large aerodynamic diameter particles was higher than that of the small ones. Other research by Klein et al. (1998) demonstrated that the diesel oxidation catalysts (DOC) were able to reduce the SOF of PM in the low temperature, thus reducing the particulate sizes. However, in the high temperature, it might oxidize the sulphur into sulfate, which could strongly influence the particulate agglomerations.

Numerous studies of the structural properties of agglomerates produced from diesel engines have been reported. Most measurements have been carried out for flame-generated agglomerates, for which the relationships between the actual properties and projected properties have been tested (Megaridis and Dobbins, 1990 and Sorensen and Feke, 1996). The fractal dimension provides useful insights into the structure of diesel agglomerates. According to Mandelbrot (1982), the number of primary particles in an agglomerate ( $N_p$ ) scales with the radius of gyration ( $R_g$ ) can be described as follows (Mandelbrot 1982):

$$N_p = k_g \left( \frac{2R_g}{d_p} \right)^{D_f} \quad (2.13)$$

Where  $k_g$  is the fractal prefactor,  $d_p$  is the primary particle diameter, and  $D_f$  is the fractal dimension. The fractal dimension also provides useful insights into the agglomeration mechanism. Previous work has shown that different agglomeration regimes result in different values of the fractal dimension.

Lee et al. (2003) employed TEM to investigate the morphology of light duty diesel PM. It revealed that PM produced at low engine loads were ambiguous with a high SOF, while at high loads, they were in graphitic structures, just as the typical carbon

graphite. The primary particle sizes were also influenced by exhaust gas recirculation (EGR), and in most cases, they increased with the increase of EGR. In addition, Park et al. (2004) also study on structural properties of diesel PM pre-classified by particle mobility and mass using TEM. By using both equipments, they were able to determine the dynamic shape factor and inherent material density of diesel PM. They found that when the particle mobility size increased from 50 to 220 nm the dynamic shape factor is increased from 1.11 to 2.21 and that the inherent material density increased from 1.27 to 1.78 g/cm<sup>3</sup>. The increase in dynamic shape factor with size occurs because large particles are more irregular than smaller particles while the increase in density occurs because the ratio of elemental carbon to condensed organics increases with increasing size.

On the other hand, Armas et al. (2008) investigated the influence of diesel engine operating conditions on the exhaust PM size distribution. Armas found that the variation of engine speed and torque consequently changed the oxidation of the formed soot and particulate nucleation. The accumulation mode particles were reduced as the engine speed is increased due to the clear decrease of the fuel air ratio and EGR ratio at low torque and the elevated oxidation at higher torques. In addition the increase of torques caused the production of nucleation mode particulates due to the EGR, which also played an important part in the exhaust particulates formation. On the other hand, decreasing torques actuate the soot oxidation due to higher oxygen, and consequently reducing the soot and accumulation mode particles.

More recent research into PM emissions includes the PM characterization from advanced combustion technology homogeneous compression charge ignition (HCCI) (Agarwal et al., 2013). Physical characterization of PM was carried out using engine exhaust particle sizer (EEPS), which measures the PM size number distribution for the nano-particles in the exhaust. The particles were collected on the filter paper for morphology study using SEM. Agarwal found that the PM mass emission decreases from the diesel HCCI engine. Most of the diesel HCCI exhaust PM was found to be ultra-fine particles. The PM number concentration tends to increase with increase in EGR rate. Otherwise, increase in the number of particles in accumulation mode is due to higher benzene soluble organic fraction (BSOF) of PM.

Shukla et al. (2014) has performed a comparative morphological analysis of the exhaust PM emitted from a common rail direct injection (CRDI) sports utility vehicle (SUV) engine for primary and aged PM by using mineral diesel and biodiesel blend B20. The diluted exhaust was passed through a customized photochemical chamber with a 2 hour retention time. While PM filters were observed by SEM. Their observation found that B20 emitted significantly lower primary PM in comparison to mineral diesel for all the loads. At lower load conditions B20 emitted lower PM for aged samples. At higher engine loads (75 % and 100 %), this reduction in aged PM for B20 compared to mineral diesel was quite significant.

## **2.7 BIODIESEL AS AN ALTERNATIVE FUEL**

With the increasing price and depletion source of crude oil, interest in biodiesel is growing remarkably. Biodiesel can be used in diesel engine with or without modification on the engine. In 1892, Rudolph Diesel invented the diesel engine with peanut oil as the fuel. However, due to the cheaper prices of petroleum oil, the diesel engine was later modified to be run on petroleum oil. Now, after centuries, as the petroleum oil sources is depleting and because of increasing concern in environmental effect, serious action are taken to bring back renewable fuel especially biodiesel to run on the diesel engine. American Society for Testing and Materials (ASTM) has defined biodiesel as fuel comprised of mono-alkyl esters of long chain fatty acids derived from vegetable oil or animal fat, designated as B100. B100 refers to the pure fuel without blending with diesel fuel. Biodiesel blends are denoted as "BXX" with "XX" representing the percentage of biodiesel contained in the blend. For example, B20 refers to the 20 % of biodiesel and 80 % of diesel blend. Biodiesel blends higher than B20 require special handling and engine modifications to avoid maintenance and performance problems (EPA, 2010). Therefore, blends of B20 or less are common blends that can be found in Europe and the United States.

Biodiesel can be produced through the chemical reaction of vegetable oil or animal fat with methyl alcohol or ethyl alcohol. The process is called transesterification with the presence of a catalyst. Commonly used catalysts are potassium hydroxide (KOH) or sodium hydroxide (NaOH). Transesterification process will produce glycerol

and ester. Usually, glycerol is used as feedstock in cosmetic products. When the methanol is used during the process, the product is called methyl ester. On the other hand, the product was called ethyl ester when ethanol is used. Methyl ester is cheaper as compared to ethyl ester due to the lower cost for methanol. Biodiesel has recently attracted significant attention of researchers, government and industries in different countries all over the world as it is biodegradable and non-toxic energy source. It is estimated that approximately 10 % of diesel fuel consumption within Europe and 5 % of Southeast Asia's total fuel demand could be replaced by biodiesel/bio-ethanol (Phan and Phan, 2008). Several studies conducted by researchers identify biodiesel as a potential alternative fuel for diesel engines. It has been found that engines running on biodiesel run successfully for longer durations and the performance and emission characteristics are quite comparable to that of petroleum based diesel fuel (Altin et al., 2001).

Buyukkaya (2010) investigated the performance, combustion and emission trends of biodiesel from rapeseed oil and its blend. It was found that CO emissions of B5 and B100 were 9 % and 32 % lower than diesel fuel, respectively. The brake specific fuel consumption (BSFC) of biodiesel at maximum torque and rated power conditions were found to be 8.5 % and 8 % higher than that of diesel fuel respectively. The study also found that the combustion characteristics of biodiesel and its blends were quite similar to those of petroleum diesel. In addition, a review by Ali (2011) has shown that biodiesel is being considered to be the best fuel for diesel engines since burning biodiesel and its blends produce the lowest greenhouse emissions on a life cycle basis. Biodiesel also reduces particulate matter, visible smoke, odor, and polyaromatic hydrocarbon emissions. Furthermore, biodiesel does not contain undesirable element like sulphur as compared to petro diesel, which have sulphur content. Numerous studies which investigate the effect of biodiesel fuel for diesel engine with different type of feedstock have been conducted world-wide. There are many potential feedstocks from various types of vegetable oils as well as animal fats are available to be used as biodiesel. Common source for biodiesel currently under vast research by many researchers all over the world are soybeans, sunflower, jathropa (Soares et al., 2010; Houa et al., 2011 and Georgogianni et al., 2009), peanuts, rapeseed (Shin et al., 2012),

palm (Ong et al., 2012), corn, canola (Lee et al., 2010), cottonseed, tallow (Teixeira et al., 2010) and waste cooking oil (Can, 2014 and Nantha Gopal et al., 2014).

### 2.7.1 Waste Cooking Oil as a Potential Feedstock for Biodiesel

Despite its various advantages, biodiesel has several problems compared with petroleum diesel such as low temperature properties (González Gómez et al., 2002) and higher production cost (Canakci and Van Gerpen, 2003). High production cost of biodiesel has been discussed among the researchers (Fore et al., 2011 and Hill et al., 2006). The production costs of biodiesel becoming approximately 1.5 times higher than diesel due to the high cost of raw material which can be up to 75 % of the total manufacturing cost (Zhang et al., 2003). Larger farm land is necessary to grow crops for biodiesel. Besides cost consideration, another obstacle encounter is a food crisis in consequence of diverting food crops from human consumption to fuel production. This has raised the major nutritional and ethical concerns among the experts. Research done by Pimentel et al. (2009) stated that production of ethanol from corn in the U.S. increases the price of beef, chicken, pork, eggs, bread, cereals, and milk by about 10 % to 30 %. In addition, Jacques Diouf, Director General of the UN Food and Agriculture Organization reports that using food grains to produce biofuels is already causing food shortages for the poor of the world (Pimentel, 2009).

In order to prevail over this obstacle, researchers were using the feedstock that does not compete with food production like waste fats and oils. Huge quantities of animal fats and WCO can be obtained all over the world. The production of large amounts of WCO has increased due to the increasing food consumption. The volume of WCO produced by the EU is approximately  $7 \times 10^5 - 1 \times 10^6$  tonnes/year (Kulkarni and Dalai, 2006) while Japan generates about  $4 \times 10^5 - 6 \times 10^5$  tonnes/year (Pugazhvadivu and Jeyachandran, 2005). In addition, it was estimated that there were 40,000 tonnes per year of WCO produced in Asia countries such as Thailand, Malaysia, Hong Kong, Indonesia, India etc (Ismail, 2005). Management of this enormous amount of WCO faced a significant challenge because of their disposal method may contaminate environmental water and land resources. Some of this waste cooking oil is used in manufacturing soap and additive in animal food production.

However, since 2002, the EU has enforced a ban on feeding these mixtures to animals. Many harmful compounds can be traced from the use of recycled cooking oils in animal feeding. By consumptions of animal origin foodstuffs like meat, milk and poultry, it could result in the return of harmful compounds back into the food chain (Cvengroš and Cvengrošová, 2004). Furthermore a major part of WCO is discharged into the environment. As large amounts of waste cooking oils are illegally dumped into rivers and landfills, causing environmental pollution, many developed countries have set policies that penalize the disposal of waste oil through the water drainage (Canakci and Van Gerpen, 2003). Recycling waste cooking oil to produce biodiesel as fuel in diesel engines is one of the best ways to utilize it efficiently, which can reduce environmental pollution (Pugazhvaivuvu and Jeyachandran, 2005 and Nantha Gopal et al., 2014). In addition, according to Figure 2.7, the price of WCO is less expensive than other oil which leads to a significant reduction in total manufacturing cost (Renewable Energy Group, 2011). Therefore, utilization of waste cooking oil significantly enhances the economic viability of biodiesel production.

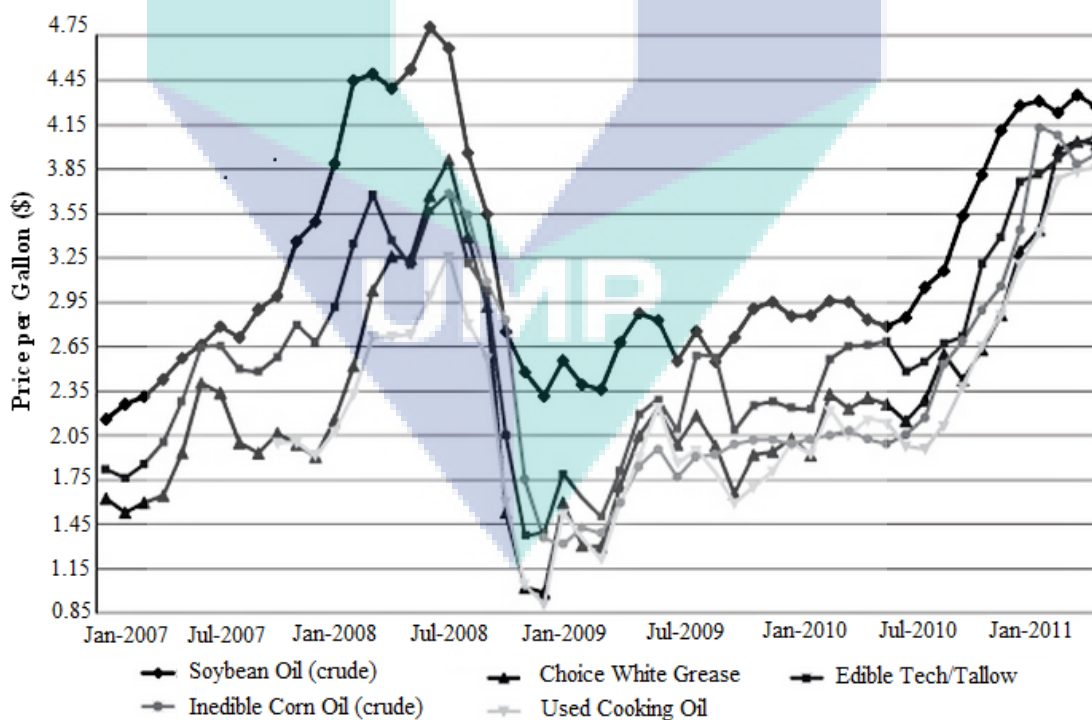


**Figure 2.7:** Feedstock price in United States

Source: Renewable Energy Group (2011)

### 2.7.2 Production of Waste Cooking Oil as a Biodiesel

According to Talens Peiro' et al. (2008) the conversion of vegetable oils and WCO to biodiesel was introduced by Nye et al. (1983) in 1983. It then developed commercially in 1988 by Mittelbach and Remschmidt (2004). WCO has different properties from refined and crude vegetable oils. During frying, vegetable oil undergoes various physical and chemical changes and many undesirable compounds are formed. The presence of heat and water accelerates the hydrolysis of triglycerides and increases the content of free fatty acids (FFA) in the oil (Marmesat et al., 2007). In addition, some polymerized triglycerides were formed which increase the molecular mass and reduce the volatility of the oil. Therefore, WCO cannot be used directly in diesel engines.

Apart from that, it also contained moisture and has higher viscosity which can lead to severe engine deposits, piston ring sticking and injector coking (Muralidharan et al., 2011). The methods in producing biodiesel from WCO do not differ from the conventional transesterification process using alkaline, acidic, and enzymatic catalysts. Each catalyst has its advantages and disadvantages depending on unwanted content, especially FFA and water. The FFA and water content have significant effects on the transesterification reaction negatively (Canakci and Özsezen, 2010). They also interfere with the separation of fatty acid, esters and glycerol. In particular, the viscosity of the oil increases considerably, because of the formation of dimeric and polymeric acids and glycerides in WCO. Molecular mass and iodine values decrease while saponification value and density increase (Ruiz-Méndez et al., 2008).

This poses a lot of challenges in the transesterification of WCO. The pre-treatment of the WCO to remove the undesirable compound is not practical. As a result, WCO is heated and filtered to remove solid particles prior to transesterification. Certainly, by applying a specific type of transesterification process, the characteristic properties of biodiesel are same as that produced from virgin oils and are generally similar to those of petroleum diesel fuel. The biodiesel is characterized by determining the density, viscosity, cetane number, flash point, calorific value, cloud and pour points. The fuel properties of biodiesel derived from WCO, all met the various national biodiesel standards. Thus, biodiesel produced from WCO can be used in diesel engines

without any engine modifications (Enweremadu and Mbarawa, 2009). The data on requirement of petroleum diesel and availability of waste cooking oil in any country indicate that biodiesel obtained from WCO may not replace petroleum diesel completely. However, a substantial amount of biodiesel fuel can be prepared from WCO, which would partially decrease the dependency on petroleum based diesel.

### 2.7.3 Waste Cooking Oil Biodiesel Properties

One of the major issues when using biodiesel is fuel properties. Generally, these properties vary for different type of biodiesel due to the fact that the feedstock has different fatty acid profiles. Fuel properties are essential for the use of biodiesel. Exhaust emissions and performance tests with biodiesel fuels derived from WCO or similar feedstock have shown that this kind of biodiesel exhibit properties similar to that of biodiesel derived from edible vegetable oil feedstock (Lapuerta et al., 2008). However, it may be expected that the properties of biodiesel derived from waste oils or fats can differ widely. The reason is that the oils or fats are likely exposed to varying degrees of use such as temperature and time, thus increasing the variability of composition and resulting in different properties than edible vegetable oil feedstock. This topic will review the properties of biodiesel from WCO.

#### *Density*

Density is the mass of unit volume of a material at a specific temperature. It is another important fuel property which directly has effects on the engine performance characteristics. Density is related to many fuel properties such as cetane number and heating value. This property influences the efficiency of fuel atomization and combustion characteristics (Barabás and Todoruț, 2011). (Alptekin and Canakci, 2009) On the other hand, diesel fuel injection systems meter the fuel by volume. So, the change of the fuel density will influence the engine output power due to a different mass injected fuel (Pratas et al., 2011). Density data are also important in numerous unit operations in biodiesel production. It was required to be known to properly design reactors, distillation units and separation process, storage tanks, and process piping.

The density depends upon the raw materials used for biodiesel fuel production and the biodiesel methyl ester profile (Veney et al., 2009). The biodiesel density according to standard ASTM D-1298 must be in a range of (0.86 - 0.90 g/ml). Density of biodiesel typically is higher than diesel fuel. This results in the delivery of a slightly greater mass of fuel since fuel equipment operates on a volume metering system (Samuel et al., 2013). Most studies showed the density of WCO is higher than diesel (Phan and Phan, 2008).

### ***Kinematic Viscosity***

Kinematic viscosity is a measure of fluid resistance to flow. It is one of the most important fuel properties that affect the quality of atomization and combustion of diesel engines. High viscosity of biodiesel provides excellent *lubricity* in diesel engine and could avoid fuel pumps from prematurely wear. However, Wang et al (2006) reported that the major disadvantage of biodiesel is their high viscosity which may lead to poor atomization of the fuel, incomplete combustion and carbon deposition on the injector. This is due to the lower spray speed and deterioration of the atomization, evaporation and air-fuel mixture formation characteristics. It is accepted fact that viscosity of biodiesel slightly higher than diesel fuel, which cause by the large molecular sizes of the triglycerides contained in vegetable oils. Thus, causes poor fuel atomization due to the large size of droplets upon injection into the cylinder and also due to high-spray jet penetration (Esteban et al., 2012).

Kinematic viscosity of biodiesel, according to ASTM D6751 must be in the range of 1.9-6.0 mm<sup>2</sup>/s at 40°C. The kinematic viscosity of WCO is about 10 times greater than diesel fuel (Shahid et al., 2012). Many techniques have been developed to reduce the kinematic viscosity and specific gravity of vegetable oils, which include pyrolysis, emulsification, leaning and transesterification. Among these techniques, most researches applied transesterification method because of the fact that this method is relatively easy, carried out in normal conditions, and gives the best conversion efficiency and quality of the converted fuel (Enweremadu and Mbarawa, 2009). The conversion of WCO into methyl esters through the transesterification process

approximately reduces the molecular weight to one-third and reduces the viscosity by about one-seventh (Demirbas, 2009).

### *Cetane Number*

The quality of biodiesel fuel can be referred to cetane number value. Cetane number is the measure of an interval between the start of injection and auto-ignition of fuel. The time interval period can be referred as an ignition delay period. In particular, high cetane number will shorten the ignition delay period. An adequate cetane number is required to increase engine performance. Higher cetane number results in more efficient ignition, less occurrence of knocking, and lower formation of NO<sub>x</sub> (Lin and Lin, 2007). In the production of diesel fuels, cetane number is an important indicator of the quality of the fuel and is usually measured using a standard engine test (ASTMD613). However, it is relatively difficult to measure and has rarely been determined for vegetable oils and fatty acid esters (Encinar et al., 2005).

Biodiesel has a higher cetane number compared to diesel fuel because of the oxygen content which ensures more complete combustion and also because some of the fatty acids present in the fuel have very high octane numbers (Laza and Bereczky, 2011). It has also been reported (Knothe, 2005) that the cetane number of biodiesel depends essentially on the distribution of fatty acids in the feedstock. The longer the fatty acid carbon chains and the more saturated the molecules, the higher the cetane number. Chetri et al. (2008) has reported that cetane number of WCO from their experiment was found to be 61. As WCO has higher amount of saturated fatty acids, the increase in the saturated fatty acid content positively enhanced the cetane number. The oxidative stability of WCO also increases due to the presence of higher amount of saturated fatty acids.

### *Calorific Value*

The calorific value or heat of combustion is the amount of heat transferred to the chamber during combustion and indicates the available energy in the fuel. It is therefore an important parameter to compare the consumption of biodiesel compared to mineral

diesel in engine performance (Klopfenstein, 1985 and Oliveira and Da Silva, 2013). Biodiesel has a calorific value which is about 12 % lower than diesel, which means that biodiesel has lower energy content. This leads to a higher consumption of biodiesel in order to achieve yield of diesel in the engine (Helwani et al., 2009). The reason for the lower value is because of the presence of chemically bound oxygen in biodiesel which lowers their calorific values. According to Phan and Phan (2008), increasing the percentage of the WCO resulted in a reduction in calorific value but an increase in other parameters such as acid number, viscosity and flash point. The reduction in calorific value for the WCO and its blends compared to diesel was due to the presence of oxygen in the biodiesel.

### ***Acid Number***

According to ASTM D 664 and EN 14104, the acid number is expressed in milligrams (mg) potassium hydroxide (KOH) required to neutralize 1 g of sample. The ASTM 6751 standard for acid number of biodiesel was set 0.5 mgKOH/g (Mahajan and Konar, 2006). The acid number of edible oils or their corresponding esters indicates the quantity of FFA and mineral acids present in the sample. The high acid number will indicate unrefined or poorly refined product oil source due to poor process control, such as ethanol carryover. Higher acid number could also cause degradation of rubber parts in older engines, resulting in filter clogging and engine deposit particularly in the fuel injector (Saifuddin et al., 2009).

There has been reported that an acid number of biodiesel will increase with time (Bondioli et al., 1995 and Thompson et al., 1998). Bouaid et al (2007) investigated the storage stability of biodiesel made from WCO over a storage time of 30-months under different storage conditions. The fuel stored in the daylight increased its acid number at a faster rate than the fuel stored in the dark after 4 months of storage. A recent study by Bezergianni and Chrysikou (2012) also indicated the similar result. In their study, WCO samples were stored for one year at room temperature under normal atmospheric conditions, but not exposed to sunlight. They found that acid value of WCO change from 0.744 to 0.931 mg KOH/g.

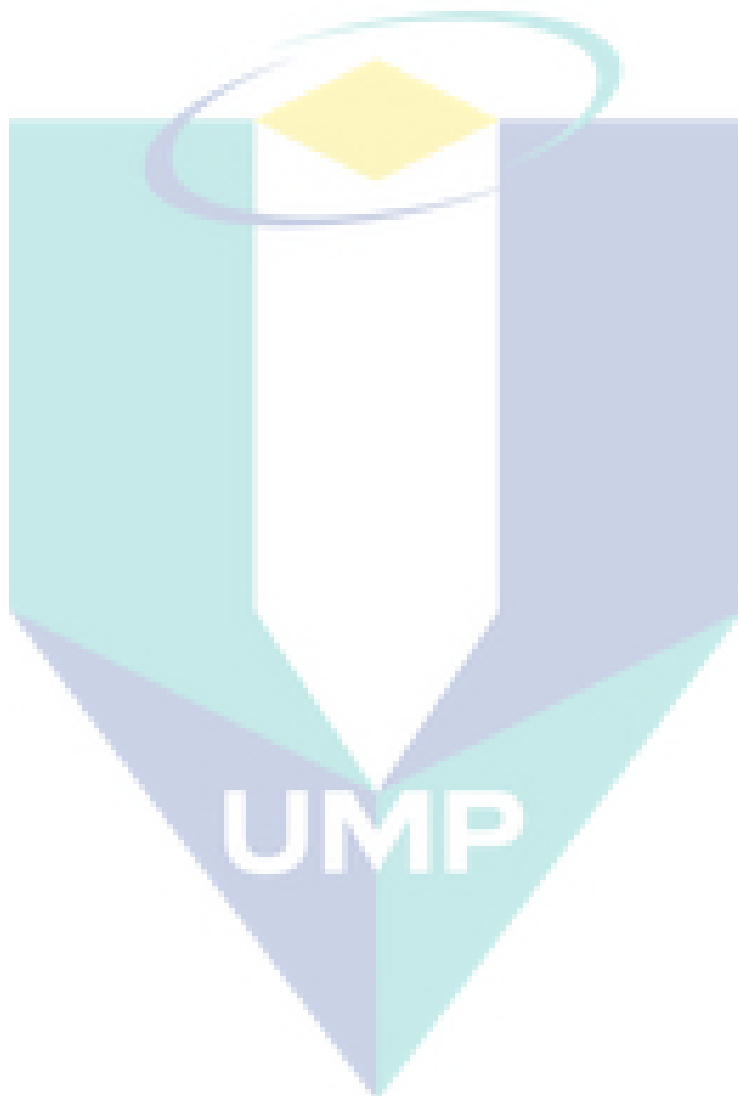
## 2.8 SUMMARY

In this chapter, the exhaust emission of diesel engine has been reviewed. Exhaust emission from diesel engine in terms of gaseous and PM contains toxic air contaminants that can affect human health and environment. Emission of NO<sub>x</sub> can contribute to the acidification and smog formations, Meanwhile, CO emission when inhaled into human body can block the delivery of oxygen and cause cellular hypoxia. Various size of PM can enter various area of human respiratory tract which can cause health problem such as coughing and severe bronchitis. Smaller particle tends to penetrate deep into lungs that will cause further result in cough and other severe respiratory problem. In addition, emission of PM can cause corrosion develop on the steel object surfaces and affect its material. Due to numerous effect of exhaust emission from diesel engine, worldwide emission regulation has becoming more stringent. The stringent emission regulation has forced the manufacturer to develop emission control technology that can meet the standard required.

In this study, the main focus is on the emission of PM fuelled with diesel and WCO biodiesel. Therefore, review on PM composition and structure, its formation, measurement method, and various study of PM emission from biodiesel especially WCO biodiesel has been made. PM is composed of two main components which are soot and SOF. Soot is formed in a locally fuel rich region where the lack of oxygen prevents complete combustion of fuel. On the other hand, SOF is produced from unburned fuel, which contains organic material that needs to be oxidized and also produced from lubrication oil that escape the process of oxidation, not combust and exist in the exhaust system. PM is divided into three types of nucleation mode, accumulation mode and coarse mode. The standard definition of atmospheric particles are classified into four main categories which are PM<sub>10</sub>, fine particles (PM<sub>2.5</sub>), ultrafine particles and nanoparticles.

Measurement and sampling of diesel PM presents a challenge due to its complex nature. There are few methods for PM measurements. Required PM information rely on different PM measurement. For decades, PM is measured mainly base on its mass. Due to increasing concern on PM size effect on human health, the measurement of PM has been push forward including the measurement of a number and size distribution. In addition, PM morphology analysis by using SEM, FE-SEM and TEM can lead to better qualitative description of the PM. From the review, exhaust emission in term of gaseous

and PM from WCO biodiesel is comparable to diesel fuel. Moreover, the fuel properties of WCO biodiesel have similar properties of biodiesel derived from edible vegetable oil in terms of density, kinematic viscosity, cetane number and calorific value. In order to obtain and observe the exhaust emission of diesel engine fuelled with diesel and WCO biodiesel blend, the next chapter which is chapter 3 will provide detail explanation on the research methodology.



## **CHAPTER 3**

### **RESEARCH METHODOLOGY**

#### **3.1 INTRODUCTION**

The whole test rig for the study is described in this chapter. It covers the experimental equipment, instrument and test fuel used in this study. In addition, detailed explanation has been given on the operating test condition and particulate matter analysis. Figure 3.1 shows the flow chart of the frame work strategy that comprises the approach of engine exhaust emission analysis. Within the frame work strategy, this chapter is divided into six subchapters. Subchapter 3.1 is introduction. Subchapter 3.2 discusses the engine and instrumentation while subchapter 3.3 discusses the exhaust emission measurement. The purpose, procedure and specification of the equipment, instrument and material will be explained in both subchapters. Subchapter 3.4 explains the test fuel used in this experiment together with their properties. Then, in subchapter 3.5, experimental procedure conducted in this study is explained in detailed while subchapter 3.6 describes the particulate matter analysis applied to find the characteristics of particulate matter.

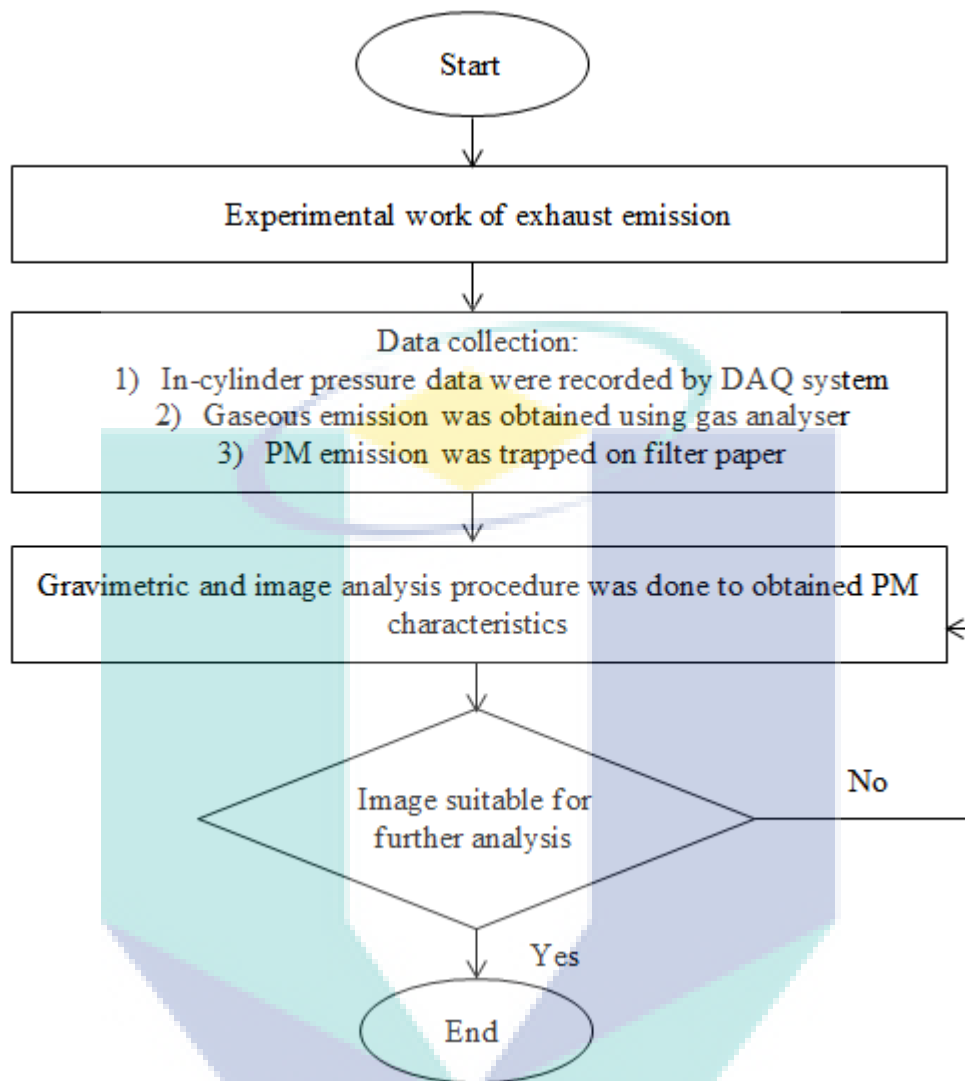


**Figure 3.1:** Flow chart

### 3.2 ENGINE AND INSTRUMENTATION

Experiments and tests are conducted at Faculty of Mechanical Engineering laboratory of automotives located at University Malaysia Pahang. A naturally aspirated YANMAR TF120 was used for the study. The engine is equipped with the cooling system, fuel delivery unit, data acquisition system, exhaust measurement equipment and dynamometer system. The schematic diagram of the overall engine test rig was shown in Figure 3.2.

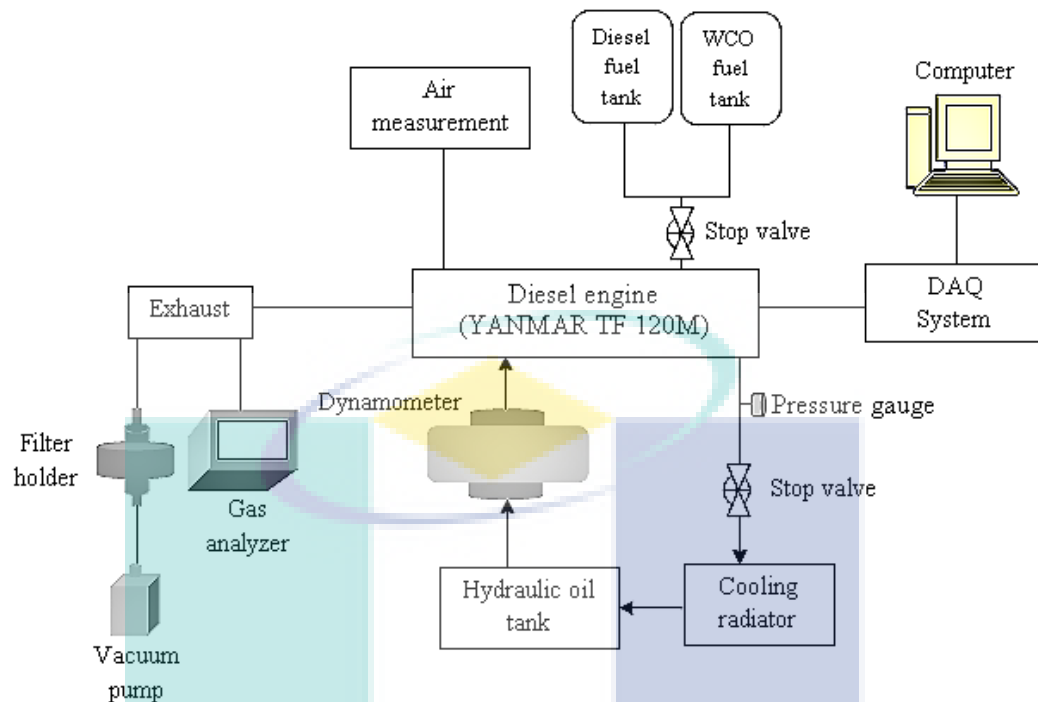


**Figure 3.2:** Schematic diagram of the test rig



**Figure 3.3:** Test engine

### 3.2.1 Engine

The engine is single cylinder direct injection combustion with the capacity of 12HP. It works on four-stroke cycle with water cooled cooling system. Table 3.1 described the details of the engine. Figure 3.3 shows the picture of the test engine used in this study. The engine is coupled with a hydraulic pump dynamometer in order to provide the load.

**Table 3.1: Engine Specification**

Description	Specification
Engine model	YANMAR TF120
Engine type	Horizontal, diesel 4 stroke cycle
Combustion system	Direct injection
Number of cylinders	1
Bore x Stroke (mm)	92 x 96
Displacement (L)	0.638
Dimensions (mm)	Length: 776 Width: 379.5 Height: 621
Injection timing	17° BTDC
Fuel injection pump	Bosch
Injection pressure (kg/cm <sup>2</sup> )	200
Compression ratio	17.7
Continuous output (HP)	10.5 HP at 2400 RPM
Rated output (HP)	12 HP at 2400 RPM
Cooling system	Water cooled (radiator type)
Cooling water capacity (L)	2.3
Dry weight (kg)	102
Connecting rod length (mm)	149.5

### 3.2.2 Hydraulic Dynamometer

A positive displacement gear pump model Hydrome model HGP-3A-F23 was used to provide the load on the motor by controlling a screw type control valve which changes the back pressure of the dynamometer. The load was kept constant at 800 psi. It was measured by controlling the pressure gauge. Figure 3.4 shows the image of the dynamometer system. The dynamometer can operate at speeds range of 400 rpm to 3000 rpm. A flexible flanged shaft coupler was used to fix the engine flywheel and

pump shaft together. Table 3.2 shows the detail specification of the engine dynamometer.

**Table 3.2:** Engine dynamometer specification

Parameter	Specification
Weight (kg)	3.35
Minimum speed drive (rpm)	400
Maximum speed drive (rpm)	3000
Maximum pressure (kg/cm <sup>2</sup> )	250
Working pressure (kg/cm <sup>2</sup> )	210



**Figure 3.4:** Dynamometer system

### 3.2.3 Data Acquisition System

Data acquisition system applied in this experiment is from TFX Engineering where it consists of cylinder pressure sensor, LCS data logger, sensor interface and transfer cable as shown in Figure 3.5. It was connected to a PC for data collection. The output parameter obtained from this instrument is in-cylinder pressure, engine power, torque exhaust temperature and maximum combustion chamber. Figure 3.4 shows the data acquisition system for the experiment. For measuring in-cylinder pressure, pressure sensor G31394-1.5 manufactured by Optrand Incorporated has been used. The pressure range is 0-200 bar (3,000 psi). The information which has been converted to digital form is stored in the PC and processed to produce the output parameter.

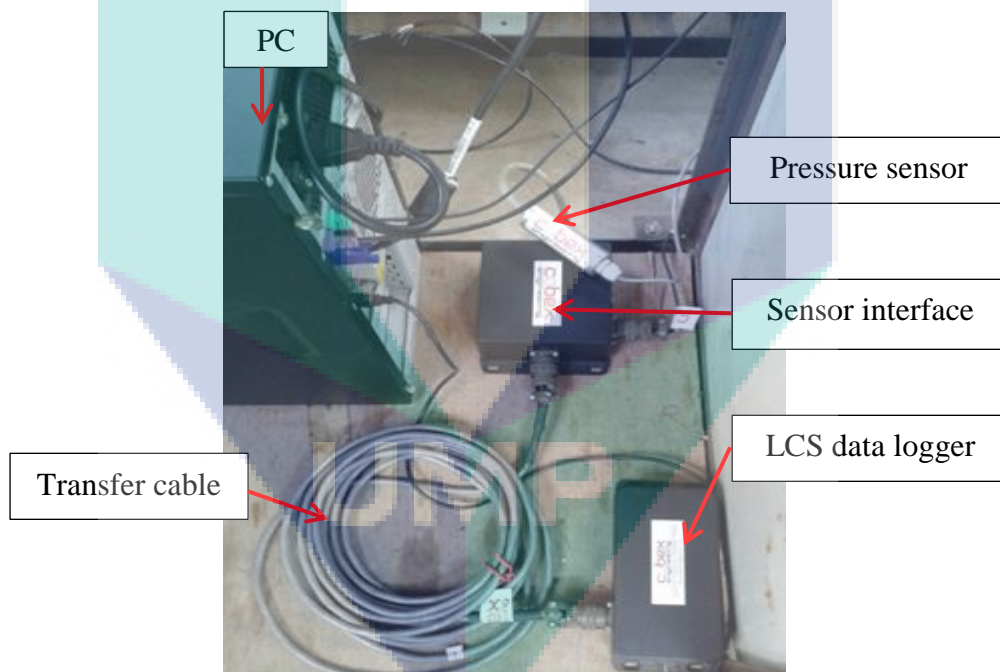


**Figure 3.5:** Data acquisition system

### 3.2.4 Temperature and Speed Measurement

Three units of K-type thermocouples were mounted to the engine for the temperature measurement. These thermocouples were able to measure exhaust gas temperature, intake temperature and ambient temperature. The temperature readings

were displayed through multipoint temperature indicator as shown in Figure 3.6. The instrument used is from Eutech System. For measuring engine speed, the photoelectric sensor is used. The sensor measure the engine speed through flywheel rotation and the reading is displayed via the digital tachometer as shown in Figure 3.6.

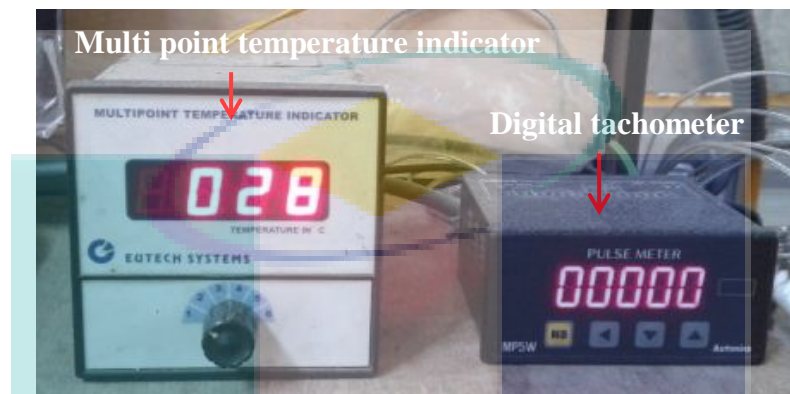


**Figure 3.6:** Temperature and speed measurement instrument

### 3.3 EXHAUST EMISSION MEASUREMENT

The exhaust emission measurement equipment consists of two main components which were PM emission sampling equipment and gaseous emission equipment. The exhaust gas was sampled at 50 cm downstream of the exhaust extractor. Figure 3.7 shows the actual setup for exhaust emission measurement equipment. Gaseous emission was measured by gas analyzer. For PM emission sampling, the instruments involved were sampling pump, filter holder, filter paper, oven and high precision electric balance.

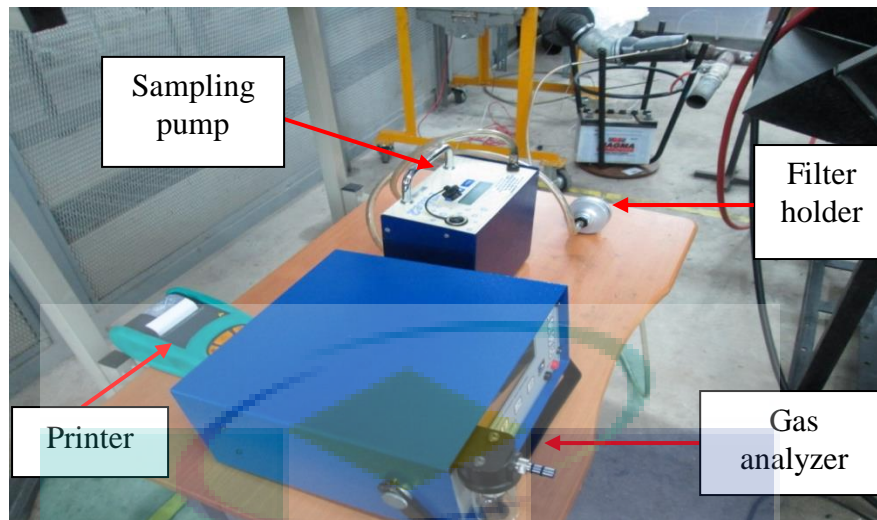


**Figure 3.7:** Exhaust sampling equipment setup

### 3.3.1 Exhaust Gas Analyzer

The gaseous emission was measured by exhaust gas analyzer. This instrument was used to measure the rate or concentration of diesel gaseous emission components. Exhaust gas analyzer used in this study is from KANE AUTOMOTIVE model Kane 4-3 as shown in Figure 3.8. The data measured was transferred to a printer via Bluetooth and printed on paper. Table 3.3 shows the specification of the exhaust gas analyzer.



**Figure 3.8:** Exhaust gas analyzer

The concentration of the components measured are NO, NO<sub>x</sub> in ppm (percent per million). CO, O<sub>2</sub> and CO<sub>2</sub> were measured in % volume. The measurement of the gaseous emission from the engine was done by connecting a heat-resistant plastic pipe with diameter about 0.75 cm. Before measurement, the device must be calibrated to obtain the data for accuracy. It was placed outdoors for air purging. The reading was taken after engine running for 15 minutes. After collecting the reading, the gas analyzer pump was switched off. The hose from the exhaust was pulled off from the gas analyzer. Then, the pump was switched on again so that the gas analyzer draws ambient air for air purging into the gas analyzer for five minutes. The step was repeated for each test fuel.

**Table 3.3:** Gas analyzer specification

Parameter	Resolution	Accuracy	Range
Carbon Monoxide (infra red)	0.01%	± 5% of reading *1 ±0.06% volume*1	0-10% Over-range 20%
Oxygen O <sub>2</sub> (Fuel Cell)	0.01%	± 5% of reading *1 ±0.06% volume*1	0-21%
Carbon Dioxides (infra red)	0.1%	± 5% of reading *1 ±0.06% volume*1	0-16% Over-range 20%
Nitrogen oxides (NO <sub>x</sub> )	1ppm	0-4,000 ppm ± 4% or 25 ppm *3	0-5,000ppm
Electrochemical		4,000-5,000 ppm ± 6*3	

### 3.3.2 Filter Holder



**Figure 3.9:** Filter holder parts

For PM emission sampling, filter holder was used to hold the filter paper to trap the particulate matter emission. In this study, 47 mm in-line aluminium filter holder from Pall Corporation was used. Figure 3.9 shows filter holder parts. The filter paper was placed between the support screen and underdrain screen at base part. The inlet cover was put on top of the support screen and aligned with the thrust ring. The placement of filter paper in filter holder is shown in sequence from left to right in Figure 3.10. Table 3.4 shows detail specification of the filter holder. Each part of filter holder must be cleaned before each sample was taken to avoid any particles left behind which will change the exact total mass of the PM and filter paper.



**Figure 3.10:** Placement of filter paper in filter holder

**Table 3.4:** Filter holder specification

Description	Specification
Effective filtration area	9.6 cm <sup>2</sup>
Diameter	5.9 cm
Length (exclude hose barb)	5.7 cm
Max. Operating temperature:	
Hose barb adapters	93 °C
O-ring	204 °C
Max. Operating pressure	14 bar

### 3.3.3 Filter Paper

The filter paper was placed in filter holder to trap the PM from the exhaust tailpipe. Filter paper used in this study is Advantec composite filter paper with the size of 47 mm. This filter paper is glass fibers covered with polytetrafluoroethylene (PTFE).

The moisture absorption is very low as the surface is coated with PTFE. Therefore, the measurement of PM concentration is not affected by humidity of the air. The absorption of acid gaseous such as NO<sub>x</sub> is very low since Fluoropolymer is used as binder.

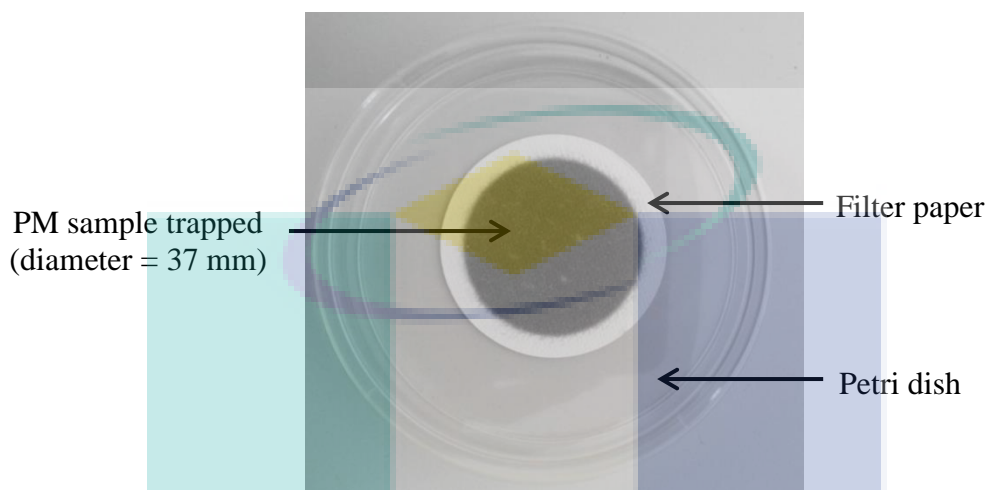


**Figure 3.11:** PM sample trapped on filter paper

The specification of the filter paper was given in Table 3.5. In order to avoid any contamination, the filter paper was handled by using tweezers and hand glove during the PM sampling measurement. The tweezers was cleaned and the hand glove was changed each time after the sample was taken. The filter paper, then quickly stored in a petri dish as shown in Figure 3.11 to avoid contamination.

**Table 3.5:** Filter paper specifications

Description	Specifications
Material	Composite filter (PTFE coated)
Trademark	ADVANTEC
Type	PG-60
Size	47 mm
Weight	60 g/m <sup>2</sup>
Thickness	0.15 mm
Max.operating temperature	260°C
Quantity	100 leaf
Lot Number	20919702
Manufacturer	Toyo Roshi Kaisya, Ltd.

### 3.3.4 Sampling Pump

The sampling pump used in this study is sampling pump Flite 2 by SKC Inc. as shown in Figure 3.12. This instrument was applied to draw air from the exhaust tailpipe through the filter holder which holds the filter paper to trap the PM. The pump was set at the flow rate of 2 liters per minute. Before the experiment, the sampling pump was calibrated by using pump calibrator in order to get accurate flow rate. The 0.75 cm diameter tube was attached to inlet hose tail and connected to filter holder to trap the PM. Detailed specification of the sampling pump was showed in Table 3.6.



Figure 3.12: Sampling pump

Table 3.6: sampling pump specification

Description	Specification
Dimensions	178 mm W x 115 mm H x 206 mm D
Flow range	2-26 litre/m
Maximum sampler back pressure	62 kPa (250 inches H <sub>2</sub> O)
Storage/ operating temperature	-5 to +50 °C
Charging temperature	-5 to +45 °C
Relative humidity	0 – 95% RH

### 3.3.5 Forced Convection Oven

Before sample collection, the filter paper was heat in the forced convection oven in order to get rid of the moisture in the filter. Other than that, it is important to associate the initial condition when the filter receives high heat from the exhaust as a result of the combustion process. The heating process needs to be done in two hours with the temperature of 50°C. This step was done after the sample collection and also after the filter paper was immersed in dichloromethane (Yusop et al., 2012).

### 3.3.6 High Precision Electric Balance

High precision electric balance was applied to weight the filter paper during the sampling process as shown in Figure 3.13. The specification of this instrument can be found in Table 3.7. The sample was weighted before sample collection to get a gross mass of filter paper. After PM sample was taken, the filter paper was weighed again to get the total mass of filter paper and PM. The PM mass was obtained by minus the gross mass of filter paper by the total mass of filter paper and PM.

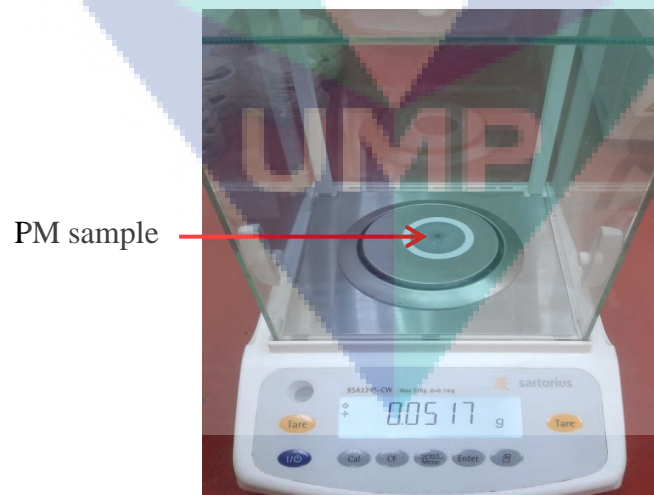


**Figure 3.13:** High Precision Electric Balance

**Table 3.7:** Electric balance specification

Description		Specification
Readability	(g)	0.0001
Weighing capacity	(g)	120
Repeatability	(g)	0.0001
Linearity	(g)	0.0002
Response time (average second)		25

### 3.3.7 Dichloromethane

Dichloromethane was used as the solvent in the extraction of SOF from the particulate matter since SOF is soluble in dichloromethane. Dichloromethane properties was showed in Table 3.8. The filter paper was immersed completely in 20 ml dichloromethane for 24 hours to extract the SOF as shown in Figure 3.14.



PM sample

**Figure 3.14:** Sample in dichloromethane**Table 3.8:** Dichloromethane properties

Description	Properties
Molecular weight	84.9
Specific gravity	1.3255 20°C/4°C
Melting point	-95°C
Boiling point	39.75°C at 760 mm Hg
Water solubility	0.24% at 20°C
Vapor pressure	435 mm Hg at 25°C
Vapor density relative to air	2.93

### 3.3.8 Field Element Scanning Electron Micrograph (FE-SEM)

In order to examine the particle size and morphology of PM, the PM sample was observed in the field element scanning electron microscope (FE-SEM) model JEOL JSM-6701F at 10 kV accelerating voltages. Figure 3.15 shows the FE-SEM used in this study. It scans the sample's surface with a high energy beam of electrons, which produce signals of the surface topography information when interacting with the sample atoms. For conventional imaging, specimens must be electrically conductive, at least at the surface and electrically grounded. As the samples in the tests were captured on filter paper, before placing them in the FE-SEM specimen chamber, they were coated with metals (gold in the tests).



**Figure 3.15:** FE-SEM

## 3.4 TEST FUEL

The transesterification, blending and analysis of the test fuel properties were carried out by laboratory of the Faculty of Chemical & Natural Resources Engineering, Universiti Malaysia Pahang. Biodiesel was originated from WCO collected from local

household. The transesterification process followed ASTM D6751 guidelines. A total of five test fuels were prepared for conducting the research. The test fuels chosen were (a) diesel fuel (b) 5 % WCO biodiesel with 95 % diesel fuel (WCO B5), (c) 10 % WCO biodiesel with 90% diesel fuel (WCO B10), (d) 20 % WCO biodiesel with 80 % diesel fuel (WCO B20) and (e) 100 % WCO biodiesel (WCO B100). The properties of each test fuel are illustrated in the Table 3.9.

**Table 3.9: Properties of test fuel**

<b>Parameter</b>	<b>ASTM method</b>	<b>ASTM D6751</b>	<b>Diesel fuel</b>	<b>WCO B5</b>	<b>WCO B10</b>	<b>WCO B20</b>	<b>WCO B100</b>
Density (g/cm <sup>3</sup> )	D 941	0.88	0.843	0.844	0.846	0.851	0.882
Kinematic Viscosity at 40°C (mm <sup>2</sup> /s)	D 445	1.9-6.0	3.718	3.754	3.776	3.829	4.282
Cetane Number	D 613	> 46	46.6	46.9	47	48.9	57.7
Calorific Value (MJ/kg)	D 240	N/A	42.32	42.08	39.29	38.67	35.02
Acid Number (mgKOH/g)	D 664	0.5 max	0.270	0.270	0.274	0.280	0.340
Cloud Point (°C)	D 97	N/A	-3	0	0	0	8
Pour Point (°C)	D 97	N/A	-10	-9	-9	-8	-4

### 3.5 TEST OPERATING CONDITION

The testing was done according to SAE J1349 Standard Engine Power Test Code as reference (SAE, 2004). The tests were carried out at a steady-state testing condition. It was conducted with 5 different test fuels (diesel fuel, B5, B10, B20, B100) at 5 different engine speeds which were 1200 rpm, 1500 rpm, 1800 rpm, 2100 rpm and 2400 rpm. The load applied on the engine was kept constant at 20 Nm. Before data collection, the engine ran steadily for 15 minutes prior to the test. In order to ensure the accuracy and consistency of the measurement data, the engine had been running roughly five minutes after changing the fuel. Certain amount of new fuel should burn before the next measurement in order to avoid the influence of previous test fuel. Table 3.10 shows the test matrix for the test fuel. The tests were repeated for four times and the average data was taken to guarantee the reproducibility of the results.

**Table 3.10:** Test matrix for test fuel

Test Fuel	Repeatability	Speed (rpm)				
		1200	1500	1800	2100	2400
Diesel	4	√	√	√	√	√
B5	4	√	√	√	√	√
B10	4	√	√	√	√	√
B20	4	√	√	√	√	√
B100	4	√	√	√	√	√

For PM sampling measurement, the PM emission was trapped on the composite filter paper. The filter was weighed before and after sampling by a high precision electric balance. It was weighted under controlled temperature and relative humidity. The oven was used to heat the filter before and after the experiment in order to avoid the humidity on the filter when the filter was being weighted. The duration and temperature of heating process are controlled within two hours at 50 °C. Using dichloromethane solution, SOF and Soot can be extracted and the concentration can be measured. Gravimetric analysis was applied to find the mass concentration of PM, SOF and soot. FE-SEM imaging was applied in order to observe the PM morphology and the information obtained from image analysis has been used to derive the PM characteristics (Ariana et al., 2006).

### 3.6 PARTICULATE MATTER ANALYSIS

This study focus on determine the PM emission from diesel engine. There are two analyses that have been done to get the PM characteristics. Gravimetric analysis was applied to get the PM concentration while image analysis was applied to obtain PM distribution. These analyses was done for all 25 samples collected.

#### 3.6.1 Gravimetric Analysis

Gravimetric analysis was applied in order to analyze the PM concentration and its component which were SOF and Soot. The difference in mass of filter paper before and after each test was determined. Therefore, the total mass concentration of PM, SOF and Soot can be calculated as mentioned below(Yusop et al., 2012). :

a) Particulate Matter (PM):

$$\text{Mass of filter (before)} = \mathbf{a} \text{ (g)} \quad (3.1)$$

$$\text{Mass of filter (after)} = \mathbf{b} \text{ (g)} \quad (3.2)$$

$$\text{PM (c)} = \mathbf{b} - \mathbf{a} \text{ (g)} \quad (3.3)$$

$$\text{PM (c/20 L)} \times 1000 = \mathbf{d} \text{ (g/m}^3\text{)} \quad (3.4)$$

b) Soluble Organic Fraction (SOF):

$$\text{Mass of filter after put in Dichloromethane solution} = \mathbf{e} \text{ (g)} \quad (3.5)$$

$$\text{SOF (f)} = \mathbf{b} - \mathbf{e} \text{ (g)} \quad (3.6)$$

$$\text{SOF (f/20 L)} \times 1000 = \mathbf{g} \text{ (g/cm}^3\text{)} \quad (3.7)$$

c) Soot:

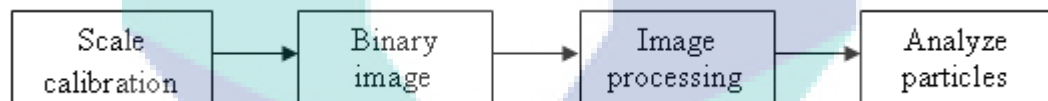
$$\text{Soot (h)} = \mathbf{d} - \mathbf{g} \text{ (g/cm}^3\text{)} \quad (3.8)$$

### 3.6.2 Image Analysis

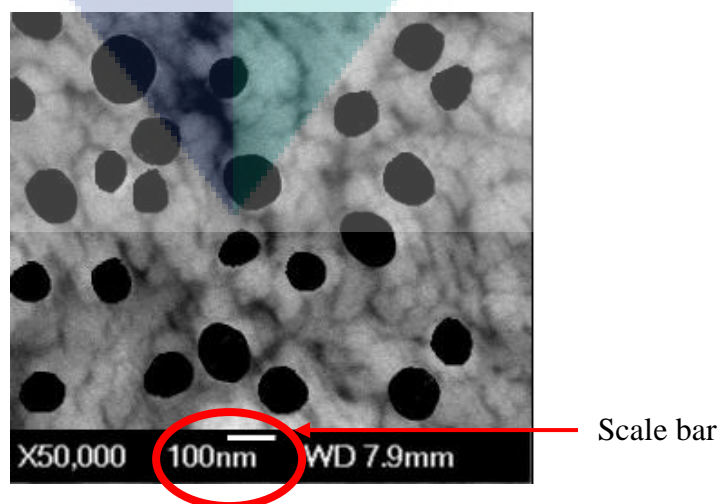
For morphological investigation, PM samples were observed with the FE-SEM and image analysis was applied. Sampling duration was kept at 1 minute with a flow rate of 2L/m. PM samples were collected on 47 mm composite filter paper PTFE coated. Each sample was cut into small size square section with dimension 5 mm<sup>2</sup> and these sections were observed with the FE-SEM. The analysis was carried out on a JEOL JSM 6701F microscope. This analysis was done to obtain the particle diameter to plot the PM distribution. Each image generated by FE-SEM was analyzed by Microsoft Paint and ImageJ software developed by the National Institute of Health (NIH). ImageJ

software can read image formats such as TIFF, GIF, JPEG, BMP, DICOM and FITS. The FE-SEM image in this study is in JPEG format.

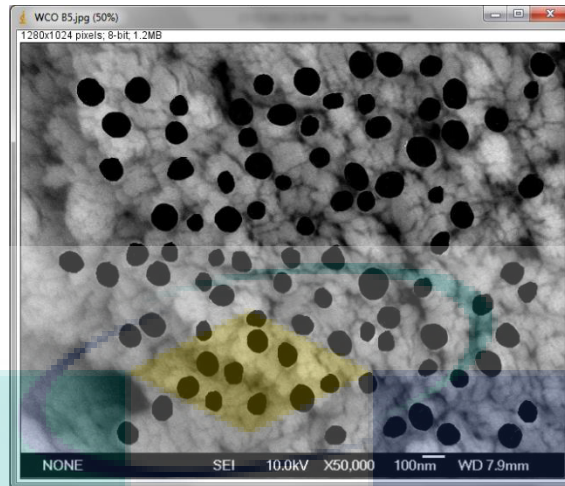
The first step involved in the image analysis procedure was to select the particle of interest with black color by using Microsoft Paint. The image then opened in ImageJ software to be analyzed. Figure 3.16 shows the image analysis process in ImageJ. The scale was calibrated by setting the measurement scale using the scale bar from the FE-SEM images as shown in Figure 3.17. The length of the scale bar in the images was reported in pixels. With the known distance of the scale bar, the pixels can be converted into nanometer (nm) by using a scale factor. The image was converted to 8 bit grayscale image which have 256 intensity graduations which can be assigned to a pixel. A pixel with an intensity of 0 is black while a pixel with a value of 255 is white. The image was then converted into binary image by thresholding the particles. Thresholding removes unwanted background information leaving behind only the particles. It assumes that the images have black object and white background.



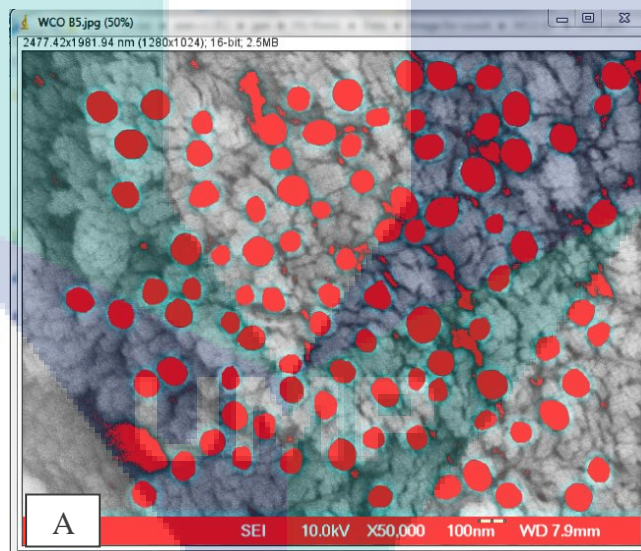
**Figure 3.16:** Image analysis process



**Figure 3.17:** Scale bar in FE-SEM image



**Figure 3.18:** Image prior to threshold



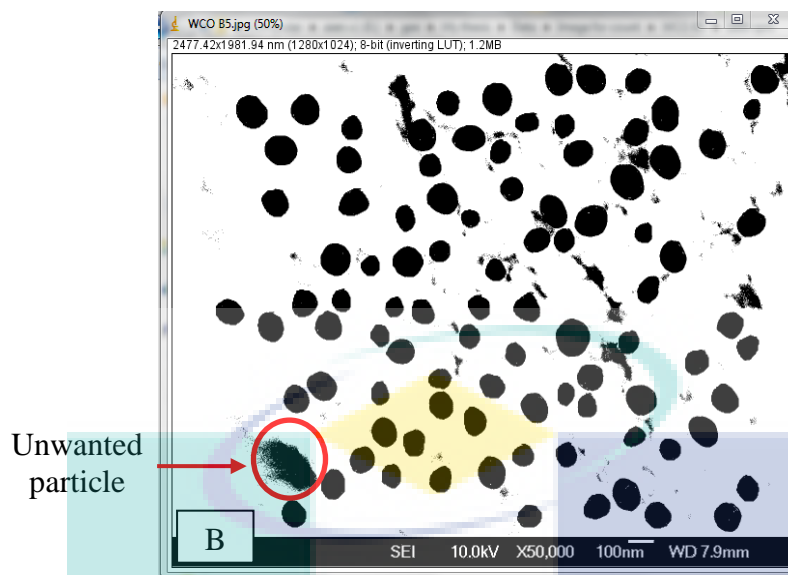


**Figure 3.19:** A) Threshold adjustment, B) Binary image

Figure 3.18 shows the image of PM which has been selected prior to threshold. Thresholding will separate the background from particle of potential images. As shown in Figure 3.19 (A) threshold adjustment was applied to match the particles. While adjusting, the threshold features are displayed in red and the background is displayed in grayscale. The threshold was set at an intensity value of 30 for all FE-SEM images. When the threshold was applied, the background is removed, leaving only the black images of particle as shown in Figure 3.19 (B). However, it is difficult to separate the background from particles of interest. Some of the unwanted particles will existed in binary image as shown in Figure 3.19 (B). Therefore, after converting to binary image, the unwanted particle was cleared and despeckle or erode function followed by dilate were applied to the image. These functions will remove any single pixel particles that are not of interest resulted in the final binary image. The final binary image which ready to be analyzed was shown in Figure 3.20.

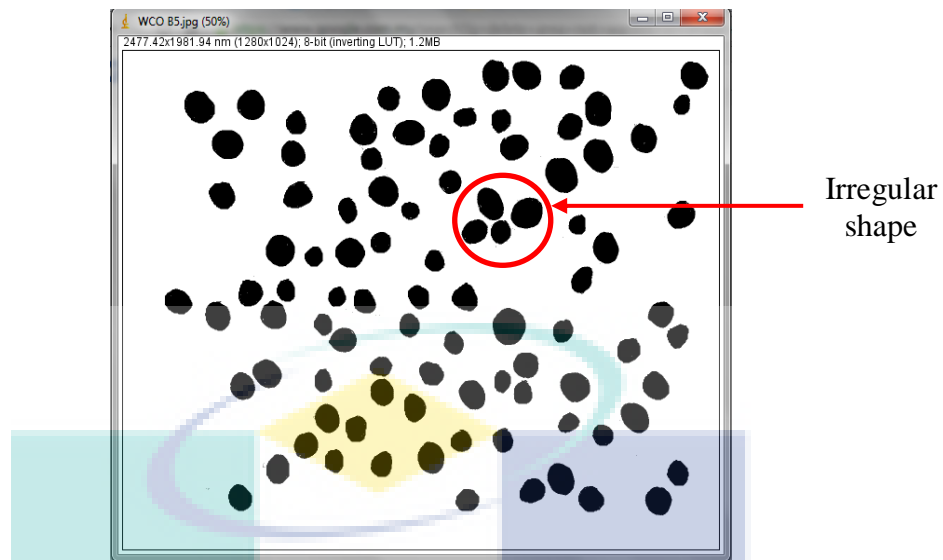


**Figure 3.20:** Final binary image

Before analyzing the particle, measurements that have to be included will be set. Since the particles are in irregular shapes as shown in Figure 3.20, *Fit Ellipse* function was used to find areas enclosed by individual particles. *Fit Ellipse* calculates the smallest area enclosed by an ellipse. Area and feret's diameter were measured in the image analysis. The result generated is in the data table. The data is saved and imported into spreadsheet software for statistical analysis. Particle size can be determined from the area as it was assumed that the particles are equivalently spherical. The diameter of the particles can be found by the formula:

$$r = \sqrt{\frac{A}{\pi}} \quad (3.9)$$

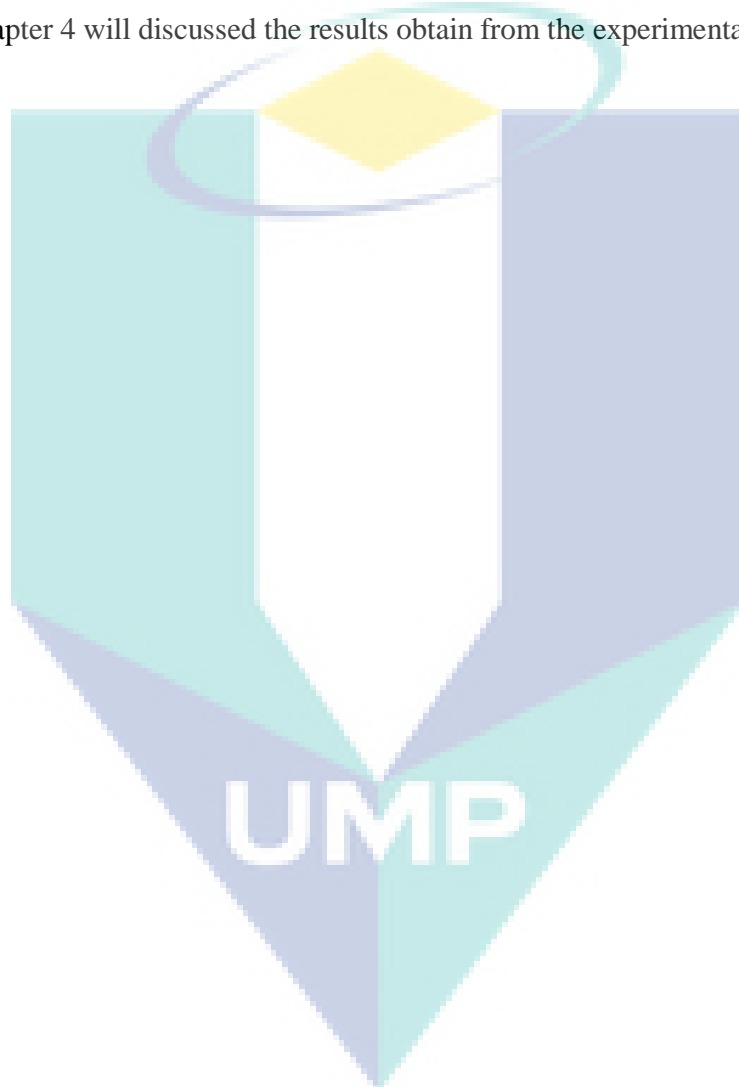
Where  $r$  is the radius and diameter,  $D = 2r$ .  $A$  is area and  $\pi = 3.14159$ . Graph of size distribution was plotted and mean diameter was found for each test fuel with different engine speed with the equation of mean diameter:

$$\bar{d} = \frac{1}{n} \sum_{i=1}^n d_i \quad (3.10)$$

Where  $d$  is PM diameter,  $n$  is the total number of PM diameter.

### 3.7 SUMMARY

This chapter describes the experiment set-up system in the tests. It includes the engine and instrumentation, where all the tests were carried out, exhaust emission measurement, test fuel properties, test operating condition and PM analysis. The specifications of the instruments and equipments were given in detail. The next chapter, which is chapter 4 will discussed the results obtain from the experimental work.



## CHAPTER 4

### RESULT AND DISCUSSIONS

#### 4.1 INTRODUCTION

This chapter will discuss the result obtained throughout the experiment conducted in this study. The engine operating parameters such as fuel type, engine speed and engine design can affect the emissions emitted by internal combustion engines. Different type of fuel has different properties which can affect the emission of diesel engine. Therefore, detailed explanation of the operating parameters, especially the properties of the fuel and operating engine speed will be discussed in this section.

The result was divided into six main sections which were in-cylinder pressure, exhaust temperature, PM mass concentration, PM morphology, PM size distribution, gaseous emission and PM/NO<sub>x</sub> trade Off. The comparison between diesel and WCO biodiesel blends at various engine speeds has been made for each section. In PM mass concentration section, the influence of SOF and soot in PM formation has been discussed in detail. The effect of engine speed and WCO biodiesel blends on PM size distribution is also deliberated in the section on PM size distribution. In gaseous emission section, influence of the engine speed and WCO biodiesel blends on CO, O<sub>2</sub>, CO<sub>2</sub>, NO<sub>x</sub>, and NO emission was discussed. The last section will be focused on the PM-NO<sub>x</sub> trade off which always been an obstacle in reducing emission of diesel engines.

## 4.2 IN-CYLINDER PRESSURE

In-cylinder pressure data must be analyzed in order to understand the complete combustion process and events occurring in the combustion chamber. The relationship between in-cylinder pressure and crank angle indicates the performance of the engine. It gives a gross indication related to engine knock, the location of peak pressure and the value of the peak pressure. Basically, the factors that affect peak pressure include compression ratio, types of fuel, air fuel ratio and types of engine. The crank angle at which peak pressure developed inside the cylinder was determined for each fuel blends and was compared with diesel fuel in terms of peak pressure magnitude and crank angle location.

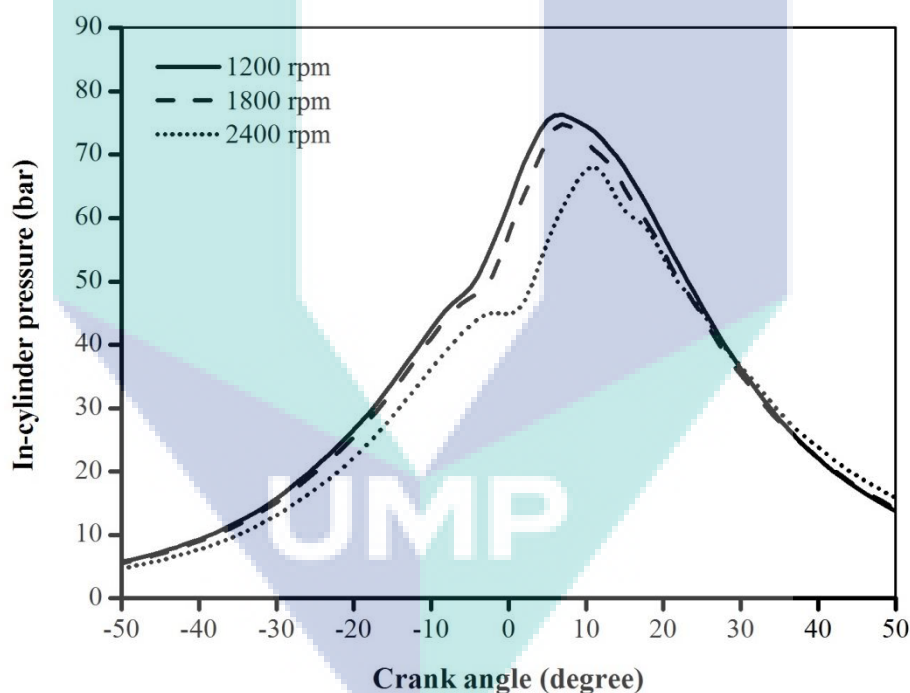


**Figure 4.1:** Variation of in-cylinder pressure of diesel fuel

Figure 4.1 shows the variation of in-cylinder pressure for diesel fuel at low engine speed 1200 rpm, moderate engine speed 1800 rpm and high engine speed 2400 rpm. From this figure, it can be seen that lower engine speed generates higher in-cylinder pressure compared to moderate and high engine speed. It gives higher peak pressure, which is 76.24 bar at crank angle 7° after top dead centre (ATDC). While peak

pressure for 1800 rpm is 74.82 bar at crank angle  $7^\circ$  ATDC and 2400 rpm gives peak pressure 68.17 bar at crank angle  $11^\circ$  ATDC. The peak pressure difference of 1800 rpm and 2400 rpm compared to 1200 rpm is 1.88 % and 11.18 %, respectively. B100 also presented similar trend with diesel fuel where lower engine speed generates higher in-cylinder pressure as shown in Figure 4.2. The highest peak pressure for B100 is at engine speed 1200 rpm with 77.39 bar at crank angle  $8^\circ$  ATDC, while at engine speed 1800 rpm, the peak pressure is 73.56 bar at  $7^\circ$  ATDC and peak pressure of engine speed 2400 rpm lies on 65.29 bar at  $11^\circ$  ATDC.

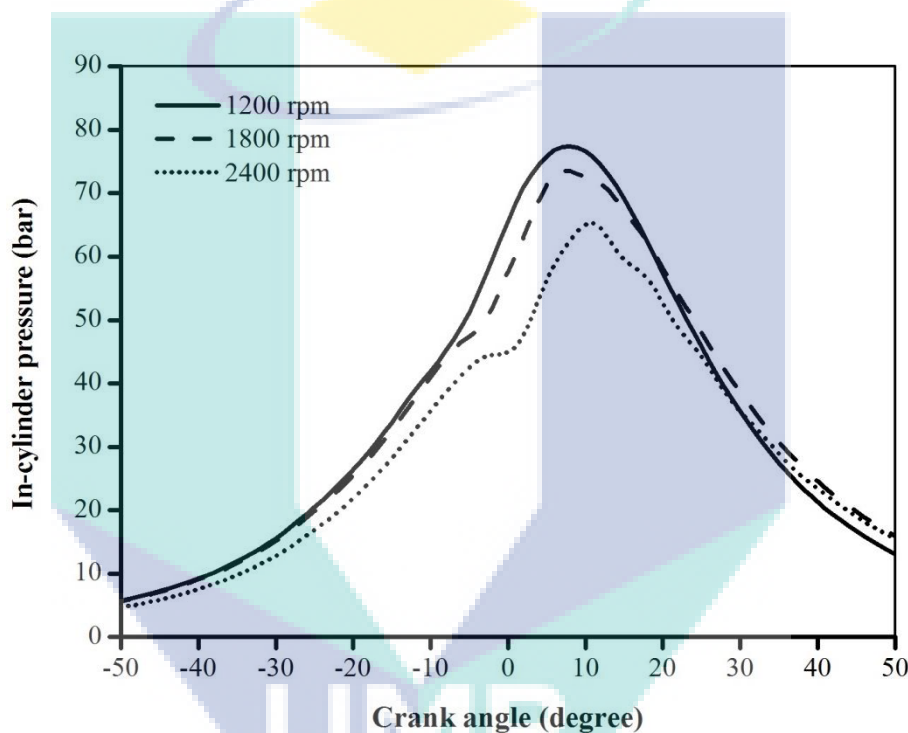


**Figure 4.2:** Variation of in-cylinder pressure of B100

From Figure 4.1 and 4.2, it can be seen that the ignition delay period for diesel fuel and B100 apparently increases with the increasing engine speed. The start of ignition point can be specified at which the pressure increases suddenly and the pressure at this point is the ignition pressure. It determines the quantity of premixed flame, forming the rate of pressure increase and its maximum value (Enweremadu and Rutto, 2010). Increasing engine speed will decrease the loss of heat during compression resulting in the increment of temperature and pressure, thus shortening the ignition

delay period in milliseconds. However, the ignition delay period is prolonging in degree of crank angle as the engine speed increase (Shankhdhar and Kumar, 2014).

The ignition delay period of the test fuel at every engine speed is shown in the graph of in cylinder pressure in Figure 4.1 and 4.2. The fuel injection of Yanmar TF120 for all engine speed is start at  $-18^\circ$  before top dead centre (BTDC). For diesel fuel, at engine speed 1200 rpm, the combustion starts at  $-5^\circ$  BTDC which means the ignition delay period is  $13^\circ$ . Meanwhile, at engine speed 1800 rpm, the combustion starts at  $-3^\circ$  BTDC with the ignition delay period of  $15^\circ$  and at engine speed 2400 rpm, the ignition delay period is  $19^\circ$  where the combustion start at  $1^\circ$  ATDC. For B100, the ignition delay period at engine speed 1200 rpm is  $11^\circ$  as the combustion starts at  $-7^\circ$  BTDC. At engine speed 1800 rpm, the combustion starts at  $-4^\circ$  BTDC with the ignition delay period is  $14^\circ$  while the combustion starts at TDC at engine speed 2400 rpm with the ignition delay period of  $18^\circ$ . The ignition delay period for diesel fuel and B100 clearly shows an increment as the engine speed is increase. Therefore, the possible reason of in-cylinder peak pressure decrement as engine speed increase is because of the longer ignition delay period for higher engine speed where combustion starts later which may lead to poor combustion. As a result, the in-cylinder peak pressure attains a lower value as it is further away from the TDC in the expansion stroke (El-Kasaby and Nemit-allah, 2013).

B100 generates slightly higher in-cylinder peak pressure compared to diesel fuel with the difference of 1.50 % at lower engine speed of 1200 rpm. The occurrence of in-cylinder peak pressures of diesel fuel is little earlier than B100. For diesel fuel, the in-cylinder peak pressure is 76.21 bar at  $6^\circ$  ATDC and B100 is 77.39 bar at  $7^\circ$  ATDC. Generally, cylinder pressure depends on the burned fuel fraction during the premixed combustion stage. B100 generates higher in-cylinder peak pressure may due to the higher cetane number and shorten ignition delay. Shorten ignition delay results in earlier combustion (Enweremadu and Rutto, 2010). In addition, the higher oxygen content of the B100 increases fuel–air mixing rate in the cylinder compared to diesel fuel. This situation may cause B100 extend the combustion duration and enhance the combustion efficiency resulting in slightly higher in-cylinder peak pressure at lower engine speed (Savariraj et al., 2013).

Despite that, B100 generates slightly lower in-cylinder peak pressure at moderate and high engine speed with the difference of 1.70 % and 4.30 %, respectively. The occurrence of in-cylinder peak pressure of both fuel happened at the same crank angle at both moderate and high engine speed. At moderate engine speed 1800 rpm, the in-cylinder peak pressure of B100 and diesel fuel is 73.56 bar and 74.82 bar at the crank angle  $7^\circ$ , respectively. While the in-cylinder peak pressure at high engine speed 2400 rpm is 65.29 bar and 68.17 bar at crank angle  $11^\circ$  for B100 and diesel fuel, respectively. The reason of lower in-cylinder peak pressure of B100 compared to diesel fuel may be that a complex and rapid pre-flame chemical reaction takes place at high temperatures. In addition, higher viscosity of B100 causes poor atomization contributes to slower air-fuel mixing thus generate slightly lower in-cylinder peak pressure at high engine speed.

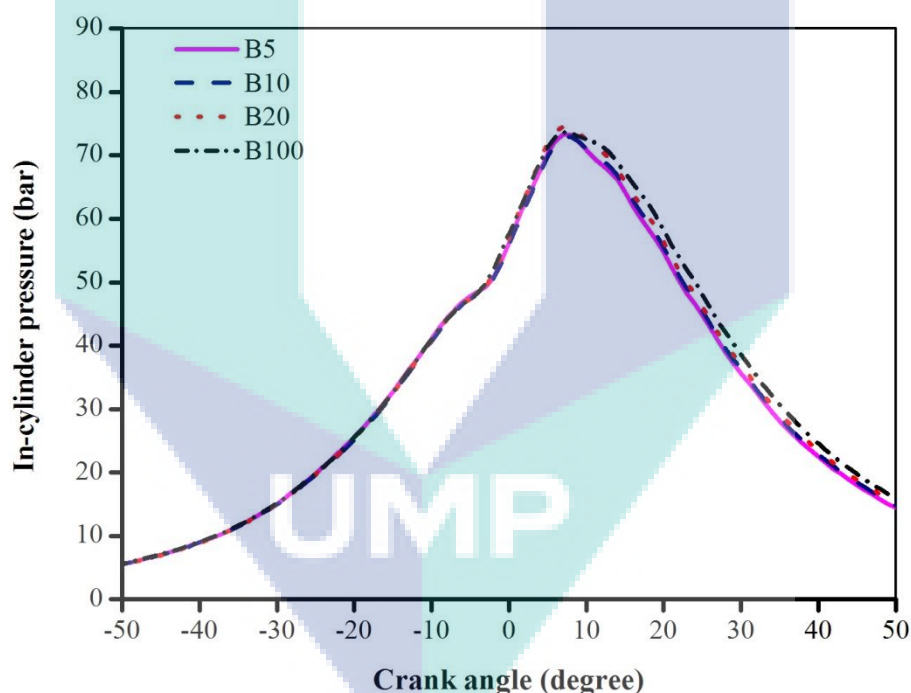


**Figure 4.3:** In-cylinder pressure of WCO biodiesel blends at 1800 rpm

Variation of in-cylinder pressure for WCO biodiesel blends was plotted in Figure 4.3. From this figure, it is observed that the peak in-cylinder pressure of B5 is 73.26 bar at  $7^\circ$  ATDC, B10 is 72.90 at  $8^\circ$  ATDC, B20 is 74.51 at  $7^\circ$  ATDC and B100 is 73.56 bar at  $7^\circ$  ATDC. The peak in-cylinder pressure is uncertain with the increasing WCO biodiesel ratio in the fuel blends. However, the combustion process of the test

fuels is similar, consisting of a phase of premixed combustion following by a phase of diffusion combustion. As mentioned before, a higher cetane number of the fuel shortens the ignition delay which results in the advanced combustion process. At the same time, the ignition delay increases with increasing aromatic compounds of the fuel (Al-Dawody and Bhatti, 2014). Therefore, decreasing blending ratio of WCO biodiesel should decrease the peak in-cylinder pressure due to higher amount of aromatic compound exist in diesel fuel.

### 4.3 EXHAUST TEMPERATURE

Observation of exhaust temperature in this study is important as it is an indication of the amount of energy released during combustion. (Li et al., 2006). The exhaust emission of diesel fuel and WCO biodiesel blends was measured and compared at five different operating engine speeds. All WCO biodiesel blends shows a significant difference in term of exhaust temperature compared to diesel fuel. Figure 4.4 shows the variation of exhaust temperature with different engine speed using diesel fuel and WCO biodiesel blends. The engine speed was set up at a range of 1200 to 2400 rpm. From the figure, it can be seen that the exhaust temperature for diesel fuel is slightly lower compared to B5, B10, B20 and B100.

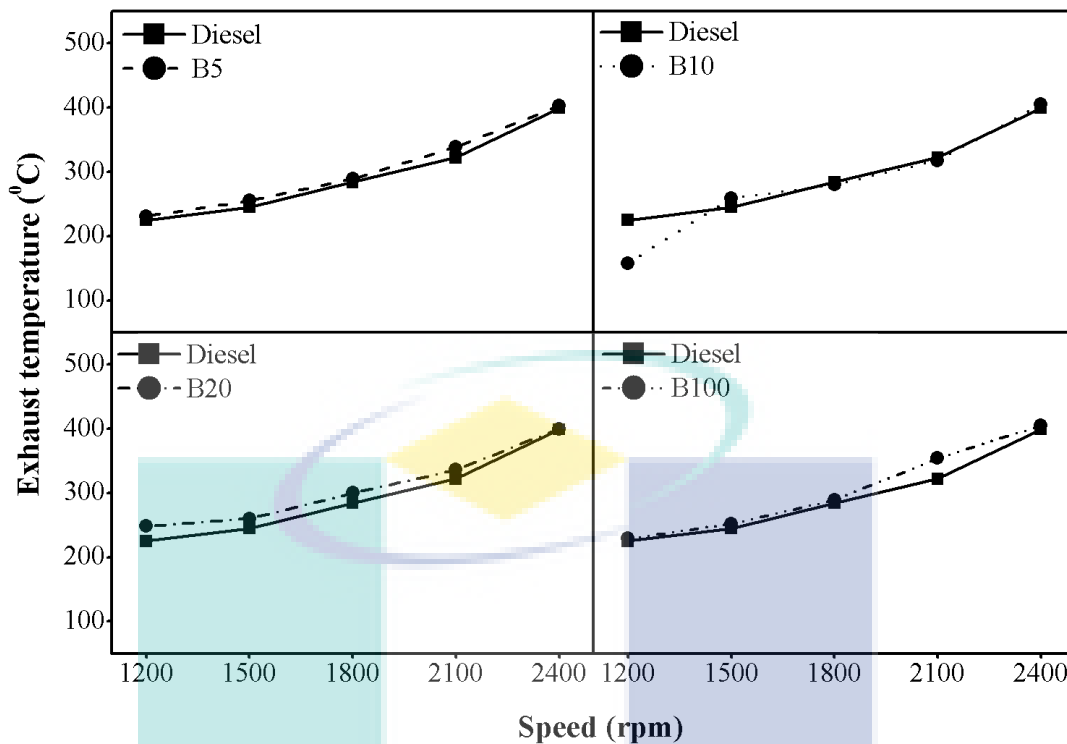


**Figure 4.4:** Variation of exhaust temperature with different engine speed and fuel

The exhaust temperature for B10 shows uncertainty trend where at engine speed 1200 rpm it recorded the lowest temperature which is 158 °C with the difference of 34.99 % lower than diesel fuel. The highest exhaust temperature observed is 405 °C with B10 and B100 at engine speed 2400 rpm with the difference of 1.49 % higher compared to diesel fuel. While the maximum exhaust temperature obtained for diesel fuel is 399 °C at engine speed 2400 rpm. WCO biodiesel blend has a higher exhaust temperature compared to diesel fuel due to its oxygen content which contributed to complete combustion thus improve the diffusion combustion rate. As a result, late burning of WCO biodiesel is reduced, therefore reduced the exhaust gas temperature (Manickam et al., 2014). In addition, referring to CO<sub>2</sub> emission in Figure 4.24, WCO biodiesel blends produce the highest amount of CO<sub>2</sub> compared to diesel fuel. Higher amount of CO<sub>2</sub> indicate more complete combustion of the fuel. This supports the higher value of exhaust temperature of WCO biodiesel blends (Shirnesan et al., 2012).

#### 4.4 PM MASS CONCENTRATION

PM is composed mainly of soot, SOF and sulphur compounds. Soot is formed in a locally fuel rich region while SOF is formed on the soot particle after the exhaust flow is dispersed in ambient air. Sulfate is formed as the result of sulphur oxides. These small compounds form agglomerates, producing in PM. Figure 4.5 illustrated the PM concentration of each test fuel for five different engine speeds. These results indicate that PM emissions were influenced by engine speed. Based on Figure 4.5, we can see that PM concentration for fuel blend B5, B10 and B20 are slightly higher at certain engine speed. This is due to the higher viscosity of WCO biodiesel, which cause deterioration of combustion quality as stated by some authors from previous studies (Aydin and Bayindir, 2010, Banapurmath and Tewari, 2008).

From Figure 4.5, B100 gives the lowest PM concentration compared to diesel and other blends. The reduction of B100 was shown in Figure 4.6. All fuel blends show reduction at low engine speed 1200 rpm to 1500 rpm and increase when the engine speed increase from 1500 rpm to 2400 rpm. Comparing PM reductions between diesel and B100, the highest reduction of PM emission occurred when the engine speed is at 2400 rpm which is 21.82 % of reduction. The lowest reduction is at 1800 rpm which is 5.56 %. From the result of in cylinder pressure obtained, the ignition delay period of diesel is longer than B100. Therefore, the combustion starts at the final stage of the expansion stroke where the temperature inside the chamber is diminishes. This will reduce the speed of oxidation increase the concentration of unburned HC that condense on the surfaces of the PM thus increase PM mass (Cataluña and da Silva, 2012). During diffusive combustion cycle at 2400 rpm, the oxygen content of the WCO and the air ratio is ending up for more effective in reducing PM for B100. The main factor for lower PM emission for B100 is it consists of higher oxygen content which leads to complete combustion and further promote the oxidation of soot. Other than that, lack aromatic and sulphur compounds also contribute to a reduction in PM emissions.

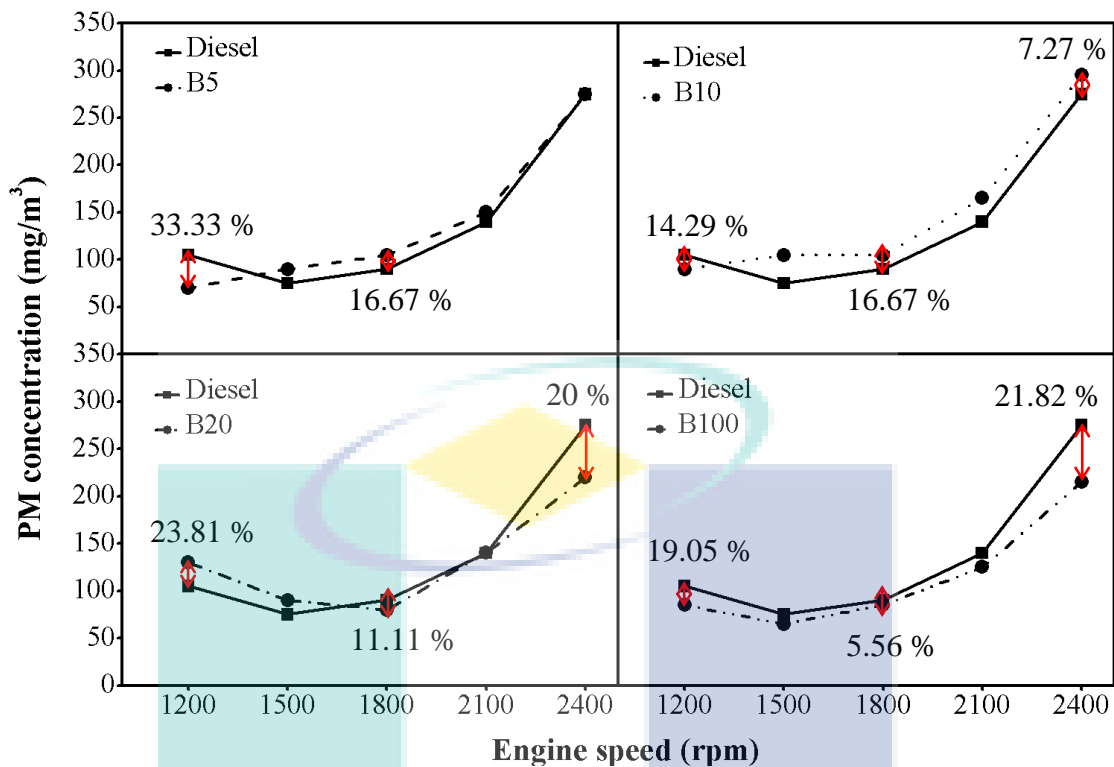


**Figure 4.5:** PM concentration of WCO biodiesel blends and diesel fuel

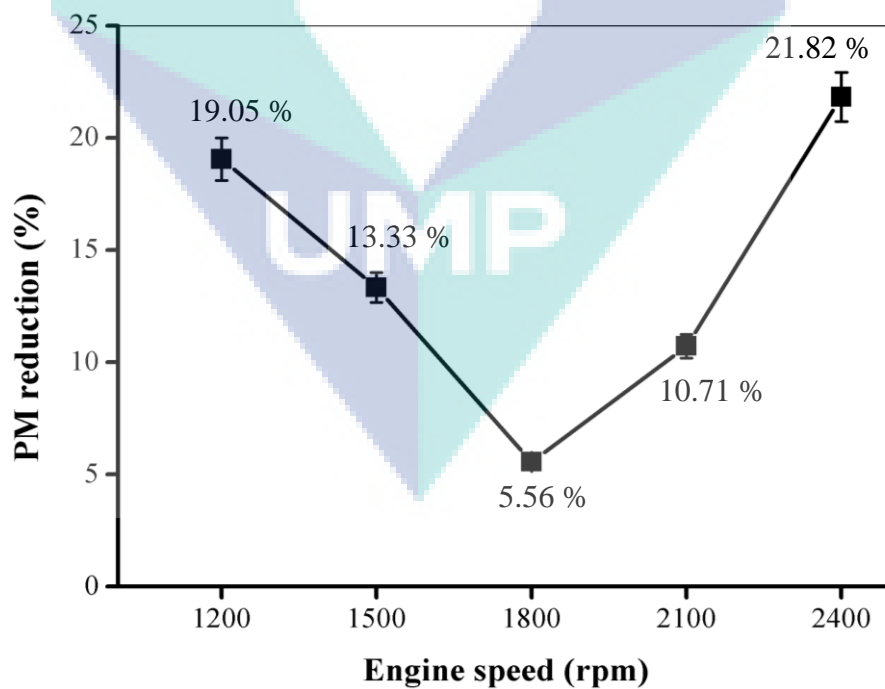


**Figure 4.6:** Percentage of PM reduction of B100 compare to diesel fuel

#### 4.4.1 SOF Component

The SOF in diesel particulate matter consists of aldehydes, alkenes and alkanes, hydrocarbon aliphatic, PAH and PAH-derivatives (Johnson et al., 1994). These elements come from unburned HC, which still contain organic material that needs to be oxidized and lubrication oil, which some lubricating oil appear in the exhaust is unchanged or not combust and escape the process of oxidation. In PM aggregation, the SOF sticks on the surface or inside of the aggregate (Ariana et al., 2006). California has required that the SOF emissions from HDDE fueled with on-road fuels sold in the state of California must not increase SOF more than 6 % above a 48 cetane, 10 % aromatic reference fuel SOF emission values (Hardin, 2009).

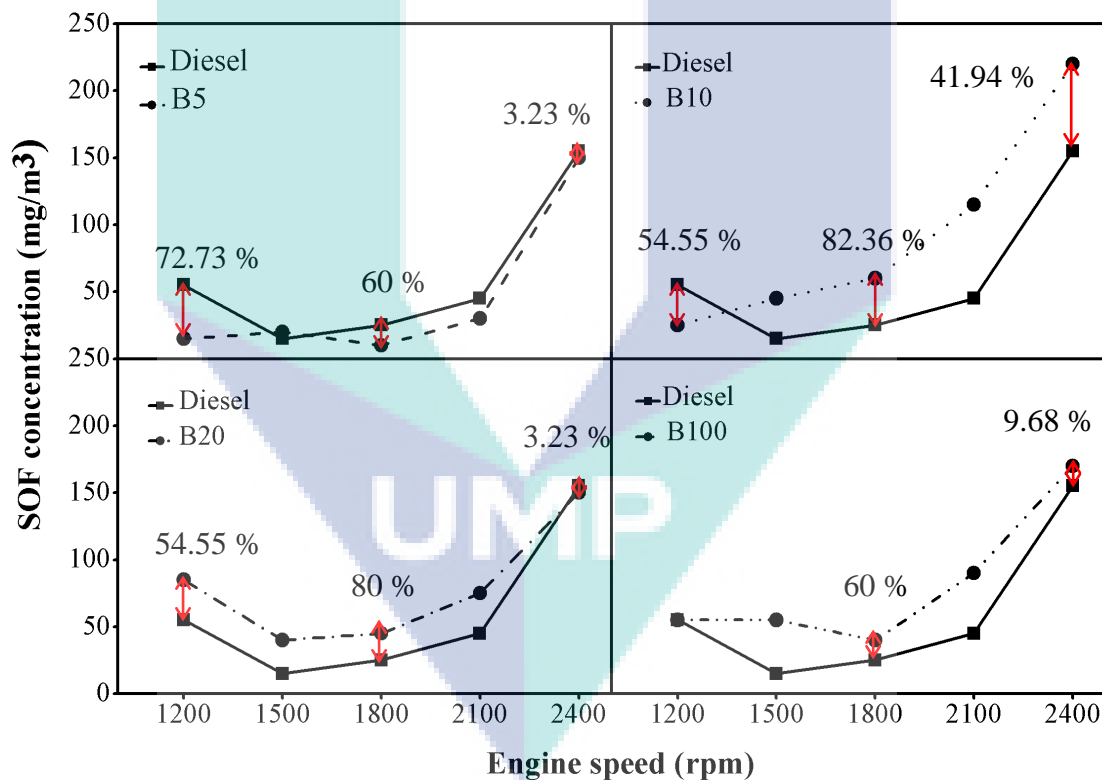


**Figure 4.7:** SOF concentration of WCO biodiesel blends and diesel fuel

From Figure 4.7, it can be seen that the SOF concentration for B10, B20 and B100 are higher than diesel fuel for engine speed 1500 rpm, 1800 rpm and 2100 rpm. This is due to the higher viscosity of the WCO biodiesel which tends to form larger droplets on injection which can cause poor fuel atomization and an incomplete

combustion process thus, increases unburned or partially burned HC emissions. These HC will condense and be absorbed on the PM surface, thus result in the increase of SOF which is the main component of PM (Armas et al., 2010). Due to that process, the PM emissions will also increase. Since biodiesel is nontoxic, the increased level of SOF may not be hazardous. (Dwivedi et al., 2006)

From the experiment, the lowest value of SOF is at 1800 rpm for B5 which is 10 mg/m<sup>3</sup>. In other word, for B5 at 1800 rpm the SOF concentration is decreased due to fuel and air ratio is effective for reducing the SOF. Thus, it has relatively low hydrocarbons and their partial oxidation products leave as SOF. It happens when the equivalent ratio of fuel-air is suitable at the particular speed. The temperature in the cylinder is enough to produce the efficient rate of oxidation. In ideal combustion, air is mixed completely with the atomized fuel. However, in reality, during the combustion, there are zones that are deficient in oxygen. Nevertheless, these zones undergo the heating of combustion, which leads to thermal decomposition. This decomposition can create shorter hydrocarbon chain lengths SOF (Schulz et al., 1999).

#### 4.4.2 Soot Component

Soot consists of a few elements such as small solid carbon particle, sulfate and metal which are formed during the fuel combustion. Figure 4.8 shows the soot concentration obtained from WCO biodiesel blends and diesel fuel. From the graph, B10, B20 and B100 show lower soot emission produced compared to diesel fuel. The lowest soot amount over total PM concentration is 15.38 % for B100 at engine speed 1500 rpm. It is 83.33 % lower than diesel fuel. At engine speed 1200 rpm, soot concentration for B100 is 40 % lower than diesel fuel. While at engine speed 1800 rpm, 2100 rpm and 2400 rpm, soot concentration of B100 are 30.77 %, 63.16 % and 62.5 % lower than diesel fuel, respectively. The figure shows WCO biodiesel has a capability to reduce the soot effectively compared to diesel fuel. Previous research has reported that biodiesel decreases the soot emission and increase the SOF. Soot was formed due to high temperature decomposition which mainly occurs in the fuel rich zone, especially within the core region of fuel spray. WCO biodiesel, which has oxygen content could reduce

locally fuel rich regions and limit soot formation, thus reducing PM emissions. Any unburned ester will condense on the filter and be measured as SOF (Angelovič, 2013).

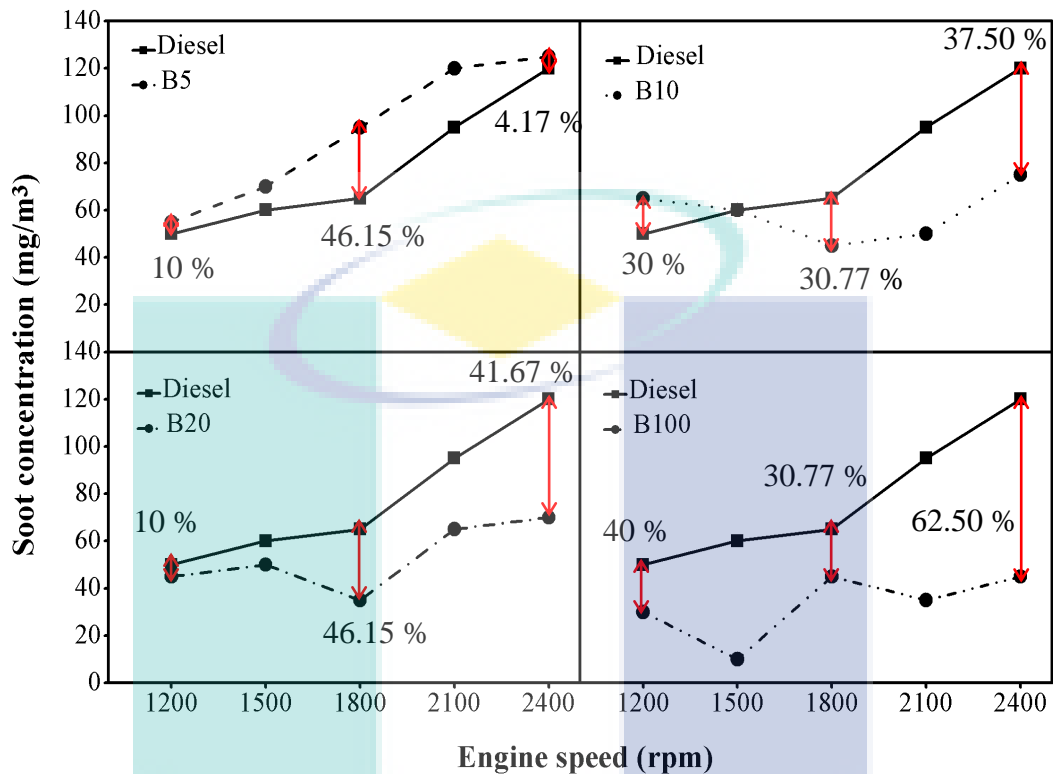
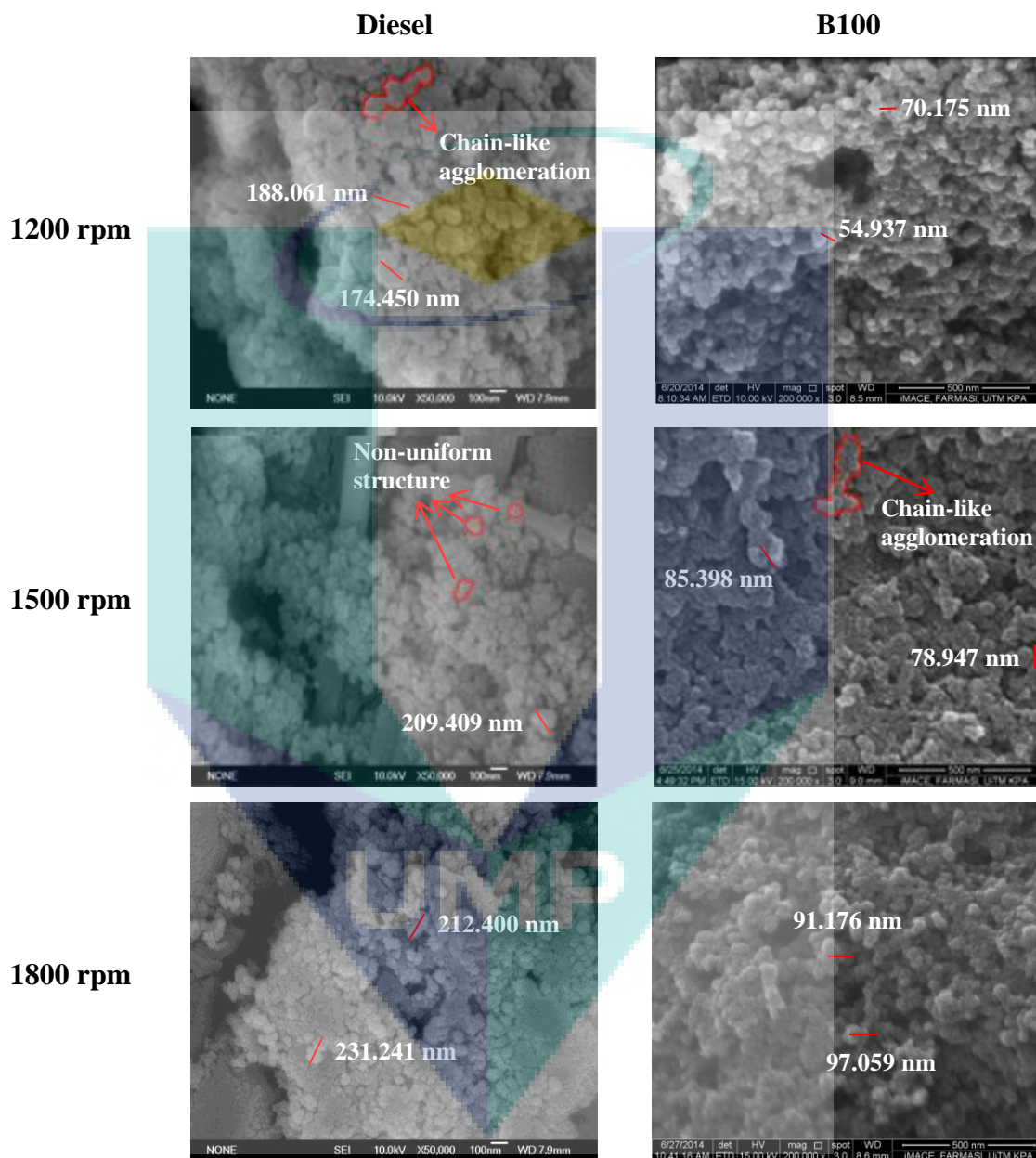


**Figure 4.8:** Soot concentration of WCO biodiesel blends and diesel fuel

#### 4.5 PM MORPHOLOGY

The FE-SEM images of diesel and B100 with engine speed of 1200 rpm, 1500 rpm, 1800 rpm, 2100 rpm and 2400 rpm are shown in Figure 4.9. While FE-SEM images of B5, B10 and B20 are shown in Figure 4.10 with engine speed 1200 rpm, 1800 rpm and 2400 rpm where it represents low, moderate and high engine speed, respectively. All the samples were collected on 47 mm composite filter paper PTFE coated for a period of 1 minute with a flow rate of 2L/m. The images actually show the surface image of the particles. It shows particles of carbon, which are chain-like agglomerations which look more like amorphous carbon. Observation shows that the surface morphology of the PM deposit obtained is non-uniform nanostructure. There are several grains with looks like carbon nanotubes formed. The particles are extremely small with a majority of the particles are approximately 150 nm in diameter. The size of

PM in the nano-range is dangerous when they enter into the human respiratory system. These PM particles can give the worst damage which can reach the finest lung space which is alveoli that can cause the respiratory disease and lung cancer.



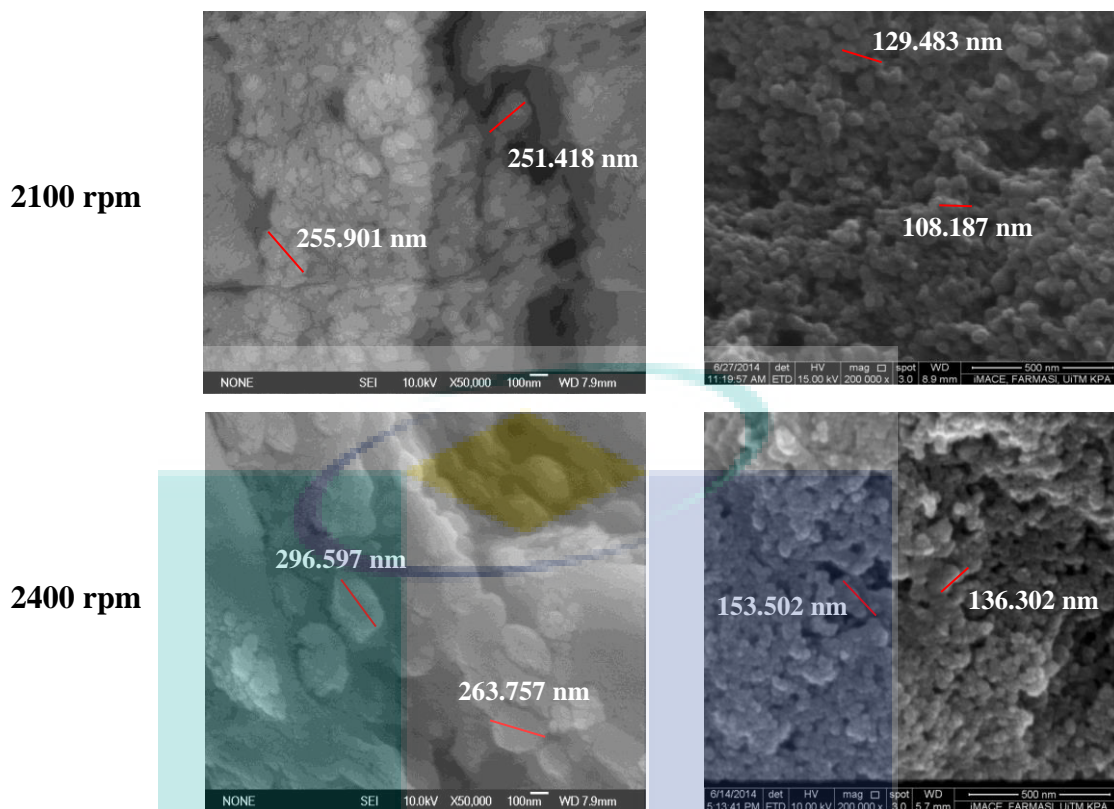


**Figure 4.9:** FE-SEM images of B100 and diesel fuel

From figure 4.9, it can be seen that the size of PM for diesel is slightly larger than B100 for every engine speed conditions. The same trend can be seen in Figure 4.10, where the size of PM is decreased when the blending ratio of WCO biodiesel is increased due to the increasing oxygen content. Combustion in a diesel engine is generally a lean combustion and the oxygen available is enough to burn every fuel droplet in the combustion chamber. However, there are localized regions, where the fuel-air ratio becomes richer than stoichiometric due to the heterogeneous mixing of fuel and air in the combustion chamber. Thus, leads to incomplete oxidation of fuel molecules due to pyrolysis. As a consequence, pyrolyzed compounds, which are primarily soot and unburned HC are formed. In case of biodiesel, the fuel molecule consists of oxygen content which helps in combustion in fuel-rich zones and limits the pyrolysis process. Therefore, B100 leads to the formation of smaller particle compared to diesel fuel (Jung et al., 2006).

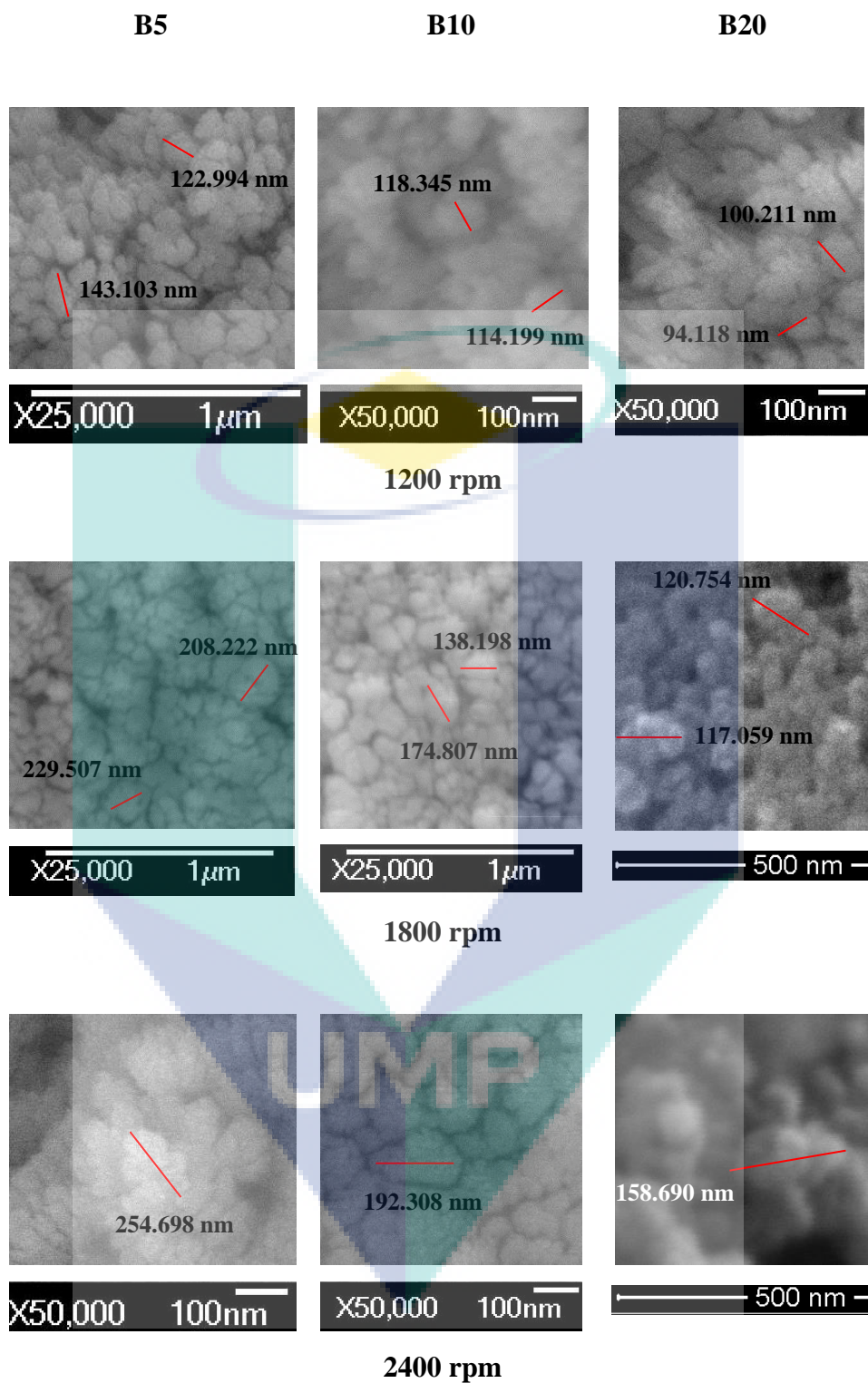


**Figure 4.10:** FE-SEM images of B5, B10 and B20

## 4.6 PM SIZE DISTRIBUTION

### 4.6.1 Effect of Engine Speed on PM Size Distribution

The measurement of PM size distribution is conducted after the engine is stabilized and the result is drawn by a single measurement of each test condition. The PM size distributions emitted from diesel fuel at various engine speeds are shown in Figure 4.8. The increasing engine speed noticeably shifted the PM size distribution from smaller size to larger size for diesel fuel. From Figure 4.11, the smallest particle shows up at engine speed of 1200 rpm which in the range of 0-50 nm with 2.80 % of the total particle count of 107 particles. In addition, 57.01 % of particles are produced in the range of 201-250 nm which the highest count for engine speed 1200 rpm. Engine speed of 1500 rpm also records the highest particle count in the range of 201-205 nm with higher particle count compared to engine speed 1200 rpm which is 60.24 % and the smallest particle is found in the range of 51-100 nm with 4.82 %.

For high engine speed of 1800 rpm, 2100 rpm and 2400 rpm the particles are most often found in the range of 251-300 nm with 56.19 %, 44.83 % and 42.06 % of total particle, respectively. The mean diameter of the particles was measured for each operating engine speed. Mean diameter of particles emitted by diesel fuel is 177.0062 nm, 202.9878 nm, 226.9067 nm, 234.3578 nm and 294.4166 nm for engine speed 1200 rpm, 1500 rpm, 1800 rpm, 2100 rpm and 2400 rpm, respectively. The size of mean diameter becomes larger as the engine speed is increased. Figure 4.12 shows the average particle count of diesel fuel for every engine speed where the highest average particle is in size range of 201-250 nm which is 34.92 % followed by size range of 251-300 nm which is 32.84 %, size range 151-200 nm with 12.95 %, size range 301-350 nm with 8.83 %, size range 101-150 nm with 5.97 %, size range 51-100 nm with 3.91 % and size range 0-50 nm with 0.56 %. From figure 4.11 and Figure 4.12, it shows that diesel fuel produced higher particles in accumulation mode compared to smaller particle in nucleation mode.

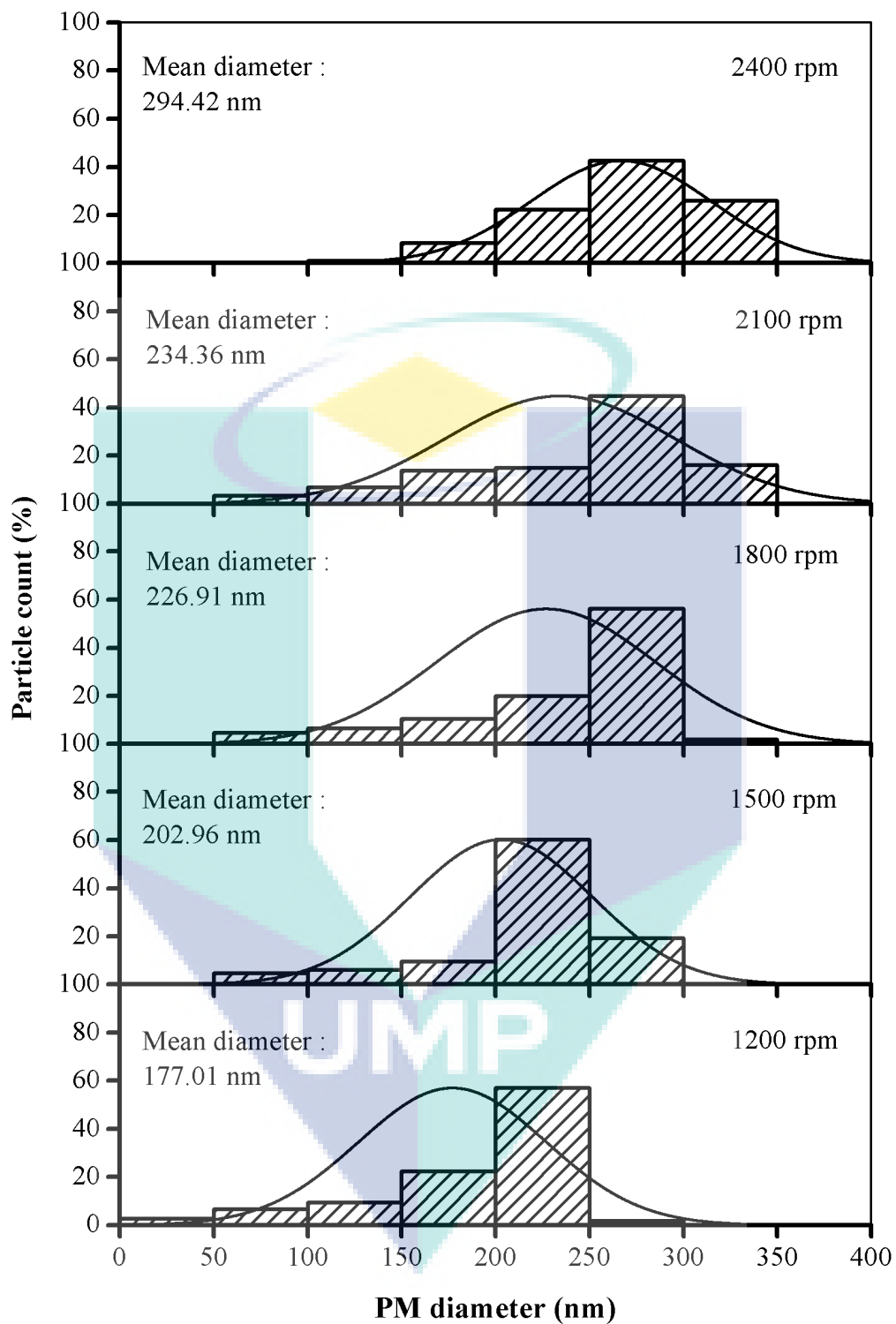


**Figure 4.11:** PM size distribution for diesel fuel

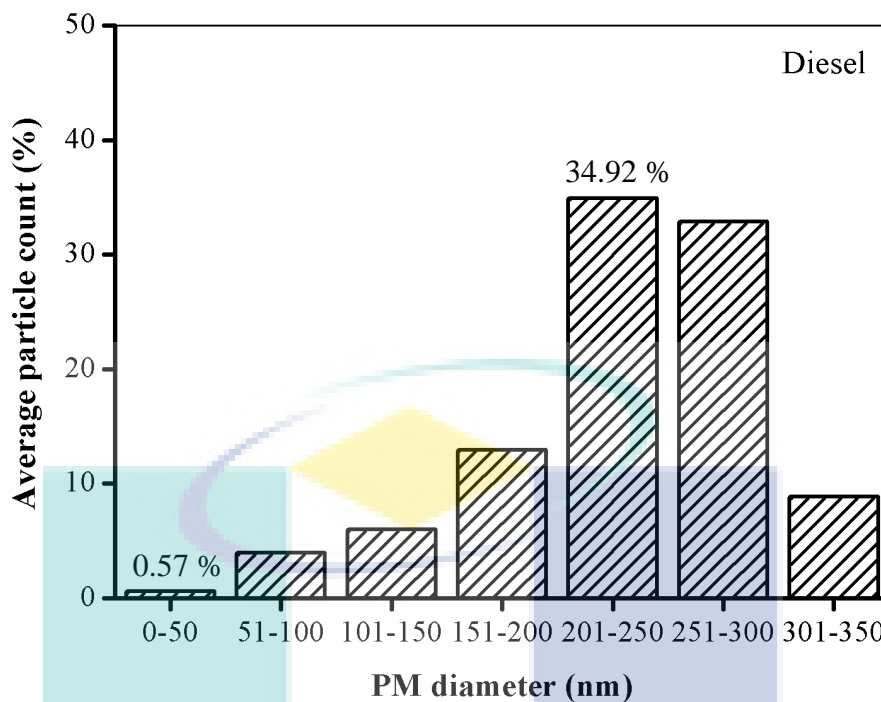


**Figure 4.12:** Average particle count of diesel fuel for each engine speed

Figure 4.13 shows PM distribution for B5 with operating engine speed of 1200 rpm, 1500 rpm, 1800 rpm, 2100 rpm and 2400 rpm. The trend is similar to diesel fuel where the increasing engine speed shifted the PM size distribution from smaller size to a larger size. For engine speed 1200 rpm, most particles are found in the size range of 101-150 nm with 54.32 % and mean diameter of 124.14 nm. While for engine speed 1500 rpm, the highest particles are recorded in the size range of 151-200 nm with 48.24 % by mean diameter of 161.82 nm.

Meanwhile, B5 produce the largest amount of particles in the size range of 201-250 nm for operating engine speed of 1800 rpm and 2100 rpm with 46.07 % and 48.75 % along with mean diameter of 237.84 nm and 236.18 nm respectively. Otherwise, 42.98 % of particles are found in the size range of 251-300 nm for engine speed 2400 rpm with mean diameter of 215.79 nm. The average particle count of B5 was illustrated in Figure 4.14. Figure shows highest average particle count is in the size range 201-250 nm with 27.95 %, followed by size range 151-200 nm with 21.95 %. While size range 101-150 nm, 251-300 nm, 51-100 nm, 301-350 nm and 0-50 nm recorded the reading of

20.85 %, 20.28 %, 7.48 %, 0.83 % and 0.66 %, respectively. Most of the particles are formed in the accumulation mode for B5 which is in the range of 100-300 nm.

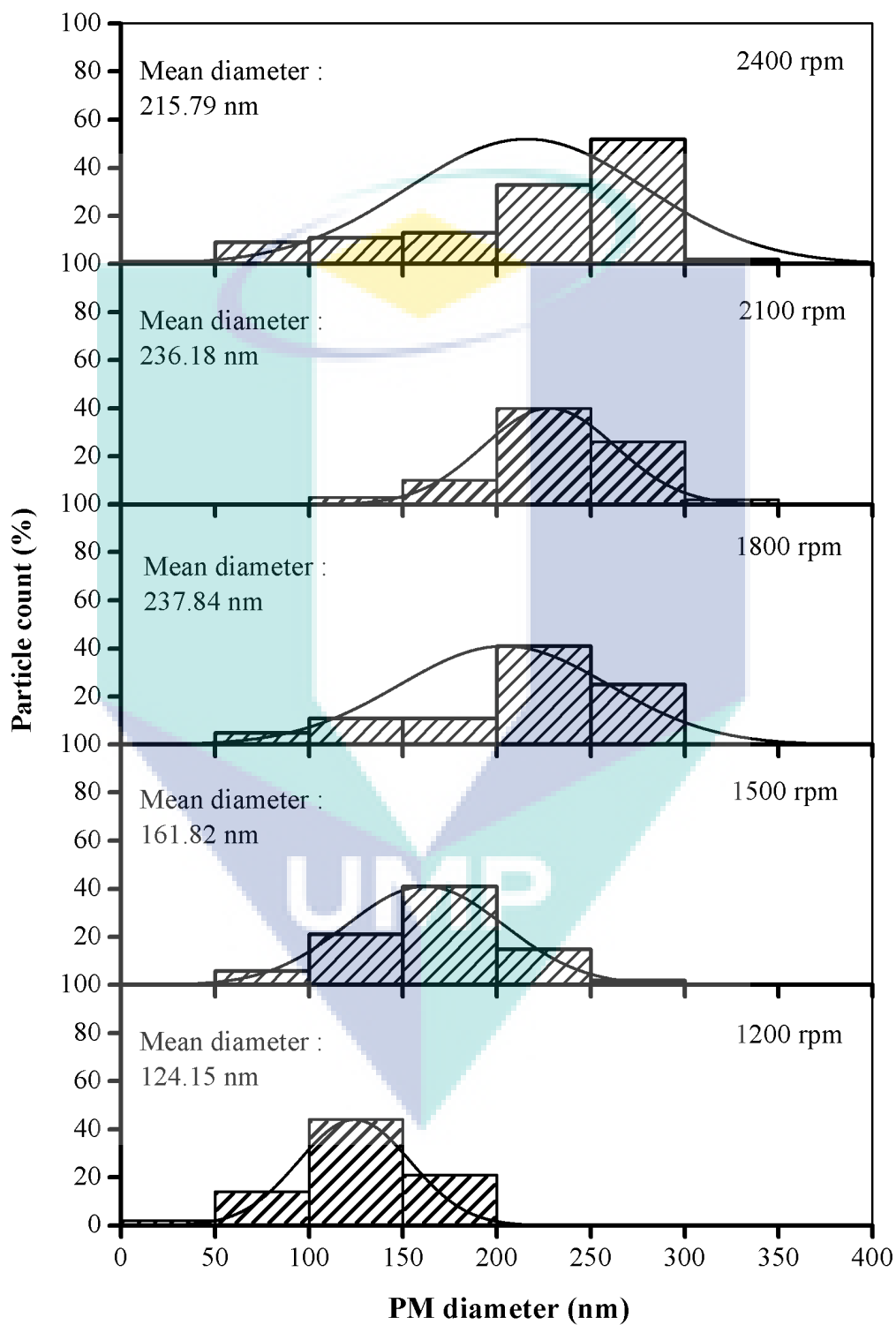


**Figure 4.13:** PM size distribution for B5

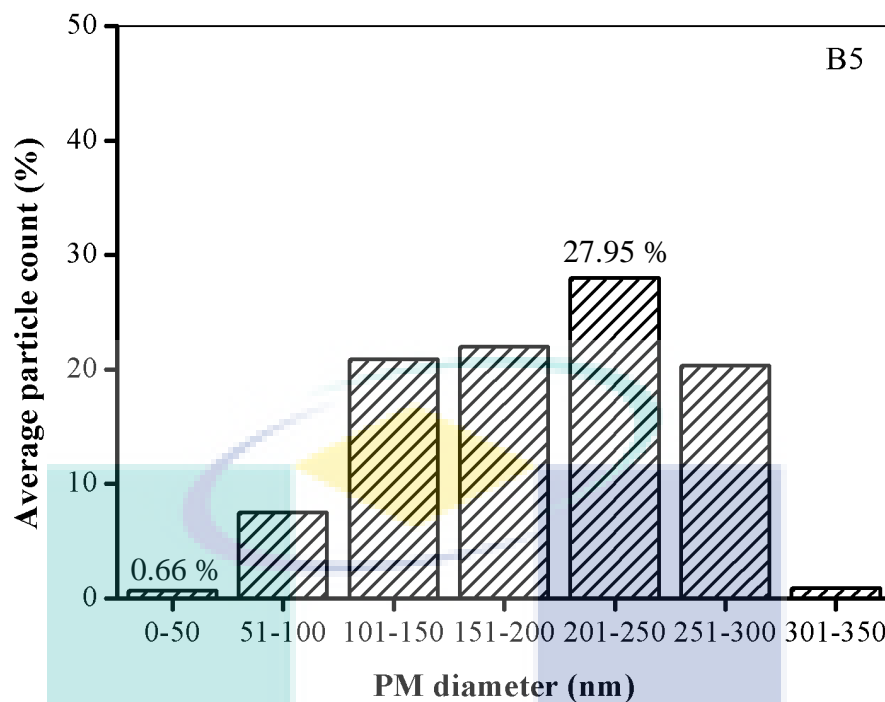
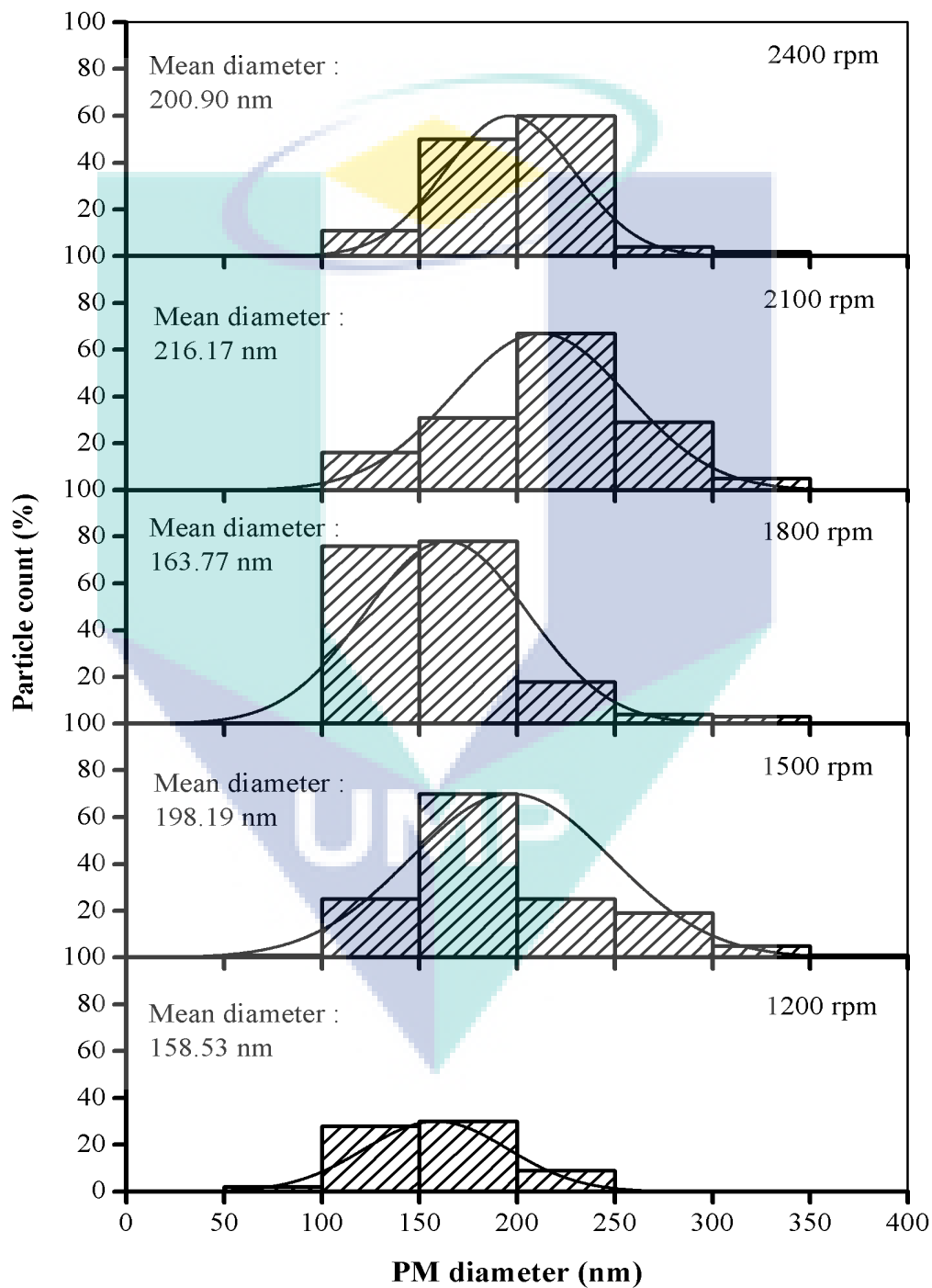


**Figure 4.14:** Average particle count of B5 for each engine speed

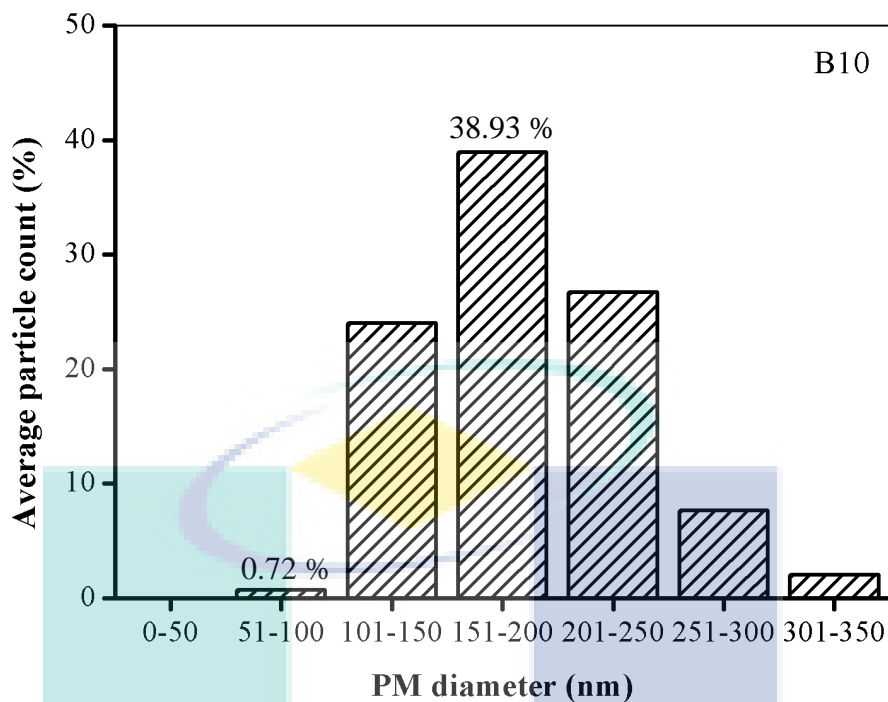
PM size distribution for B10 is shown in Figure 4.15. The distribution also shows the similar trend with diesel fuel and B5 where the PM size distribution is shifted to the larger size as the engine speed is increased. The highest particles found at the engine speed 1200 rpm is in the size range of 151-200 nm with particle count of 43.48 %. Similar with the engine speed 1200 rpm, the highest particles for engine speed 1500 rpm and 1800 rpm also found in the size range of 151-200 nm with 48.28 % and 43.58 %, respectively. Meanwhile, most particles are found in the size range of 201-250 nm for both engine speed 2100 rpm and 2400 rpm with particle count of 45.58 % and 47.62 %, respectively.

Figure 4.16 shows average particle count of B10 for each engine speed. The highest average particle count is at the size range of 151-200 nm with 38.92 %, followed by the size range of 201-250 nm with 26.71 %. While particles in the size range 101-150 nm is 23.98 %. On the other hand, few particles are in the size range of 251-300 nm, 301-350 nm and 51-100 nm with an average percentage of 7.65 %, 2.02 % and 0.72 % respectively. Similar to the diesel fuel and B5, B10 also formed higher particle at the accumulation mode. Operating engine speed 2100 rpm recorded the

largest mean diameter of 216.17 nm followed by engine speed 2400 rpm with mean diameter of 200.90 nm. While mean diameter for engine speed 1500 rpm is 198.20 nm. Meanwhile, mean diameter for engine speed 1800 rpm and 1200 rpm is 163.77 nm and 158.53 respectively.



**Figure 4.15:** PM size distribution for B10



**Figure 4.16:** Average particle count of B10 for each engine speed

Figure 4.17 shows the PM size distribution for B20. The distribution trend followed the diesel fuel, B5 and B10 where the distribution is shifted toward the larger size when the engine speed becomes higher. In case of engine speed of 1200 rpm the particles are found in 3 size ranges which were 51-100 nm, 101-150 nm and 151-200. The highest particles are found in size range of 101-150 nm where it consist of 75 % of the total particle count followed by size range 51-100 nm with 16.30 % and size range 151-200 nm with 8.70 %. Whereas, at engine speed 1500 rpm, the particles are found in 5 different size ranges where the highest particles found in the size range of 101-50 nm with 40.58 % of the total particles count. There are about 28.99 % particles in size range of 151-200 nm, 18.84 % particles in size range of 201-250, 7.24 % particles in size range 51-100, 3.62 % particles in size range 251-300 and 0.72 % particles in size range 301-350.

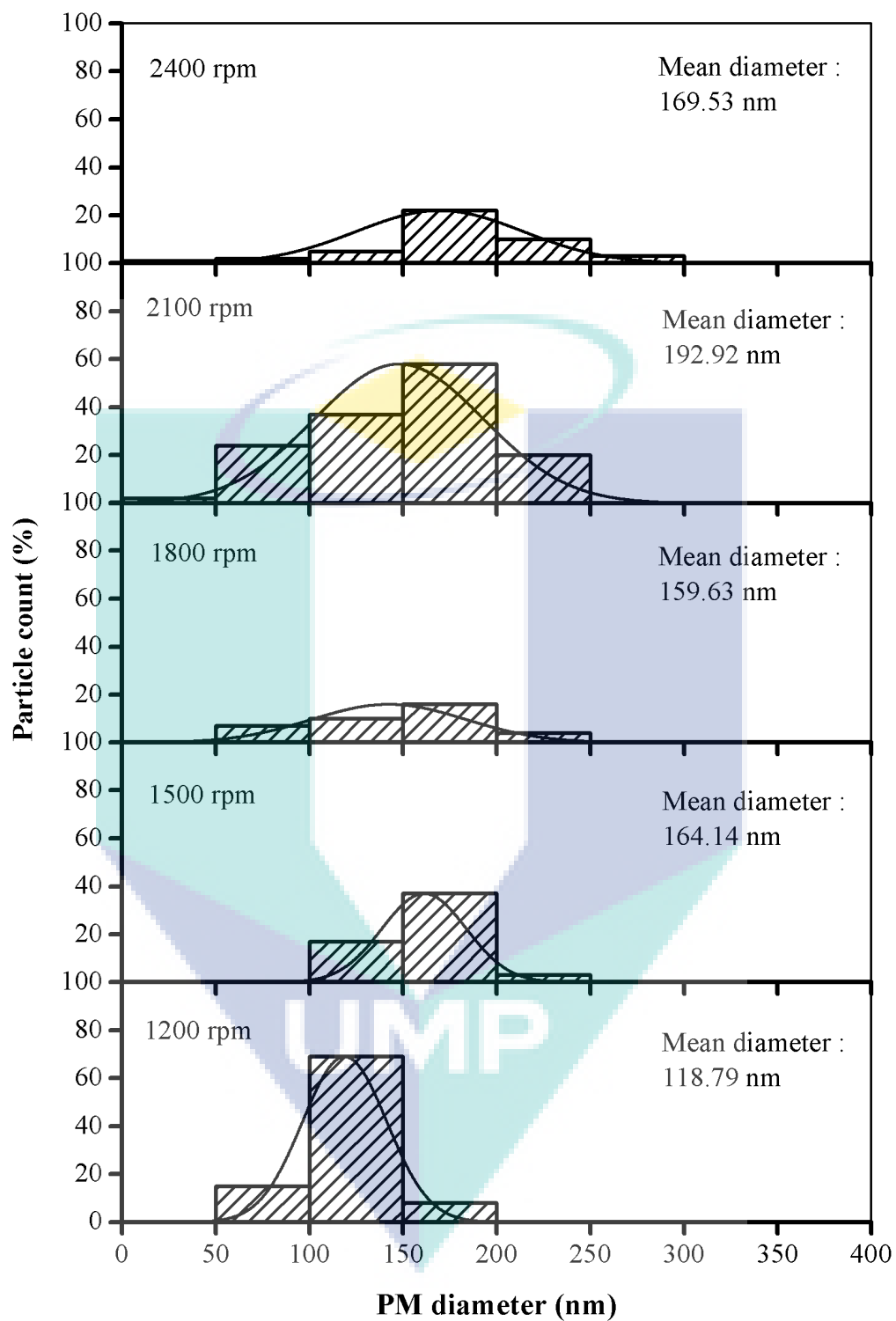


**Figure 4.17:** PM size distribution for B20

For engine speed 1800 rpm, the particles are found in 4 size ranges which the highest particles are in the size range of 151-200 nm with 48.48 % particles. Other

particles are found in the size range of 101-150 nm, 51-100 nm and 201-250 nm with percent count of 30.30 %, 21.21 % and 12.12 %, respectively. The highest particle count for engine speed 2100 rpm is found in the size range of 151-200 nm with 49.07 % of the total particles count. It is followed by the size range of 101-150 nm, 51-100 nm, 201-250 nm and 0-50 nm with the percent count of 32.41 %, 18.52 %, 16.67 % and 1.85 %, respectively. Similar with the engine speed 1800 rpm and 2100 rpm, the highest particles count for engine speed 2400 rpm are found in the size range of 151-200 nm with 51.16 %. About 23.26 % of the particles are found in the size range of 201-250 nm, while 11.63 % particles are in the size range of 101-150 nm. The rest of the particles are found in the size range of 251-300 nm, 51-100 nm and 0-50 nm with percent count of 6.98 %, 4.65 % and 2.32 %, respectively. The PM size distribution of B20 shows higher particles in the accumulation mode with the increment at the nucleation mode compared to B10, B5 and diesel fuel.

PM mean diameter of B20 is 118.79 nm, 164.14 nm, 159.63 nm, 192.92 nm and 169.53 nm for engine speed 1200 rpm, 1500 rpm, 1800 rpm, 2100 rpm and 2400 rpm, respectively. Figure 4.18 shows the average particle count of PM size distribution from all engine speed. Most particles found for B20 is in the size range of 101-150 nm and 151-200 nm which consist of 37.98 % and 37.28 % of the total particles count. While some particles are found in the size range of 201-250 nm, 51-100 nm, 251-300 nm, 0-50 nm and 301-350 nm with the average percentage of 14.55 %, 13.22 %, 2.12 %, 0.84 % and 0.14 % respectively.

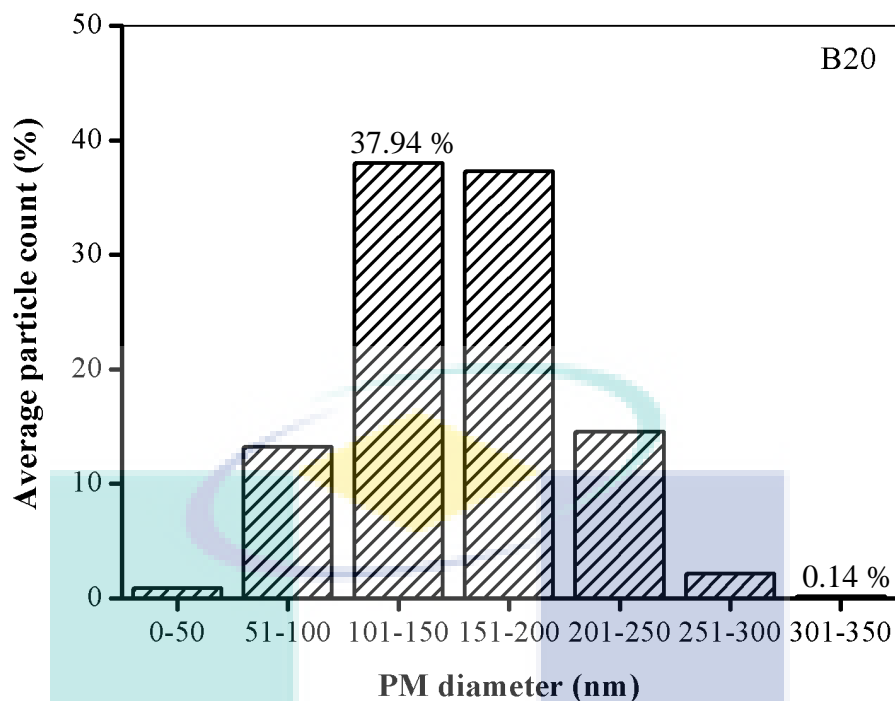


**Figure 4.18:** Average particle count of B20 for each engine speed

Similar with other fuel, the PM size distribution of B100 also shifted to the larger size as the engine speed increases. It can be seen clearly in Figure 4.19. For engine speed 1200 rpm, 1500 rpm and 1800 rpm, the particles are found in 3 size ranges which were 0-50 nm, 51-100 nm and 101-150 nm with the highest particles is found in the size range of 51-100 nm. Engine speed 1200 rpm recorded about 83.82 % particles in this size range followed by engine speed 1500 rpm and 1800 rpm with 72.36 % and 60.87 %, respectively. For engine speed 2100 rpm, the highest particle is found in the range of 101-150 nm with 39.47 % of the total particle count. While other particles are found in the size range of 151-200 nm and 51-100 nm, with particle count of 36.84 % and 18.42 %, respectively. While size range 0-50 nm and 201-250 have the same amount of particle count which is 2.63 %.

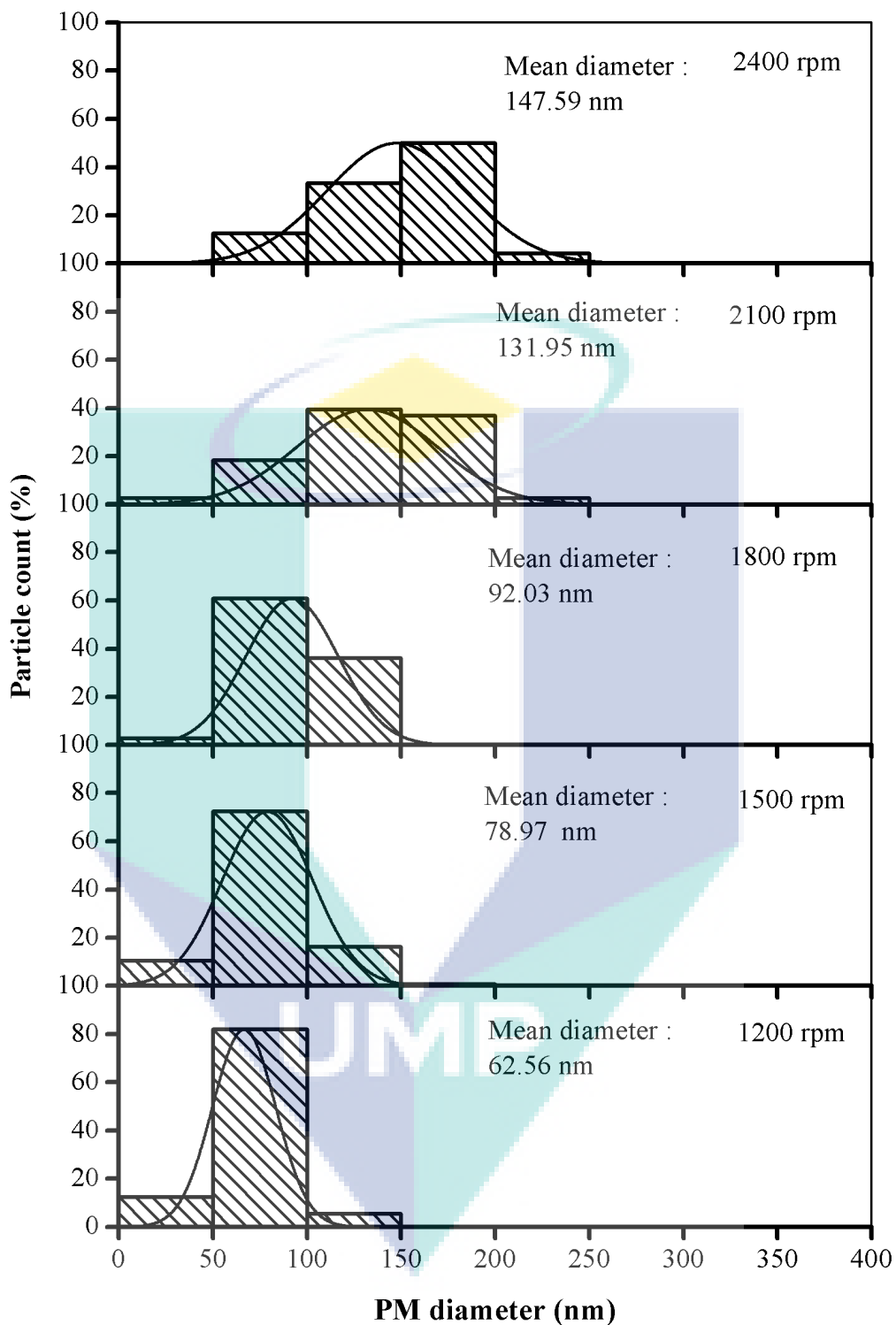


**Figure 4.19:** PM size distribution for B100

Differ from engine speed 2100 rpm, 50 % of the total particles count found for engine speed 2400 rpm is in the range of 151-200. The rest of the particles are found in

the size range of 101-150 nm, 51-100 nm and 210-250 nm with the percent count of 33.33 %, 12.5 % and 4.17 %, respectively. The mean particle diameter of B100 for engine speed 1200 rpm is 62.56 nm, while for engine speed 1500 rpm is 78.97 nm. Meanwhile, mean particle diameter for engine speed 1800 rpm, 2100 rpm and 2400 rpm were 92.03 nm, 131.95 nm and 147.60 nm, respectively. Figure 4.20 represents the average particle count for B100 where the highest percentage is in the range of 51-100 nm which is in the nucleation mode with the 49.59 % of the total particle count from every engine speed. It is followed by size range of 101-150 nm with average percentage of 26.23 %. Around 17.53 % of particles are in the size range 151-200 nm. Other particles are located in the size range of 151-200 nm, 0-50 nm and 201-250 nm with the average percentage of 17.53 %, 5.28 % and 1.36 %, respectively.

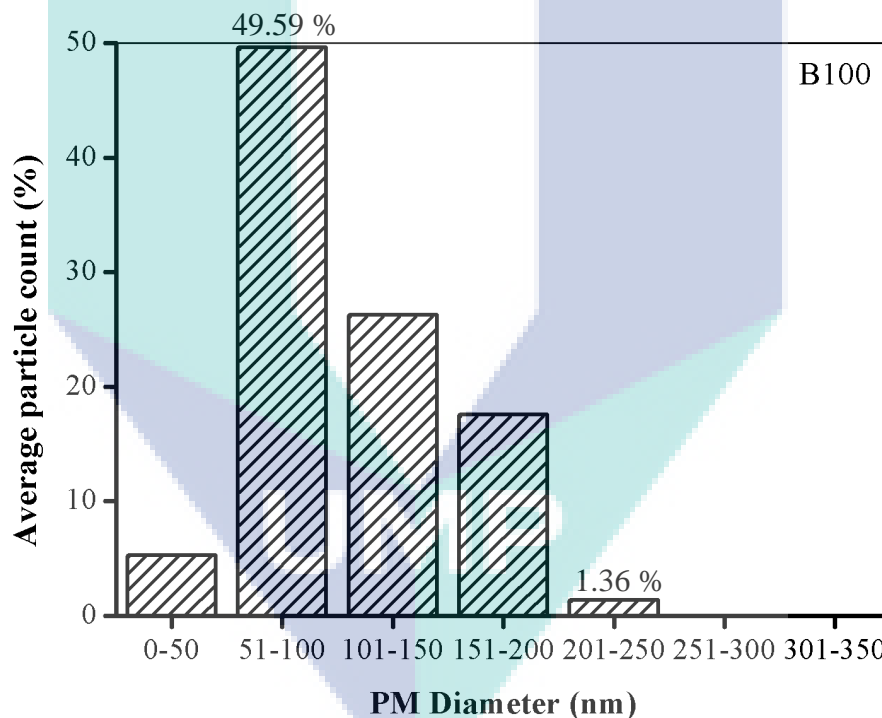


**Figure 4.20:** Average particle count for B100 for each engine speed

From the results obtained, each fuels show a similar trend where PM size distribution is shifted to the larger size as the engine speed increases. As explained in the chapter 2, PM is formed in the locally fuel rich regions of the inhomogeneous combustion in the combustion chamber. Due to high temperature and available oxygen at the boundary of diffusive flame, the fuel burns at that region (Dec, 1997). Referring

back to the result of in cylinder pressure in section 4.2, the ignition delay period is prolong as engine speed is increase. This lead to the delayed combustion event beyond TDC and premixed spikes were lowered. Accordingly, the reaction rate for oxidation of the particulates produced during the combustion will be reduced. Thus, increase bigger particulate emissions at high engine speed at constant load.

#### **4.6.2 Effect of WCO Biodiesel Blends on PM size Distribution**

PM size distribution for diesel fuel and WCO biodiesel blends at engine speed 1800 rpm is shown in Figure 4.21. The figure shows that the higher blending ratio of WCO biodiesel blends shifted the PM size distribution towards smaller PM diameter. While the larger size particles which strongly contribute to the volume and weight of PM, were remarkably decreased. This is due to the enhanced fuel spray characteristics creating an increased proportion of SOF known also as liquid PM (Rounce et al., 2012). From the result obtained in section 4.2, the ignition delay period of WCO biodiesel is shorter than diesel fuel due to higher cetane number of WCO biodiesel. This will generates smaller particles of PM in the pre combustion process. Furthermore, higher oxygen content of WCO biodiesel fuel optimizes at later diffusion combustion process and prevents the transformation of particles from small to large particles (nucleation mode to accumulation mode). Thus, WCO biodiesel greatly improves the combustion process and larger size particles in accumulation mode, decrease rapidly because of its high oxygen content and high cetane number (Puzun et al., 2011).

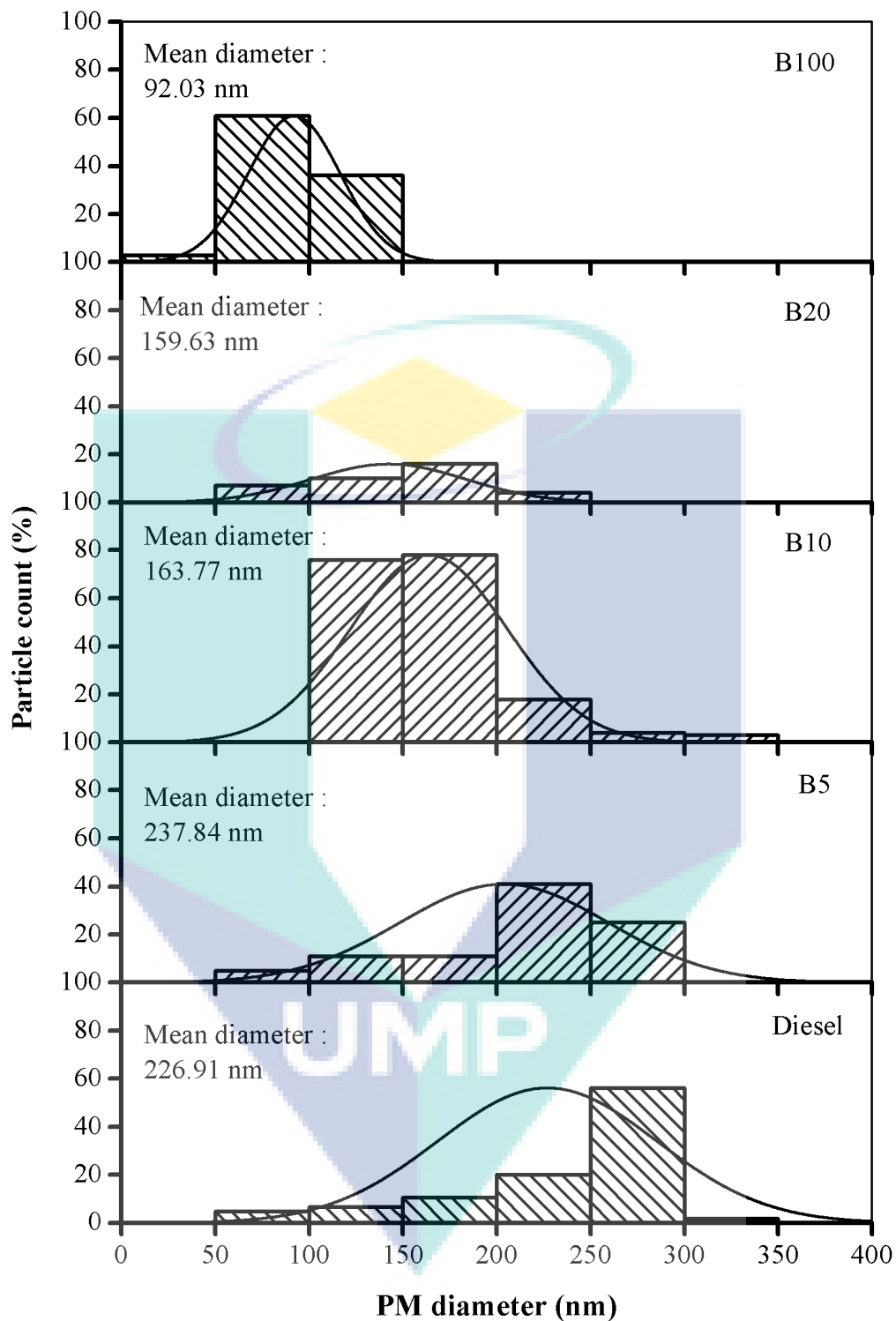


**Figure 4.21:** PM size distribution at engine speed 1800 rpm

## 4.7 GASEOUS EMISSION

### 4.7.1 CO Emission

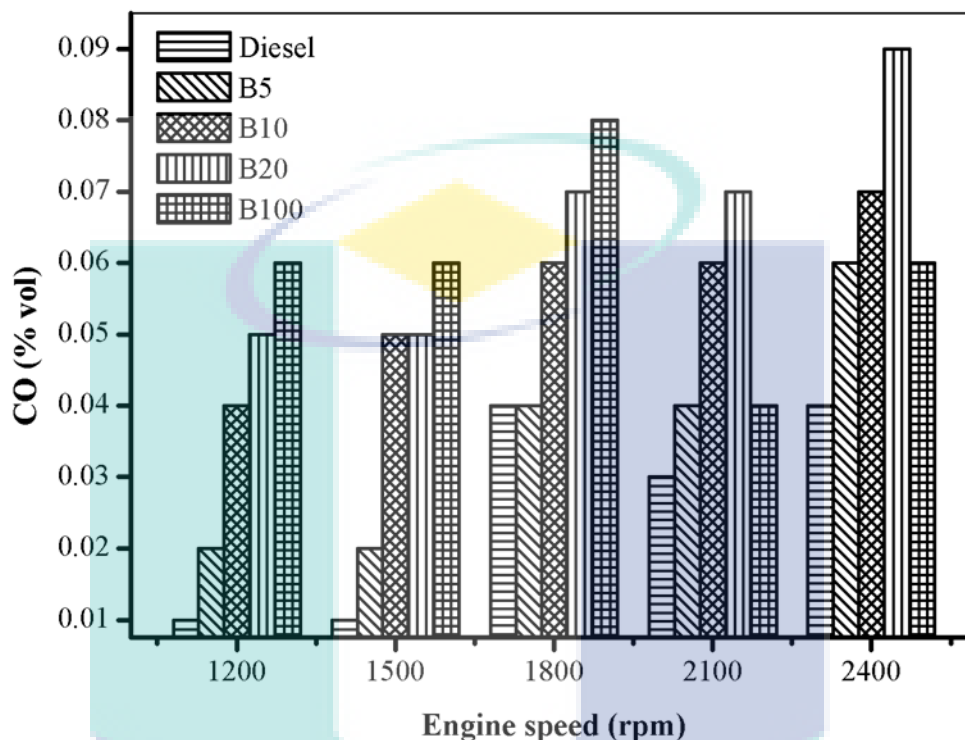


**Figure 4.22:** Emission of CO at various engine speeds

Figure 4.22 shows the emission of CO for each test fuel with different engine speed. At low and moderate engine speed, which is from 1200 rpm until 1800 rpm, the CO emission is found to be increased with the increasing engine speed for all test fuel. However, CO emission of all the test fuel decreased at engine speed 2100 rpm except for B5 which remain no changes for 1800 rpm and 2100 rpm. CO emissions are mostly coming from the incomplete combustion and depend on many parameters such as air fuel ratio and engine temperature. At low speed operation, poor atomization and uneven distribution of small portions of fuel across the combustion chamber, along with low temperature, may lead to local oxygen deficiency and incomplete combustion (Aksoy, 2011). In particular, high oxygen content in biodiesel will promote completes combustion, thus leads to the reduction of CO emissions. Unexpectedly, this study

found that the increment of WCO concentration in the fuel blend causes the increment of the CO emissions compared to diesel fuel.

As shown in Figure 4.22, at engine speed 1800 rpm, CO emission of B5 showed no increment compared to diesel fuel because the concentration of diesel fuel is still higher in B5 blend. The increment of CO emission for B10, B20 and B100 are 50 %, 75 % and 100 % respectively. The contrary results from Figure 4.22 with other studies can be related to the biodiesel production process as explained by Meng et.al. (2008) who's also observed higher CO emission from washed WCO biodiesel in comparison with diesel fuel which has higher viscosity than diesel fuel that causes poor atomization incomplete combustion process. Other than that, according to Valente et. al. (2012) CO formation increase with the increasing fuel injection. As the density of the biodiesel is higher than diesel fuel, the fuel mass amount injected is larger than for diesel engine fuelled with biodiesel. Another possible explanation comes from a higher acid number in the WCO in comparison with diesel fuel. Hamasaki et. al. (2001) discovered that increasing in acid number will increase hydroperoxide concentration which participates in CO formation.

#### 4.7.2 O<sub>2</sub> Emisison

The O<sub>2</sub> emission of diesel and WCO biodiesel blends at various engine speeds are shown in Figure 4.23. Comprehensively, the O<sub>2</sub> emission for diesel fuel and WCO biodiesel blends show a similar trend where O<sub>2</sub> emission is decreased along with the increasing engine speed due to better combustion at high engine speed. B100 shows slightly higher O<sub>2</sub> emission at engine speed 1200 rpm, 2100 rpm and 2400 rpm with difference of 0.14 %, 0.83 % and 0.71 % compared to diesel fuel. This indicates good burning quality of B100 inside the cylinder.

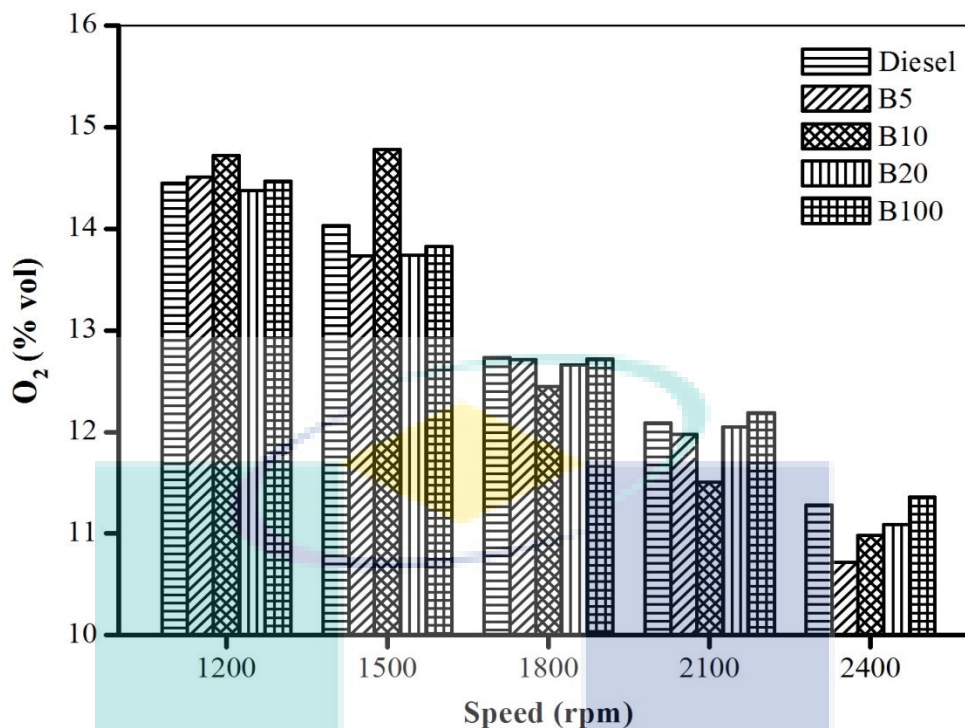


**Figure 4.23:** Emission of O<sub>2</sub> at various engine speeds

### 4.7.3 CO<sub>2</sub> Emission

The emission of CO<sub>2</sub> can contribute to serious public health problem and play a major role in global warming, which is one of the most important environmental concerns of the world (Ozsezen and Canakci, 2011). In Figure 4.24, it is observed that CO<sub>2</sub> emission concentration increases with the increasing engine speed. This is due to the increase in combustion temperature which leads to more complete and efficient combustion (Sayin et al., 2013). CO<sub>2</sub> emissions of WCO biodiesel are higher than diesel fuel for almost each blend at every speed except for B5 at 1200 rpm and B10 at 1500 rpm which record the reduction of 1.9 % and 3.9 %, respectively. While at engine speed 1200 rpm, CO<sub>2</sub> emission of B10 is similar with diesel fuel. The CO<sub>2</sub> emission reaches a maximum value at 2400 rpm with B5 blend which is 8 % Vol, 12.68 % higher than diesel fuel. It is an indication of efficient combustion of biodiesel due to its oxygenated nature which helps for more complete combustion (El\_Kassaby and Nemit\_allah, 2013). It is observed that CO<sub>2</sub> emissions of B5, B10, B20 and B100 were 12.68 %, 9.86 %, 8.45 % and 4.22 %, respectively higher compared to diesel fuel at 2400 rpm. This

shows that a higher percentage of biodiesel in fuel blends emits a lower amount of CO<sub>2</sub> emission at high engine speed. The CO<sub>2</sub> trend discrepancy may be happening due to the variation of biodiesel feedstock sources, engine types and testing procedures (Pala-En et al., 2013, Tesfa et al., 2014).

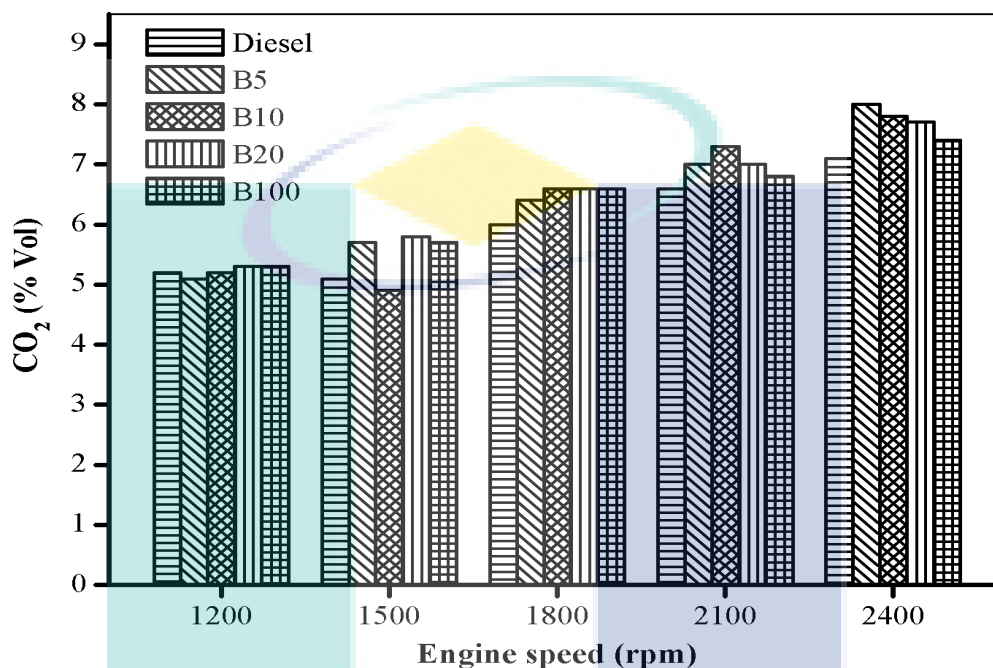


**Figure 4.24:** Emissions of CO<sub>2</sub> at various engine speeds

#### 4.7.4 NO<sub>x</sub> Emission

The effect of WCO biodiesel blends on NO<sub>x</sub> emissions is shown in Figure 4.25. At lower speed which is 1200 rpm, NO<sub>x</sub> emission of diesel is low compared to other fuel. While B100 is highest with increment of 35.68 % compared to diesel. B100 produce NO<sub>x</sub> at amount higher than diesel at 1200 rpm due to higher temperature from improved combustion and higher oxygen content (Agarwal, 2007). Most of researchers reported that biodiesel fuelled diesel engines caused an increase in NO<sub>x</sub> emissions (Tesfa et al., 2014). However, contrary to others, this study shows the value of NO<sub>x</sub> emission is inconsistent where at certain engine speeds, certain fuel shows unordinary increment. From engine speed 1500 rpm to 2400 rpm, NO<sub>x</sub> for B100 is lower than diesel with the variance of 0.21 % to 7.38 %. The explanation for this event is due to

higher cetane number of B100 which shorten the ignition delay as mention in the section 4.2. In addition of higher degree of saturation and longer chain lengths of B100, the time for reactants to preheat will reduce due to lower flame temperature. Accordingly, B100 produced lower NO<sub>x</sub> emissions (Pala-En et al., 2013). The graph also shows NO<sub>x</sub> emission is slightly decreased at higher engine speed 2400 rpm. At higher engine speed, ignition delay period is reduced at the mean time, which resulted in shorter residence time of the peak burning gas temperature available for NO<sub>x</sub> formation (Lin and Li, 2009). Therefore, reduction of NO<sub>x</sub> emission at high engine speed was observed.

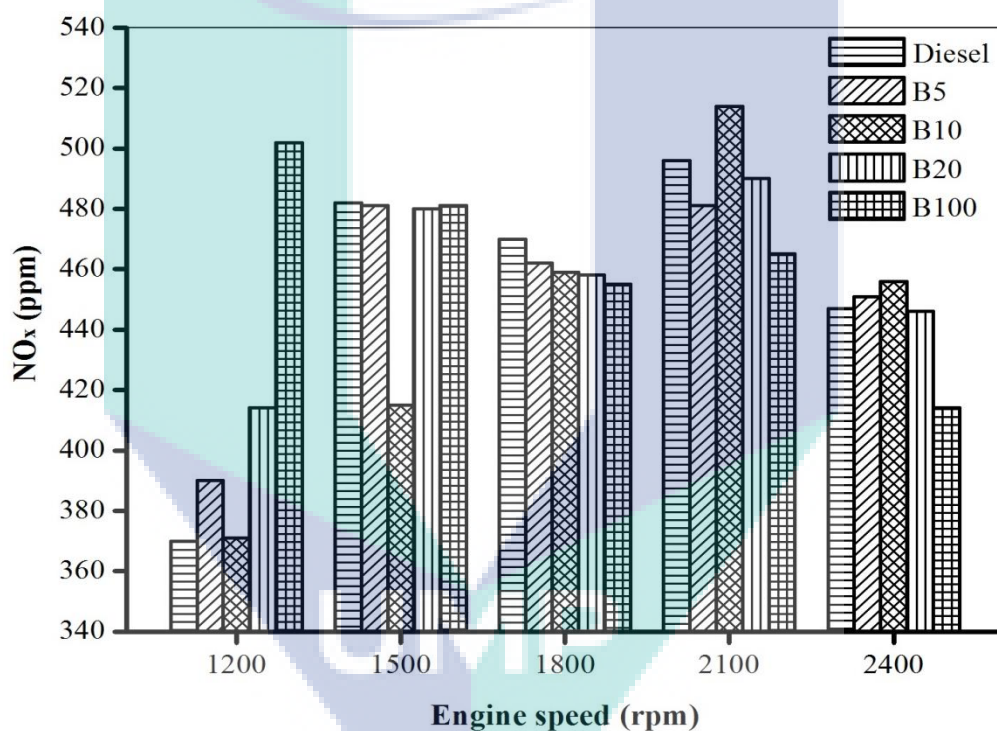


Figure 4.25: Emission of NO<sub>x</sub> at various engine speeds

#### 4.7.5 NO Emission

The variation of NO emission for diesel fuel and WCO biodiesel blends at various engine speeds is illustrated in Figure 4.26. NO emission formed similar trend with NO<sub>x</sub> emission. It has been known that, NO<sub>x</sub> is a collection of NO and NO<sub>2</sub> with NO is the major components which contribute to 90 % of NO<sub>x</sub> (Benajes et al., 2014 and Thangaraja and Mehta, 2014). The NO emission for each fuel is increase as engine

speed increases. However, at moderate engine speed which is 1800 rpm, NO emission is decrease and increase at engine speed 2100 rpm. At high engine speed which is 2400 rpm, the NO emission is decrease again. The lowest NO emission for diesel fuel is at engine speed 1200 rpm with 372 ppm vol while the highest NO emission is at engine speed 2100 rpm with 462 ppm vol. B100 produced lower NO emission at engine speed 1500 rpm, 1800 rpm, 2100 rpm and 2400 rpm with reduction of 0.22 %, 0.23 %, 4.11 % and 8.71 %, respectively compared to diesel fuel. Lower NO emission of B100 probably attributable to the lower amount of premixed combustion due to its higher cetane number compared to diesel fuel (Monyem et al., 2001)

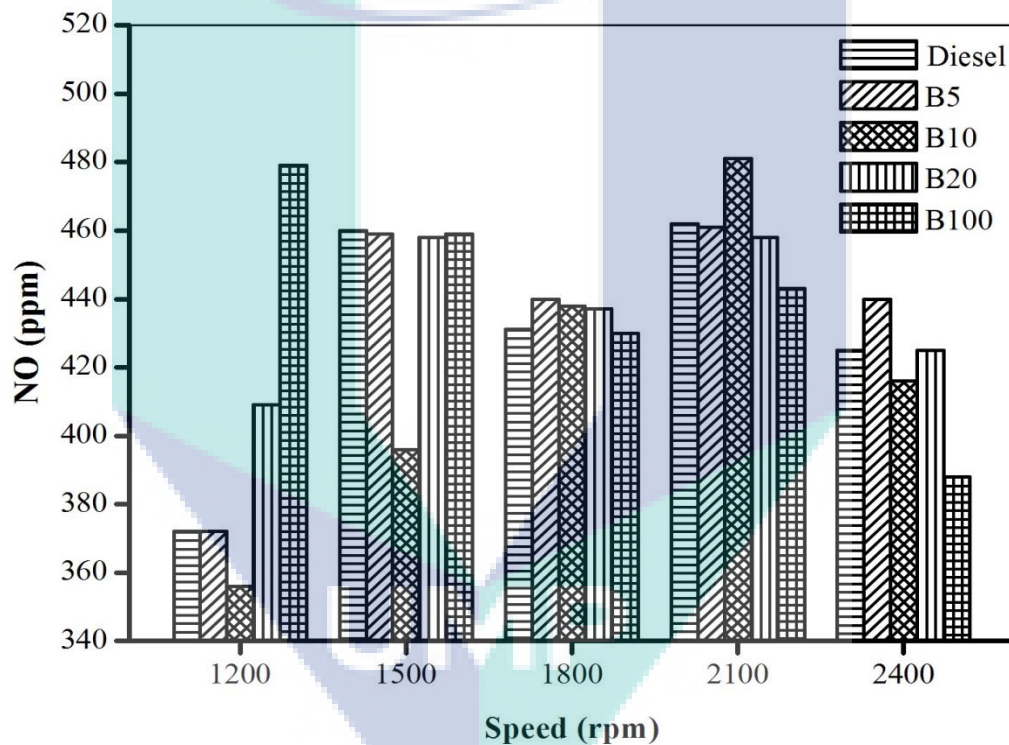
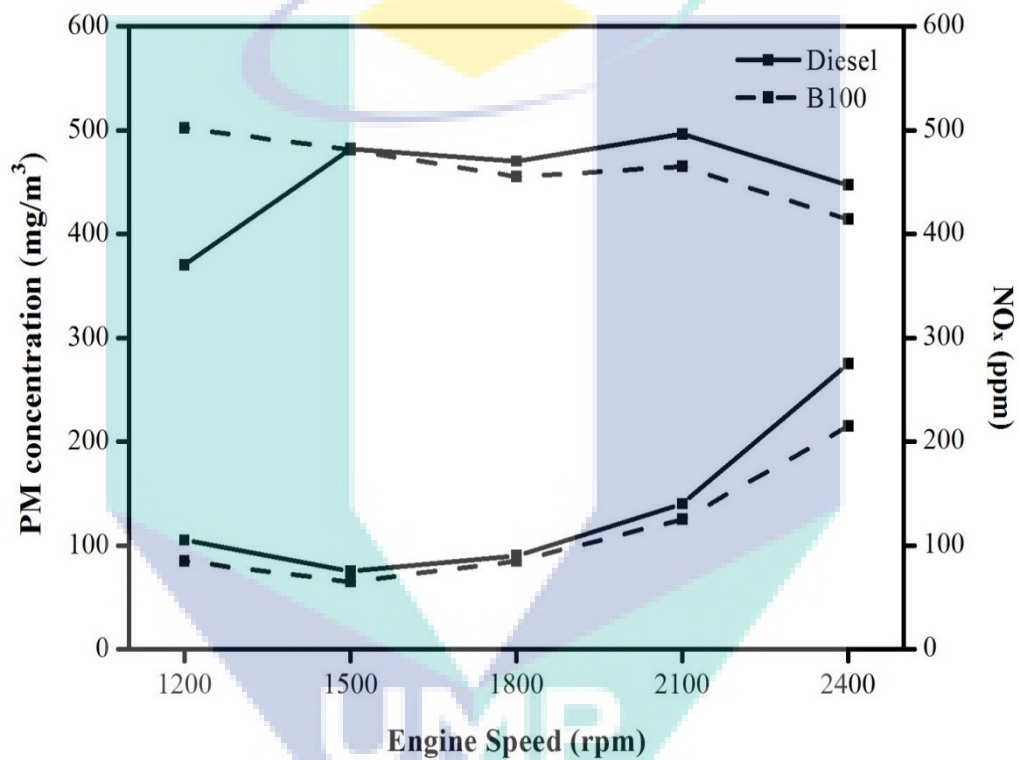


Figure 4.26: Emission of NO at various engine speeds

#### 4.8 PM - NO<sub>x</sub> TRADE OFF

The formation of NO<sub>x</sub> as well as PM is strongly influenced by the combustion temperature. As mention before, soot particles, which heavily contribute to the total mass of PM emitted by the engine, are formed in the cylinder in the locally fuel rich regions of the inhomogeneous combustion. Due to high temperature, subsequent soot

burns at the boundary of the diffusion flame. Conversely, formation of NO<sub>x</sub> also favor by this high temperature, hence, decreasing the combustion temperature to obtain a reduction in NO<sub>x</sub> emissions will result in an increasing PM. This dilemma is known as the NO<sub>x</sub>-PM trade off (Hussain et al., 2012). It is very difficult to reduce both NO<sub>x</sub> and PM emission simultaneously during the combustion process. Many emission-reduction technologies developed so far tend to increase PM emission while reducing NO<sub>x</sub> emission, and vice versa (Han et al., 1996).



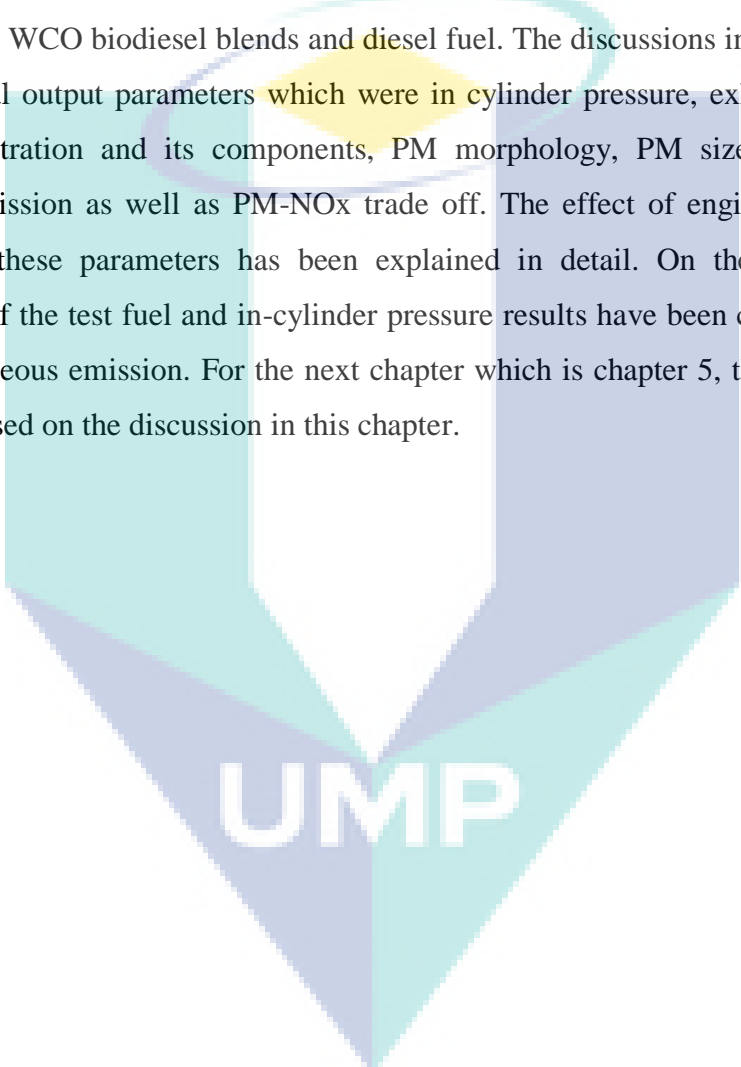
**Figure 4.27:** PM-NO<sub>x</sub> graph for diesel and B100

Figure 4.27 illustrated the graph of PM and NO<sub>x</sub> emission produced from the experiment. The upper lines represent NO<sub>x</sub> emission while lines at the bottom represented PM concentration of both fuel diesel and B100. As shown in the figure, it can be seen that the emission of NO<sub>x</sub> for B100 is lower than diesel fuel except at engine speed 1200 rpm. B100 has the percentage difference from 0.21 % to 7.38 % lower compared to diesel fuel for NO<sub>x</sub> emissions. On the other hand, B100 also shows lower PM emission compared to diesel fuel with varied from 5.56 % to 21.82 %. Contrary with other researchers, where most of the studies showed an increment in NO<sub>x</sub> emission

at the same time decrease the PM emission with biodiesel used in diesel engine (Karavalakis et al., 2011 and Fontaras et al., 2014). This study attained lower NO<sub>x</sub> and PM emission simultaneously.

#### 4.9 SUMMARY

This chapter has discussed the experimental results obtained from diesel engine fuelled with WCO biodiesel blends and diesel fuel. The discussions include the analysis from several output parameters which were in cylinder pressure, exhaust temperature, PM concentration and its components, PM morphology, PM size distribution and gaseous emission as well as PM-NO<sub>x</sub> trade off. The effect of engine speed and fuel blends on these parameters has been explained in detail. On the other hand, the properties of the test fuel and in-cylinder pressure results have been correlated with the PM and gaseous emission. For the next chapter which is chapter 5, the conclusion will be made based on the discussion in this chapter.

The logo for UMP (Universiti Malaysia Perlis) is a large, downward-pointing arrow shape. It is composed of several overlapping geometric shapes in shades of teal, light blue, and yellow. The letters 'UMP' are printed in white, bold, sans-serif font across the bottom of the arrow.

UMP

## CHAPTER 5

### CONCLUSION AND RECOMMENDATION

#### 5.1 CONCLUSION

The results presented in this thesis have covered the objectives of this study. The objectives consists of three major parts which is to study the exhaust emission comparison between diesel fuel and WCO biodiesel blends (B5, B10, B20, B100), the influence of SOF and soot on PM formation, and study the particulate matter characteristics and gaseous emission from these fuel. In order to achieve the objectives of this study, four main output parameter was observed. It includes PM emission characteristics, gaseous emission, exhaust temperature and in-cylinder pressure. In-cylinder pressure, which is one of the important combustion characteristics was observed for each test fuel at different operating engine speed to understand the event occur in the combustion chamber. Therefore, more information on emission formation were obtained. In addition, exhaust temperature parameter was observed conducive to gain more information on effectiveness of fuel combustion in the combustion cylinder.

From observation on in-cylinder pressure in this study, it can be concluded that, each blended fuel shows a similar trend with the diesel fuel where in-cylinder pressure is decreases with the increasing engine speed. This is due to ignition delay period which prolong as the engine speed increases. On the other hand, ignition delay period of WCO biodiesel is shorter than diesel fuel due to higher cetane number of WCO biodiesel. Comparing the in-cylinder pressure of the WCO biodiesel blends, this study shows that peak in-cylinder pressure is uncertain with the increasing of WCO biodiesel concentration in the fuel blends. In terms of exhaust temperature, both WCO biodiesel

blends and diesel fuel shows increment of the exhaust temperature as operating engine speed is increased. At the same time, WCO biodiesel blend gives higher value of exhaust temperature which is 1.49 % compared to diesel fuel due to its oxygen content which contribute to complete combustion thus improve the diffusion rate.

In view of PM mass concentration, B100 gives the lower value at all engine speed compared to diesel fuel and other blend. This is due to oxygen content of B100 which leads to complete combustion. The PM reductions for B100 is from 5.56% to 21.82 % compared to diesel fuel. As for SOF concentration, blended fuels B10, B20, and B100 have higher SOF value which is in the range of 3.23 % to 82.36 % compared to diesel fuel at moderate and high engine speed due to higher viscosity of the WCO biodiesel which leads to poor atomization and increases unburned or partially burned HC emissions. The lowest value of SOF appear at moderate engine speed 1800 rpm with WCO B5 which is 10 mg/m<sup>3</sup>. Meanwhile, soot concentration for B10, B20 and B100 is lower compared to diesel fuel with variation of 10 % to 62.50 %. WCO biodiesel, which has oxygen content could reduce locally fuel rich regions and limit soot formation. The lowest soot amount over total PM concentration is 15.38 % for B100 at engine speed 1500 rpm.

In observation of PM morphology, the images from FE-SEM shows particles of carbon, which are chain-like agglomeration which look like amorphous carbon. The particle is in non-uniform nanostructure which is extremely small with majority of particle are approximately 150 nm in diameter. As for the PM size distribution, the trend was similar to diesel and WCO blends. The size distribution of diesel fuel and WCO biodiesel blends were shifted to the larger size as the engine speed is increased. Simultaneously, the size distribution is shifted to the smaller PM diameter as blending ratio of WCO biodiesel in the fuel blends is increased.

In terms of gaseous emission, increasing engine speed increased the CO and CO<sub>2</sub> while decrease the O<sub>2</sub> emission. The emission of NO<sub>x</sub> and NO as the engine speed increases is uncertain. On the other hand, the effect of WCO biodiesel blends on the gaseous emission also shows an uncertain trend. The increment of WCO biodiesel concentration in the fuel blends unexpectedly causes the increment of CO emission. At

engine speed 1800 rpm, the variation of CO emission for biodiesel blend is 50 % to 100 % higher than diesel fuel. Meanwhile, O<sub>2</sub> emission of B100 is slightly higher than diesel fuel at low and high engine speed. Whereas, almost each WCO biodiesel blends shows higher CO<sub>2</sub> emission compared to diesel fuel except B5 at 1200 rpm and B10 at 1500 rpm with the reduction of 1.9 % and 3.9 %, respectively. As for NO<sub>x</sub> and NO emission, both have similar trend where from engine speed 1500 rpm to 2400 rpm, B100 has lower value of NO<sub>x</sub> and NO compared to diesel fuel with variation of 0.21 % to 7.38 % and 0.22% to 4.11 % respectively. From the PM concentration and NO<sub>x</sub> emission result, PM-NO<sub>x</sub> trade off is observed. The trend shows that B100 simultaneously decrease both NO<sub>x</sub> and PM emission at the same time. This finding shows contrary result with other researcher where most of the studies shows lower PM emission will increase the emission of NO<sub>x</sub> with biodiesel used in diesel engine.

## 5.2 SUMMARY OF FINDINGS

The findings from the experimental results have achieved the objectives of the study. The findings can be summarized based on the objectives as follow:

- (i) To compare the engine exhaust PM emission of WCO biodiesel and diesel fuelled engine.

Only PM mass concentration of B100 gives the lower value at all engine speed compared to diesel fuel.

- (ii) To analyze the influence of soluble organic fraction (SOF) and soot in particulate matter (PM) formation using various waste cooking (WCO) biodiesel blends.

From the results obtained, the SOF concentration for WCO biodiesel blends is higher than diesel fuel. Meanwhile, soot concentration of WCO biodiesel blends is lower than diesel fuel. This indicates that SOF component dominates the PM formation of the WCO biodiesel while soot component dominates the PM formation of the diesel fuel.

- (iii) To study the PM characteristics and gaseous emissions from WCO biodiesel blends.

The PM size distribution of WCO biodiesel and diesel fuel is shifted to the larger size as engine speed increase while the PM size distribution is shifted to the smaller size as blending ratio of WCO biodiesel increases in fuel blends. On the other hand, increasing engine speed increases the CO and CO<sub>2</sub> while decreases O<sub>2</sub> emission. Meanwhile, the change of NO<sub>x</sub> and NO emissions due to engine speed is uncertain. The effect of WCO biodiesel blends on the gaseous emission also shows an uncertain trend.

This study shows that the PM and gaseous emission as well as combustion characteristic of the WCO biodiesel are comparable with diesel fuel without any modification of the diesel engine. Therefore, WCO biodiesel has potential as an alternative fuel to be used in diesel engine in the future.

## 5.2 RECOMMENDATIONS

Based on the experimental observation, there are a few recommendations for future research related to this study in order to improve and get better outcome.

### 5.2.1 TEM Employment to Obtain PM Image

Recently, the most common method to characterize the structure of PM is by using TEM. This study employed FE-SEM to obtain the PM image for PM characterization due to its cost which is cheaper than TEM. Similar with FE-SEM, TEM also can be governed by computer based image processing in order to analyze PM characteristics. However, the TEM technique provides projected two-dimensional properties of PM agglomerates which give higher resolution compared to FE-SEM. Therefore, the characteristics of PM obtained by TEM will be more accurate compared to FE-SEM. Thus, it is recommended that TEM is employ in future research in order to obtain PM image.

### 5.2.3 PM Chemical Composition Analysis

The component such as sulphur, nitrites, and ashes with the use of alternative fuels, may rise as new problems in the future. In addition, the chemical composition in PM can give more information on health effect when PM enters into the human body. Therefore, studies into the chemical composition of particulates are also recommended. The chemical characterization of the PM can be obtained by SEM, in association with an energy-dispersive X-ray (EDS) system.

### 5.2.4 Transient Mode Testing

The present work has shown that WCO emission and combustion is comparable with diesel fuel under steady-state condition. However, this result may be different in engine transient mode. As we all know, real vehicle driving conditions are mostly in transient mode. Therefore, transient engine testing is recommended to meet the transient emissions regulations and operating requirements in real vehicle driving.

### 5.2.5 Specific Sources for WCO Biodiesel

The feedstock for biodiesel plays an important role in order to get high quality of biodiesel which meet the required standard. Different type of raw material used in biodiesel production will give different results in term of combustion characteristics and exhaust emission. In this study, the oil sources of WCO biodiesel was collected from various types of waste cooking oil from households, such as palm oil, sunflower oil, olive oil, and corn oil. In addition to differences in cooking oil stocks, variations in frying temperatures and times can affect the composition of the final fuel. Therefore, specific source of WCO biodiesel from specific place for example food chain store which has use same type of cooking and employ same frying methods standard of cooking such as KFC, Burger King or Mc Donald is recommended. In addition, the comparison can be made between the source of oil from specific place and the source of oil which collected from various place for future research to gain more information on the quality of WCO biodiesel sources.

## REFERENCES

- Agarwal, A. K. 2007. Biofuels (alcohols and biodiesel) applications as fuels for internal combustion engines. *Progress in Energy and Combustion Science*. **33** (3): 233-271.
- Agarwal, A. K., Dhar, A., Gupta, J. G., Kim, W. I., Choi, K., Lee, C. S. & Park, S. 2015. Effect of fuel injection pressure and injection timing of Karanja biodiesel blends on fuel spray, engine performance, emissions and combustion characteristics. *Energy Conversion and Management*. **91**: 302-314
- Agarwal, A. K., Singh, A. P., Lukose, J. & Gupta, T. 2013. Characterization of exhaust particulates from diesel fueled homogenous charge compression ignition combustion engine. *Journal of Aerosol Science*. **58**: 71-85.
- Aksoy, F. 2011. The effect of opium poppy oil diesel fuel mixture on engine performance and emissions. *International Journal of Environmental Science & Technology*. **8** (1): 57-62.
- Al-Dawody, M. F. & Bhatti, S. 2014. Effect of Variable Compression Ratio on the Combustion, Performance and Emission Parameters of a Diesel Engine Fuelled with Diesel and Soybean Biodiesel Blending. *World Applied Sciences Journal*. **30** (12): 1852-1858.
- Ali, R. 2011. Biodiesel A Renewable Alternate Clean and Environment Friendly Fuel for Petrodiesel Engines: A Review *International Journal of Engineering Science & Technology*. **3** (10): 7707-7713
- Alptekin, E. & Canakci, M. 2009. Characterization of the key fuel properties of methyl ester–diesel fuel blends. *Fuel*. **88** (1): 75-80.
- Altın, R., Cetinkaya, S. & Yücesu, H. S. 2001. The potential of using vegetable oil fuels as fuel for diesel engines. *Energy conversion and management*. **42** (5): 529-538.
- Angelovič, M. 2013. Particulate Emissions and Biodiesel: A review. *Scientific Papers Animal Science and Biotechnologies*. **46** (1): 192-198.
- Ariana, I. M., Nishida, O., Fujita, H., Harano, W. & Fujio, M. 2006. Removal of Marine Diesel Particulate Matter by Electrostatic Precipitator. Working paper. The International Conference on Electrostatic Precipitation (ICESP). Cairns, Australia: 25 - 29 June.
- Armas, O., Ballesteros, R. & Gomez, A. 2008. The effect of diesel engine operating conditions on exhaust particle size distributions. *Journal of Automobile Engineering*. **222**: 1513-1525.

- Armas, O., Yehliu, K. & Boehman, A. L. 2010. Effect of alternative fuels on exhaust emissions during diesel engine operation with matched combustion phasing. *Fuel*. **89** (2): 438-456.
- Asif, M. & Muneer, T. 2007. Energy supply, its demand and security issues for developed and emerging economies. *Renewable and Sustainable Energy Reviews*. **11** (7): 1388-1413.
- ASTM. 2008. Standard specification for biodiesle fuel blend stock (B100) for middle distillate fuels.
- Aydin, H. & Bayindir, H. 2010. Performance and emission analysis of cottonseed oil methyl ester in a diesel engine. *Renewable Energy*. **35** (3): 588-592.
- Baccarelli, A., Martinelli, I., Zanobetti, A., Grillo, P., Hou, L.-F., Bertazzi, P. A., Mannucci, P. M. & Schwartz, J. 2008. Exposure to Particulate Air Pollution and Risk of Deep Vein Thrombosis. *Arch Intern Med*. **168** (9): 920-927.
- Banapurmath, N. & Tewari, P. 2008. Performance of a low heat rejection engine fuelled with low volatile Honge oil and its methyl ester (HOME). *Proceedings of the Institution of Mechanical Engineers, Part A: Journal of Power and Energy*. **222** (3): 323-330.
- Banús, E., Ulla, M., Miró, E. & Milt, V. 2013. Structured Catalysts for Soot Combustion for Diesel Engines. *Diesel Engine-Combustion, Emissions and Condition Monitoring*, 117-142. <http://www.intechopen.com>.
- Barabás, I. & Todoruț, I.-A. 2011. *Utilization of biodiesel-diesel-ethanol blends in CI engine. Biodiesel-quality, emissions and by-products*. Dr. Gisela Montero (Ed.), ISBN: 978-953-307-784-0, InTech, DOI: 10.5772/27137. Available from: <http://www.intechopen.com/books/biodiesel-quality-emissions-and-by-products/utilization-of-biodiesel-diesel-ethanol-blends-in-ci-engine>
- Beelen, R., Hoek, G., Brandt, P. A. v. d., Goldbohm, R. A., Fischer, P., Schouten, L. J., Jerrett, M., Hughes, E., Armstrong, B. & Brunekreef, B. 2008. Long-term effects of traffic-related air pollution on mortality in a Dutch cohort. *Environment Health Perspective*. **116** (2): 196–202.
- Benajes, J., López, J. J., Novella, R. & Redón, P. 2014. Comprehensive modeling study analyzing the insights of the NO–NO<sub>2</sub> conversion process in current diesel engines. *Energy Conversion and Management*. **84**: 691-700.
- Bezergianni, S. & Chrysikou, L. P. 2012. Oxidative stability of waste cooking oil and white diesel upon storage at room temperature. *Bioresource Technology*. **126**: 341-344.
- Bondioli, P., Gasparoli, A., Lanzani, A., Fedeli, E., Veronese, S. & Sala, M. 1995. Storage stability of biodiesel. *Journal of the American Oil Chemists' Society*. **72** (6): 699-702.

- Bouaid, A., Martinez, M. & Aracil, J. 2007. Long storage stability of biodiesel from vegetable and used frying oils. *Fuel*. **86** (16): 2596-2602.
- Bowman, C. T. 1975. Kinetics of pollutant formation and destruction in combustion. *Progress in Energy and Combustion Science*. **1** (1): 33-45.
- BP. 2014. BP Statistical Review of World Energy 2014. *63rd edition*.
- Buyukkaya, E. 2010. Effects of biodiesel on a DI diesel engine performance, emission and combustion characteristics. *Fuel*. **89** (10): 3099-3105.
- Can, Ö. 2014. Combustion characteristics, performance and exhaust emissions of a diesel engine fueled with a waste cooking oil biodiesel mixture. *Energy Conversion and Management*. **87**: 676-686.
- Canakci, M. & Özsezen, A. N. 2010. Evaluating waste cooking oils as alternative diesel fuel. *Gazi University Journal of Science*. **18** (1): 81-91.
- Canakci, M. & Van Gerpen, J. 2003. A pilot plant to produce biodiesel from high free fatty acid feedstocks. *Transactions of the ASAE*. **46** (4): 945-954.
- Cataluña, R. & da Silva, R. 2012. Effect of cetane number on specific fuel consumption and particulate matter and unburned hydrocarbon emissions from diesel engines. *Journal of Combustion*. **2012**.
- Chauhan, B. S., Kumar, N., Cho, H. M. & Lim, H. C. 2013. A study on the performance and emission of a diesel engine fueled with Karanja biodiesel and its blends. *Energy*. **56**: 1-7.
- Chhetri, A. B., Watts, K. C. & Islam, M. R. 2008. Waste cooking oil as an alternate feedstock for biodiesel production. *Energies*. **1** (1): 3-18.
- Chryssakis, C. A., Hagen, J. R., Knafl, A., Hamosfakidis, V. D. & Filipi, Z. S. 2006. In-cylinder reduction of PM and NO<sub>x</sub> emissions from diesel combustion with advanced injection strategies. *International Journal of Vehicle Design*. **41** (1): 83-102.
- CAI-Asia. 2010. *Factsheet No. 2 – Particulate matter (PM) standards in Asia*. Clean Air Asia.
- Cvengroš, J. & Cvengrošová, Z. 2004. Used frying oils and fats and their utilization in the production of methyl esters of higher fatty acids. *Biomass and bioenergy*. **27** (2): 173-181.
- Dec, J. E. 1997. A conceptual model of DI diesel combustion based on laser-sheet imaging. *SAE Technical Paper*. **970873**.
- Demirbas, A. 2008. Economic and environmental impacts of the liquid biofuels. *Energy Education Science and Technology*. **22** (1): 37-58.

- Dorado, M. P., Ballesteros, E., Arnal, J. M., Gómez, J. & López, F. J. 2003. Exhaust emissions from a Diesel engine fueled with transesterified waste olive oil. *Fuel*. **82** (11): 1311-1315.
- Dwivedi, D., Agarwal, A. K. & Sharma, M. 2006. Particulate emission characterization of a biodiesel vs diesel-fuelled compression ignition transport engine: A comparative study. *Atmospheric Environment*. **40** (29): 5586-5595.
- Eastwood, P. 2008. *Particulate Emissions From Vehicles*. London John Wiley & Sons, Ltd.
- El-Kasaby, M. & Nemit-allah, M. A. 2013. Experimental investigations of ignition delay period and performance of a diesel engine operated with Jatropha oil biodiesel. *Alexandria Engineering Journal*. **52** (2): 141-149.
- El\_Kassaby, M. & Nemit\_allah, M. A. 2013. Studying the effect of compression ratio on an engine fueled with waste oil produced biodiesel/diesel fuel. *Alexandria Engineering Journal*. **52** (1): 1-11.
- Encinar, J. M., Gonzalez, J. F. & Rodríguez-Reinares, A. 2005. Biodiesel from used frying oil. Variables affecting the yields and characteristics of the biodiesel. *Industrial & Engineering Chemistry Research*. **44** (15): 5491-5499.
- Energy Commission. 2014. *National Energy Balance 2012*. Energy Commission of Malaysia. Putrajaya.
- Enweremadu, C. & Mbarawa, M. 2009. Technical aspects of production and analysis of biodiesel from used cooking oil - A review. *Renewable and Sustainable Energy Reviews*. **13** (9): 2205-2224.
- Enweremadu, C. C. & Rutto, H. L. 2010. Combustion, emission and engine performance characteristics of used cooking oil biodiesel - A review. *Renewable and Sustainable Energy Reviews*. **14** (9): 2863-2873.
- EPA. 1988. New emission standards for nonroad diesel engines *EPA420-F-98-034* United States Environmental Protection Agency.
- EPA. 2002a. *A Comprehensive Analysis of Biodiesel Impacts on Exhaust Emissions*. United States Environmental Protection Agency. EPA420-P-02-001.
- EPA. 2002b. *Health assessment document for diesel engine exhaust*. EPA/600/8-90/057F. Washington, DC.
- EPA. 2008. Particulate matter. <http://www.epa.gov/pm/>.
- EPA. 2010. *Biodiesel, technical highlights*. Office of Transportation and Air Quality. EPA-420-F-10-009.

- EPA. 2012a. *Diesel Fuel Explained: Diesel Prices and Outlook*. U.S Department of Energy.
- EPA. 2012b. *Our Nation's Air: Status and Trends Through 2010*. North Carolina.
- EPA. 2014. *Inventory of U.S. greenhouse gas emissions and sinks: 1990-2012*. EPA 430-R-13-001. Washington, DC.
- Esteban, B., Riba, J.-R., Baquero, G., Rius, A. & Puig, R. 2012. Temperature dependence of density and viscosity of vegetable oils. *Biomass and Bioenergy*. **42**: 164-171.
- Farrar-Khan, J. R., Andrews, G. E., Williams, P. T. & Bartle, K. D. 1992. The influence of nozzle sac volume on the composition of diesel particulate fuel derived SOF. *SAE Technical Paper*. **921649**.
- Ferreira, T. M., Forti, M. C. & Alcaide, R. L. M. 2013. Inhalable particulate matter characterization in a medium-sized urban region in Brazil (São José dos Campos Town)-Part I: Morphology. *Química Nova*. **36** (9): 1380-1387.
- Flynn, P. F., Durrett, R. P., Hunter, G. L., Loye, A. O. z., Akinyemi, O. C., Dec, J. E. & Westbrook, C. K. 1999. Diesel Combustion: An Integrated View Combining Laser Diagnostics, Chemical Kinetics, And Empirical Validation. *SAE Technical Paper*. **1999-01-0509**.
- Fontaras, G., Kalogirou, M., Grigoratos, T., Pistikopoulos, P., Samaras, Z. & Rose, K. 2014. Effect of rapeseed methylester blending on diesel passenger car emissions – Part 1: Regulated pollutants, NO/NO<sub>x</sub> ratio and particulate emissions. *Fuel*. **121**: 260-270.
- Fore, S. R., Lazarus, W., Porter, P. & Jordan, N. 2011. Economics of small-scale on-farm use of canola and soybean for biodiesel and straight vegetable oil biofuels. *Biomass and Bioenergy*. **35** (1): 193-202.
- Frenklach, M. 2002. Reaction mechanism of soot formation in flames. *Physical Chemistry Chemical Physics*. **4** (11): 2028-2037.
- Georgogianni, K. G., Katsoulidis, A. P., Pomonis, P. J. & Kontominas, M. G. 2009. Transesterification of soybean frying oil to biodiesel using heterogeneous catalysts. *Fuel Processing Technology*. **90**: 671–676.
- Gomez, M. G., Howard-Hildige, R., Leahy, J., O'reilly, T., Supple, B. & Malone, M. 2000. Emission and performance characteristics of a 2 litre Toyota diesel van operating on esterified waste cooking oil and mineral diesel fuel. *Environmental Monitoring and Assessment*. **65** (1-2): 13-20.
- González Gómez, M. E., Howard-Hildige, R., Leahy, J. J. & Rice, B. 2002. Winterisation of waste cooking oil methyl ester to improve cold temperature fuel properties. *Fuel*. **81** (1): 33-39.

- Grewe, V., Dahlmann, K., Matthes, S. & Steinbrecht, W. 2012. Attributing ozone to NOx emissions: Implications for climate mitigation measures. *Atmospheric Environment*. **59**: 102-107.
- Hall, D. E., Goodfellow, C. L., Heinze, P., Rickeard, D. J., Nancekievill, G., Martini, G., Hevesi, J., Rantanen, L., Merino, P. M., Morgan, T. D. B. & Zemroch, P. J. 1998. A study of the size, number and mass distribution of the automotive particulate emissions for European light-duty vehicles. *SAE Technical Paper*. **982600**.
- Hamasaki K, Kinoshita E, Tajima S, Takasaki K & D., M. 2001. Combustion characteristics of diesel engines with waste vegetable oil methyl ester. *Proceeding of the Fifth International Symposium on Diagnostics and Modeling of Combustion in Internal Combustion Engines*. **200**: 410-416.
- Han, Z., Uludogan, A., Hampson, G. J. & Reitz, R. D. 1996. Mechanism of soot and NOx emission reduction using multiple-injection in a diesel engine. **960633**.
- Hardin, J. W. 2009. *Quantification of soluble organic fraction measurement variation in diesel particulate matter emissions*. Phd. Thesis. West Virginia University, USA.
- Helwani, Z., Othman, M., Aziz, N., Kim, J. & Fernando, W. 2009. Solid heterogeneous catalysts for transesterification of triglycerides with methanol: a review. *Applied Catalysis A: General*. **363** (1): 1-10.
- Herfatmanesh, M. R., Lu, P., Attar, M. A. & Zhao, H. 2013. Experimental investigation into the effects of two-stage injection on fuel injection quantity, combustion and emissions in a high-speed optical common rail diesel engine. *Fuel*. **109**: 137-147
- Heywood, J. B. 1988. *Internal combustion engine fundamentals*. McGraw-hill New York.
- Hill, J., Nelson, E., Tilman, D., Polasky, S. & Tiffany, D. 2006. Environmental, economic, and energetic costs and benefits of biodiesel and ethanol biofuels. *Proceedings of the National Academy of Sciences*. **103** (30): 11206-11210.
- Hoefl, I., Steude, K., Wrage, N. & Veldkamp, E. 2012. Response of nitrogen oxide emissions to grazer species and plant species composition in temperate agricultural grassland. *Agriculture, Ecosystems & Environment*. **151**: 34-43.
- Home Air Purifier Expert. 2010. The complete guide to your lungs and respiratory health. (online). <http://www.home-air-purifier-expert.com/lungs.html#imageofdustinhallation>. (26 February 2015).
- Houa, J., Zhanga, P., Yuana, X. & Zhenga, Y. 2011. Life cycle assessment of biodiesel from soybean, jatropha and microalgae in China conditions. *Renewable and Sustainable Energy Reviews*. **15**: 5081– 5091.

- Hussain, J., Palaniradja, K., Algumurthi, N. & Manimarana, R. 2012. Diesel engines emissions and after treatment techniques- A review. *Journal of Engineering Research and Studies* **3**(3): 34-44.
- IARC. 2012. IARC: Diesel Engine Exhaust Carcinogenic. *Press release NO 213*.
- IEA. 2014. World Energy Outlook 2014. International Energy Agency.
- Ismail, R. 2005. Palm oil and palm olein frying applications. *Asia Pacific journal of clinical nutrition*. **14** (4): 414-419.
- Jin, T., Qu, L., Liu, S., Gao, J., Wang, J., Wang, F., Zhang, P., Bai, Z. & Xu, X. 2014. Chemical characteristics of particulate matter emitted from a heavy duty diesel engine and correlation among inorganic and PAH components. *Fuel*. **116**: 655-661.
- Johnson, J. H., Bagley, S. T., Gratz, L. D. & Leddy, D. G. 1994. A review of diesel particulate control technology and emissions effects-1992 horning memorial award lecture. *Training*. **2013**: 11-04.
- Johnson, T. J., Symonds, J. P. & Olfert, J. S. 2013. Mass-Mobility Measurements Using a Centrifugal Particle Mass Analyzer and Differential Mobility Spectrometer. *Aerosol Science and Technology*. **47** (11): 1215-1225.
- Johnson, T. V. 2006. Diesel Emission Control in Review. *SAE International Journal of Fuels and Lubrication*. **2009-01-0121**.
- Jung, H., Kittelson, D. B. & Zachariah, M. R. 2006. Characteristics of SME biodiesel-fueled diesel particle emissions and the kinetics of oxidation. *Environmental science & technology*. **40** (16): 4949-4955.
- Kampa, M. & Castanas, E. 2008. Human health effects of air pollution. *Environmental Pollution*. **151** (2): 362-367.
- Karavalakis, G., Bakeas, E., Fontaras, G. & Stournas, S. 2011. Effect of biodiesel origin on regulated and particle-bound PAH (polycyclic aromatic hydrocarbon) emissions from a Euro 4 passenger car. *Energy*. **36** (8): 5328-5337.
- Kittelson, D. & Kraft, M. 2014. Particle Formation and Models in Internal Combustion Engines. **Preprint No. 142**: University of Cambridge
- Kittelson, D., Watts, W. & Johnson, J. 2002. Diesel Aerosol Sampling Methodology-CRC E-43. University of Minnesota, Minneapolis: Final report, Coordinating Research Council
- Kittelson, D. B. 1998. Engines and nanoparticles: A Review. *J. Aerosol Sci.* **29** (5/6): 575-588.

- Klein, H., Lox, E., Kreuzer, T., Kawanami, M., Ried, T. & Bächmann, K. 1998. Diesel Particulate Emissions of Passenger Cars - New Insights into Structural Changes During the Process of Exhaust Aftertreatment Using Diesel Oxidation Catalysts. *SAE Technical Paper*. **980196**.
- Klopfenstein, W. 1985. Effect of molecular weights of fatty acid esters on cetane numbers as diesel fuels. *Journal of the American Oil Chemists Society*. **62** (6): 1029-1031.
- Knothe, G. 2005. Dependence of biodiesel fuel properties on the structure of fatty acid alkyl esters. *Fuel Processing Technology*. **86** (10): 1059-1070.
- Kulkarni, M. G. & Dalai, A. K. 2006. Waste cooking oil an economical source for biodiesel: a review. *Industrial & engineering chemistry research*. **45** (9): 2901-2913.
- Kumar, N., Varun & Chauhan, S. R. 2013. Performance and emission characteristics of biodiesel from different origins: A review. *Renewable and Sustainable Energy Reviews*. **21**: 633-658.
- Lapuerta, M., Rodríguez-Fernández, J. & Agudelo, J. R. 2008. Diesel particulate emissions from used cooking oil biodiesel. *Bioresource Technology*. **99** (4): 731-740.
- Laza, T. & Bereczky, Á. 2011. Basic fuel properties of rapeseed oil-higher alcohols blends. *Fuel*. **90** (2): 803-810.
- Lee, B.-K. & Vu, V. T. 2010. Sources, Distribution and Toxicity of Polyaromatic Hydrocarbons (PAHs) in Particulate Matter. *Air Pollution* ISBN **978-953-307-143-5**: <http://www.intechopen.com>.
- Lee, K. O., Zhu, J., Ciatti, S., Yozgatligil, A. & Choi, M. Y. 2003. Sizes, Graphitic Structures and Fractal Geometry of Light-Duty Diesel Engine Particulates. *SAE Technical Paper*. **2003-01-3169**.
- Lee, S. B., Han, K. H., Lee, J. D. & Hong, I. K. 2010. Optimum process and energy density analysis of canola oil biodiesel synthesis. *Journal of Industrial and Engineering Chemistry*. **16**:1006–1010.
- Li, Y., McLaughlin, N., Patterson, B. & Burt, S. 2006. Fuel efficiency and exhaust emissions for biodiesel blends in an agricultural tractor. *Canadian Biosystems Engineering*. **48** 2.
- Lin, C.-Y. & Li, R.-J. 2009. Engine performance and emission characteristics of marine fish-oil biodiesel produced from the discarded parts of marine fish. *Fuel Processing Technology*. **90** (7–8): 883-888.

- Lin, C.-Y. & Lin, H.-A. 2007. Engine performance and emission characteristics of a three-phase emulsion of biodiesel produced by peroxidation. *Fuel Processing Technology*. **88** (1): 35-41.
- Lin, Y.-C., Hsu, K.-H. & Chen, C.-B. 2011. Experimental investigation of the performance and emissions of a heavy-duty diesel engine fueled with waste cooking oil biodiesel/ultra-low sulfur diesel blends. *Energy*. **36** (1): 241-248.
- Luján, J. M., Bermúdez, V., Tormos, B. & Pla, B. 2009. Comparative analysis of a DI diesel engine fuelled with biodiesel blends during the European MVEG-A cycle: Performance and emissions (II). *Biomass and Bioenergy*. **33** (6-7): 948-956.
- Mačković, M. 2012. *Characterization of soot particles from diesel engines and tin dioxide particles milled in stirred media mills*. Phd Thesis. Erlangen, Universität Erlangen-Nürnberg, Diss.
- Mahajan, S. & Konar, S. K. 2006. Determining the acid number of biodiesel. *Journal of the American Oil Chemists' Society*. **83** (6): 567-570.
- Mandelbrot, B. B. 1982. *The Fractal Geometry of Nature*. San Francisco, W. H. Freeman and Company.
- Manickam, A., Rajan, K., Manoharan, N. & Kumar, K. 2014. Reduction of Exhaust Emissions on a Biodiesel fuelled Diesel Engine with the Effect of Oxygenated Additives. *International Journal of Engineering & Technology* **6**(5): 2406-2411.
- Marmesat, S., Rodrigues, E., Velasco, J. & Dobarganes, C. 2007. Quality of used frying fats and oils: comparison of rapid tests based on chemical and physical oil properties. *International journal of food science & technology*. **42** (5): 601-608.
- Megaridis, C. M. & Dobbins, R. A. 1990. Morphological Description of Flame-Generated Materials. *Combustion Science and Technology*. **71** (1-3): 95-109.
- Meng, X., Chen, G. & Wang, Y. 2008. Biodiesel production from waste cooking oil via alkali catalyst and its engine test. *Fuel Processing Technology*. **89** (9): 851-857.
- Mittelbach, M. & Remschmidt, C. 2004. *Biodiesel: the comprehensive handbook*. Martin Mittelbach.
- Monyem, A., Van Gerpen, J. & Canakci, M. 2001. The effect of timing and oxidation on emissions from biodiesel-fueled engines. *Carbon*. **44** (1): 35-42.
- MPIC. 2014. *Implementation of the B7 Programme for the Subsidized Sector*. Ministry of Plantation Industries and Commodities. Kuala Lumpur.
- MSHA. 2005. Diesel Particulate Matter Exposure of Underground Metal and Nonmetal Miners; Final Rule. 70. Mine Safety and Health Administration.

- Muralidharan, K., Vasudevan, D. & Sheeba, K. 2011. Performance, emission and combustion characteristics of biodiesel fuelled variable compression ratio engine. *Energy*. **36** (8): 5385-5393.
- Nantha Gopal, K., Pal, A., Sharma, S., Samanchi, C., Sathyanarayanan, K. & Elango, T. 2014. Investigation of emissions and combustion characteristics of a CI engine fueled with waste cooking oil methyl ester and diesel blends. *Alexandria Engineering Journal*. **53** (2): 281-287.
- Naydenova, I. I. 2007. *Soot formation modeling during hydrocarbon pyrolysis and oxidation behind shock waves*. Phd Thesis. Rupertus Carola University of Heidelberg, Germany.
- Nazar, A. M., Silva, F. A. & Ammann, J. J. 1996. Image processing for particle characterization. *Materials Characterization*. **36** (4-5): 165-173.
- Nye, M., Williamson, T., Deshpande, W., Schrader, J., Snively, W., Yurkewich, T. & French, C. 1983. Conversion of used frying oil to diesel fuel by transesterification: preliminary tests. *Journal of the American Oil Chemists' Society*. **60** (8): 1598-1601.
- Oliveira, L. & Da Silva, M. 2013. Relationship between cetane number and calorific value of biodiesel from Tilapia visceral oil blends with mineral diesel. International Conference on Renewable Energies and Power Quality (ICREPQ'13) Bilbao, Spain: 20-22 March 2013.
- Ong, H. C., Mahlia, T. M. I., Masjuki, H. H. & Honnery, D. 2012. Life cycle cost and sensitivity analysis of palm biodiesel production. *Fuel*. **98** 131-139.
- Ozsezen, A. N. & Canakci, M. 2011. Determination of performance and combustion characteristics of a diesel engine fueled with canola and waste palm oil methyl esters. *Energy Conversion and Management*. **52** (1): 108-116.
- Ozsezen, A. N., Canakci, M., Turkcan, A. & Sayin, C. 2009. Performance and combustion characteristics of a DI diesel engine fueled with waste palm oil and canola oil methyl esters. *Fuel*. **88** (4): 629-636.
- Öztürk, E. 2015. Performance, emissions, combustion and injection characteristics of a diesel engine fuelled with canola oil-hazelnut soapstock biodiesel mixture. *Fuel Processing Technology*. **129**: 183-191.
- Pala-En, N., Sattler, M., Dennis, B. H., Chen, V. C. & Muncrief, R. L. 2013. Measurement of Emissions from a Passenger Truck Fueled with Biodiesel from Different Feedstocks. *Journal of Environmental Protection*. **4** (8A): 74-82.
- Park, K., Kittelson, D. B. & McMurry, P. H. 2004. Structural Properties of Diesel Exhaust Particles Measured by Transmission Electron Microscopy (TEM): Relationships to Particle Mass and Mobility. *Aerosol Science and Technology*. **38**: 881-889.

- Peiró, L. T., Méndez, G. V. & Durany, X. G. i. 2008. Exergy analysis of integrated waste management in the recovery and recycling of used cooking oils. *Environmental science & technology*. **42** (13): 4977-4981.
- Peng, R. D., Chang, H. H., Bell, M. L., McDermott, A., Zeger, S. L., Samet, J. M. & Dominici, F. 2008. Coarse particulate matter air pollution and hospital admissions for cardiovascular and respiratory diseases among Medicare patients. *Jama*. **299** (18): 2172-2179.
- Phan, A. N. & Phan, T. M. 2008. Biodiesel production from waste cooking oils. *Fuel*. **87** (17): 3490-3496.
- Pimentel, D. 2009. Biofuel food disasters and cellulosic ethanol problems. *Bulletin of Science, Technology & Society*. **29** (3): 205-212.
- Pimentel, D., Marklein, A., Toth, M. A., Karpoff, M. N., Paul, G. S., McCormack, R., Kyriazis, J. & Krueger, T. 2009. Food versus biofuels: environmental and economic costs. *Human ecology*. **37** (1): 1-12.
- Pope III, CA, Burnett RT, Thun MJ, Calle EE, Krewski D, Ito K & Thurston GD 2002. Lung cancer, cardiopulmonary mortality, and long-term exposure to fine particulate air pollution. *Journal of the American Medical Association*. **287** (9): 1132-41.
- Pratas, M. J., Freitas, S. V., Oliveira, M. B., Monteiro, S. C., Lima, Á. S. & Coutinho, J. A. 2011. Biodiesel density: Experimental measurements and prediction models. *Energy & Fuels*. **25** (5): 2333-2340.
- Pugazhivadivu, M. & Jeyachandran, K. 2005. Investigations on the performance and exhaust emissions of a diesel engine using preheated waste frying oil as fuel. *Renewable energy*. **30** (14): 2189-2202.
- Puhan, S., Balasubramanian, K. & Sharma, K. N. 2013. Experimental Investigation of performance and Emission Characteristics of Biodiesel From Sterculia Striata. *Asian Journal of Computer Science & Information Technology*. **3** (2): 19-25.
- Puzun, A., Wanchen, S., Guoliang, L., Manzhi, T., Chunjie, L. & Shibao, C. 2011. Characteristics of Particle Size Distributions About Emissions in A Common-rail Diesel Engine with Biodiesel Blends. *Procedia Environmental Sciences*. **11, Part C**: 1371-1378.
- Renewable Energy Group. 2011. Form s-1 registration statement. Available: <http://www.sec.gov/Archives/edgar/data/1463258/000119312511189855/ds1.htm>.
- Richter, H. & Howard, J. B. 2000. Formation of polycyclic aromatic hydrocarbons and their growth to soot—a review of chemical reaction pathways. *Progress in Energy and Combustion Science*. **26** (4–6): 565-608.

- Rounce, P., Tsolakis, A. & York, A. P. E. 2012. Speciation of particulate matter and hydrocarbon emissions from biodiesel combustion and its reduction by aftertreatment. *Fuel*. **96**: 90-99.
- Ruiz-Méndez, M., Marmesat, S., Liotta, A. & Dobarganes, M. C. 2008. Analysis of used frying fats for biodiesel production. *Grasas y aceites*. **59** (1): 45-50.
- SAE. 2004. Engine Power Test Code-Spark Ignition and Compression Ignition-Net Power Rating. *SAE J1349, Rev Aug2004*. SAE Power Test Code Committee.
- Saifuddin, N., Raziah, A. & Farah, H. 2009. Production of biodiesel from high acid value waste cooking oil using an optimized lipase enzyme/acid-catalyzed hybrid process. *Journal of Chemistry*. **6** (S1): S485-S495.
- Samoli E, Peng R, Ramsay T, Pipikou M, Touloumi G, Dominici F, Burnett R, Cohen A, Krewski D, Samet J & Katsouyanni K 2008. Acute effects of ambient particulate matter on mortality in Europe and North America. *Environment Health Perspective*. **116** (11): 1480–1486.
- Samuel, O., Waheed, M., Bolaji, B. & Dairo, O. 2013. Production of Biodiesel from Nigerian Restaurant Waste Cooking oil using Blender. *International Journal of Renewable Energy Research (IJRER)*. **3** (4): 976-979.
- Savariraj, S., Ganapathy, T. & Saravanan, C. 2013. Performance, emission and combustion characteristics of fish-oil biodiesel engine. *European Journal of Applied Engineering and Scientific Research*. **2** (3): 26-32.
- Sayin, C., Gumus, M. & Canakci, M. 2013. Influence of injector hole number on the performance and emissions of a DI diesel engine fueled with biodiesel–diesel fuel blends. *Applied Thermal Engineering*. **61** (2): 121-128.
- Schulz, H., Bandeira De Melo, G. & Ousmanov, F. 1999. Volatile organic compounds and particulates as components of diesel engine exhaust gas. *Combustion and Flame*. **118** (1–2): 179-190.
- Shahid, E., Jamal, Y., Shah, A., Rumzan, N. & Munsha, M. 2012. Effect of Used Cooking Oil Methyl ester on Compression Ignition Engine. *Journal of Quality and Technology Management*. **8** (2): 91-104.
- Shandilya, K., Khare, M. & Gupta, A. 2002. *Characterization and speciation of fine particulates in ambient air in Delhi*. ME thesis. Malaviya National Institute of Technology, Jaipur, India,
- Shankhdhar, V. & Kumar, N. 2014. Theoretical Study of the effects of Ignition Delay on the Performance of DI Diesel Engine. *International Journal of Research*. **1** (7): 230-236.

- Sharma, M., Agarwal, A. K. & Bharathi, K. V. L. 2005. Characterization of exhaust particulates from diesel engine. *Atmospheric Environment*. **39**: 3023-3028.
- Shin, H.-Y., Lim, S.-M., Kang, S. C. & Bae, S.-Y. 2012. Statistical optimization for biodiesel production from rapeseed oil via transesterification in supercritical methanol. *Fuel Processing Technology*. **98**: 1-5.
- Shirnesan, A., Almassi, M., Ghobadian, B., Borghei, A. M. & Najafi, G. H. 2012. Effects of Biodiesel and Engine Load on Some Emission Characteristics of a Direct Injection Diesel Engine. *Current World Environment*. **7** (2): 207-212.
- Shukla, P. C., Gupta, T. & Agarwal, A. K. 2014. A Comparative Morphological Study of Primary and Aged Particles Emitted from a Biodiesel (B20) vis-à-vis Diesel Fuelled CRDI Engine. *Aerosol and Air Quality Research*. **14** (3): 934-942.
- Soares, C. M., Itavo, L. C. V., Dias, A. M., Arruda, E. J., Delben, A. A. S. T., Oliveira, S. L. & Oliveira, L. C. S. d. 2010. Forage turnip, sunflower, and soybean biodiesel obtained by ethanol synthesis: Production protocols and thermal behavior. *Fuel*. **89** 3725–3729.
- Sorensen, C. M. & Feke, G. D. 1996. The Morphology of Macroscopic Soot. *Aerosol Science and Technology*. **25**: 328–337.
- Stanek, L. W., Sacks, J. D., Dutton, S. J. & Dubois, J.-J. B. 2011. Attributing health effects to apportioned components and sources of particulate matter: An evaluation of collective results. *Atmospheric Environment*. **45**: 5655-5663.
- Talebian-Kiakalaieh, A., Amin, N. A. S. & Mazaheri, H. 2013. A review on novel processes of biodiesel production from waste cooking oil. *Applied Energy*. **104**: 683-710.
- Tanaka, T., Ando, A. & Ishizaka, K. 2002. Study on pilot injection of DI diesel engine using common-rail injection system. *JSAE Review*. **23** (3): 297-302.
- Teixeira, L. S. G., Couto, M. B., Souza, G. S., Filho, M. A., Assis, J. I. C. R., Guimaraes, P. R. B., Pontes, L. A. M., Almeida, S. Q. & Teixeira, J. S. R. 2010. Characterization of beef tallow biodiesel and their mixtures with soybean biodiesel and mineral diesel fuel. *biomass and bioenergy*. **34** 438–441.
- Tesfa, B., Gu, F., Mishra, R. & Ball, A. 2014. Emission Characteristics of a CI Engine Running with a Range of Biodiesel Feedstocks. *Energies*. **7** (1): 334-350.
- Thangaraja, J. & Mehta, P. 2014. Effect of Biodiesel on Thermal NO Formation. *Journal of The Institution of Engineers (India): Series C*: 1-9.
- Thompson, J., Peterson, C., Reece, D. & Beck, S. 1998. Two-year storage study with methyl and ethyl esters of rapeseed. *Transactions of the ASAE*. **41** (4): 931-939.

- Ulusoy, Y., Tekin, Y., Cetinkaya, M. & Karaosmanoglu, F. 2004. The engine tests of biodiesel from used frying oil. *Energy Sources*. **26** (10): 927-932.
- Usta, N., Öztürk, E., Can, Ö., Conkur, E., Nas, S., Con, A., Can, A. & Topcu, M. 2005. Combustion of biodiesel fuel produced from hazelnut soapstock/waste sunflower oil mixture in a diesel engine. *Energy Conversion and Management*. **46** (5): 741-755.
- Valente, O. S., Pasa, V. M. D., Belchior, C. R. P. & Sodr , J. R. 2012. Exhaust emissions from a diesel power generator fuelled by waste cooking oil biodiesel. *Science of The Total Environment*. **431**: 57-61.
- Veny, H., Baroutian, S., Aroua, M. K., Hasan, M., Raman, A. A. & Sulaiman, N. M. N. 2009. Density of *Jatropha curcas* Seed Oil and its Methyl Esters: Measurement and Estimations. *International Journal of thermophysics*. **30**:529–541.
- Wang, Y. D., Al-Shemmeri, T., Eames, P., McMullan, J., Hewitt, N., Huang, Y. & Rezvani, S. 2006. An experimental investigation of the performance and gaseous exhaust emissions of a diesel engine using blends of a vegetable oil. *Applied Thermal Engineering*. **26**:1684–1691.
- WHO. 2006. *Air Quality Guidelines: Global Update 2005. Particulate matter, ozone, nitrogen dioxide and sulfur dioxide*. World Health Organization Regional Office for Europe. ISBN 92 890 2192 6.
- WHO. 2007. *Health relevance of particulate matter from various sources: Report on a WHO Workshop* World Health Organization Regional Office for Europe. EUR/07/5067587
- WHO. 2010. *Exposure to Air Pollution: A Major Public Health Concern*. World Health Organization Regional Office for Europe Geneva.
- WHO. 2013. *Health effects of particulate matter: Policy Implications for countries in eastern Europe, Caucasus and central Asia*. World Health Organization Regional Office for Europe. ISBN 978 92 890 0001 7.
- Yusop, A. F., Mamat, R., Sudrajad, A. & Yasin, M. H. M. 2012. Characteristics of Particulate Matter (PM) of Diesel engine using Palm Oil Methyl Ester (PME) fuel. *Journal of Biobased Materials and Bioenergy*. **6** : 1-4.
- Zhang, Y., Dube, M., McLean, D. & Kates, M. 2003. Biodiesel production from waste cooking oil: 2. Economic assessment and sensitivity analysis. *Bioresource technology*. **90** (3): 229-240.

## APPENDIX

### List of Publications

#### A) International and National Journal

1. **Nur Fauziah Jaharudin**, Abdul Adam Abdullah, Ahmad Fitri Yusop, Rizalman Mamat, Nur Atiqah Ramlan and Mohd Herzwan Hamzah, Study on Particulate Matter (PM) Emissions of Diesel Engine using Palm Oil Methyl Ester, **Applied Mechanics and Materials**, Volume 465-466, 2014, Pages 433 to 437.
2. Nur Atiqah Ramlan, Mohd Herzwan Hamzah, **Nur Fauziah Jaharudin**, Abdul Adam Abdullah, and Rizalman Mamat, Analysis of Diesel Engine Performance Fueled with Waste Cooking Oil, **Applied Mechanics and Materials**, Volume 465-466, 2014, Pages 418 to 422.
3. Mohd Herzwan Hamzah, Abdul Adam Abdullah, Agung Sudrajad, Nur Atiqah Ramlan and **Nur Fauziah Jaharudin**, Performance of Diesel Engine Operating with Waste Plastic Disposal fuel, **Applied Mechanics and Materials**, Volume 465-466, 2014, Pages 423 to 427.

#### B) International and National Conference Papers

1. **Nur Fauziah Bt Jaharudin**, Abdul Adam Abdullah and Rizalman Mamat.  
A review on biodiesel characteristics, its spray characteristics and exhaust emission. National Conference for Postgraduate Research (NCON-PGR 2012), 8-9 September 2012 Kuantan, Pahang.
2. **Nur Fauziah Jaharudin**, Nur Atiqah Ramlan, Mohd Herzwan Hamzah, Abdul Adam Abdullah, Rizalman Mamat.  
Study On Particulate Matter Of Diesel Engine Using Waste Cooking Oil.  
International Integrated Engineering Summit (IIES 2014), 1-4 December 2014, UTHM, Johor, Malaysia.